STRUCTURAL DESIGN OF CAR SEATS

ARAÇ KOLTUKLARININ YAPISAL TASARIMI

BENGÜSU EYYÜPOĞLU USTA

ASSIST. PROF. DR. SELÇUK HİMMETOĞLU

Thesis Supervisor

Submitted to Graduate School of Science and Engineering of Hacettepe University as a Partial Fulfillment to the Requirements for the Award of the Degree of Master of Sciences in Mechanical Engineering

2025

Hayatta öğrendiğim en değerli şeyleri bana öğreten, her zaman arkamda duran kıymetli babama, minnet ve sevgiyle…

ABSTRACT

STRUCTURAL DESIGN OF CAR SEATS

Bengüsu EYYÜPOĞLU USTA

Master of Science, Department of Mechanical Engineering

Supervisor: Assist. Prof. Dr. Selçuk HİMMETOĞLU

June 2025, 76 pages

This thesis focuses on evaluating the structural performance of vehicle seats under rear-end collision scenarios. The study involves static and dynamic analyses considering design parameters such as material selection, sheet thickness, and hinge configuration of the seat frame. Static structural analyses were performed using ANSYS to investigate the deformation behavior of the seatback under crash loads. To obtain results closer to real crash conditions, time-dependent dynamic simulations were carried out using LS-DYNA, and a multi-body system model was built in MSC Nastran. As a result of the study, the mass and inertia properties of the seat system were determined, and it was concluded that these data can contribute to the literature for future research.

Keywords: rear-end collisions, seat structural design, car seat, seat deformation

ÖZET

ARAÇ KOLTUKLARININ YAPISAL TASARIMI

Bengüsu EYYÜPOĞLU USTA

Yüksek Lisans, Makine Mühendisliği Bölümü

Tez Danışmanı: Dr. Öğr. Üyesi Selçuk HİMMETOĞLU

Haziran 2025, 76 sayfa

Bu tez, araç koltuklarının arkadan çarpma senaryolarında yapısal performansını değerlendirmek amacıyla yürütülmüştür. Çalışmada, koltuk iskeletinin malzeme seçimi, sac kalınlığı ve menteşe tasarımı gibi parametreler dikkate alınarak statik ve dinamik analizler gerçekleştirilmiştir. Statik yapısal analizler ANSYS ortamında yapılmış, çarpışma yükleri altında koltuk sırtlığının deformasyon davranışı incelenmiştir. Gerçek çarpışma koşullarına daha yakın sonuçlar elde etmek amacıyla LS-DYNA ile zaman bağımlı dinamik analizler yapılmış, ayrıca MS-Nastran yazılımı ile çok cisimli sistem modeli kurulmuştur. Çalışma sonunda koltuk sistemine ait kütle ve atalet bilgileri elde edilmiş, bu verilerin benzer çalışmalar için literatüre katkı sağlayabileceği değerlendirilmiştir.

Anahtar Kelimeler: arkadan çarpışmalar, koltuk yapısal tasarımı, araba koltuğu, koltuk deformasyonu

ACKNOWLEDGEMENTS

I would like to express my sincere gratitude to my advisor, Assist. Prof. Dr. Selçuk Himmetoğlu, for their valuable guidance, support, and encouragement throughout the preparation of this thesis. His insights and feedback have been essential at every stage of this study.

I would like to thank Bilal Toprak, for providing dynamic analysis support.

I would also like to thank Eyüp Gözükara for helping me to learn analysis environment and his support.

My sincere thanks go to my family, especially my husband, for his endless patience during this challenging process. Their presence has been my greatest source of strength.

Finally, I am thankful to all my friends and colleagues who shared this journey with me and contributed to this work, directly or indirectly.

TABLE OF CONTENTS

LIST OF FIGURES

LIST OF TABLES

SYMBOLS AND ABBREVIATIONS

Symbols

σ	Stress
Ø	Diameter

Abbreviations

FMVSS	Federal Motor Vehicle Safety Standards
UNECE	United Nation Economic Comission for Europe
EURONCAP	European New Car Assessment Program
FEM	Finite Element Method
MBD	Multi Body Dynamics
NIC	Neck Injury Criterion
MPa	Megapascal
kg	kilogram
mm	milimeter
N	Newton

1. INTRODUCTION

One of the most crucial aspects of the vehicle design process in the automotive industry is safety. Car seats must be able to absorb crash loads and protect the occupants in traffic accidents. By limiting passenger movement within the vehicle and absorbing forces during a collision, seats must help lower the risk of injuries. Reducing injuries and fatalities in traffic accidents is largely dependent on well-designed seats.

Various international safety standards are applied in seat design. These standards include different crash cases to evaluate the structural integrity and rear, front or side crash performance of the seat. Among these, rear-end collisions are very common and they can have serious effects on passengers. During rear impacts, the head and neck areas are at high risk due to forces transferred to the seatback.

The main goal of this thesis is to design and analyze the seatback frame to create a safe seat structure that can absorb crash loads under rear impact scenarios, stay within acceptable deformation limits, and protect the passenger. For this purpose, a detailed 3D model of the seatback frame was created, and its structural performance under crash conditions was analyzed using the Finite Element Method (FEM). The analyses inputs were based on FMVSS 207 and FMVSS 301, which are Federal Motor Vehicle Safety Standards. While FMVSS 301 concentrates on fuel system integrity in rear crashes and indirectly influences seat strength requirements, FMVSS 207 specifies static and quasi-static loading conditions for seatback strength.

The 3D model used in this study was created in CATIA V6 3DEXPERIENCE software using the real dimensions of a passenger car seat. The model was transferred to ANSYS Static Structural for linear elastic finite element analysis. The goal is to ensure that the deformation results stayed below the limits defined in the standards and to evaluate if the design is safe.

Although the analysis focused on the strength of the seatback, the full seat frame structure was also modeled to match the mass of real vehicle seats. A model with polyurethane foam was added to the seat frame to estimate the total mass and inertia properties.

In conclusion, the mass and inertia values of the seatback frame and headrest obtained from the analysis are used in multi-body dynamics simulations. Thesis provided a comprehensive analysis of car seat structures under rear-end collisions, using both static and dynamic methods. An optimal seat structure with appropriate material and dimensions was successfully designed, meeting international safety standards.

A significant achievement of this study is calculating precise mass and inertia values. These outputs provide essential input data for future crash simulations and serve as valuable references for automotive safety research.

This study also aims at determining the dynamic response of the seat under impact loads; with this obtained data multi-body models of the seats will be improved. Multi-body modelling is computationally more efficient that finite element modelling. Hence the obtained seat response characteristics in this thesis are valuable inputs for a multi-body seat model.

2. GENERAL INFORMATION

2.1 Importance of the Car Seat Structural Design

Automotive seats are critical components not only for comfort and ergonomics but also for structural integrity and crash safety. Especially in rear-end collision scenarios, the strength of the seatback and its energy absorption capacity have a direct impact on passenger safety. Therefore, the structural design of the seat must ensure safe performance under both static loads and dynamic impact conditions.

Car seats need to serve multiple functions as maintaining the occupant's position, carrying loads transferred to the seat structure in the whole lifecycle of the vehicle, supporting adjustability features such as angle and height adjustment, providing comfort during long journeys, and enhancing safety by maintaining structural integrity during crashes. In addition to support the occupant's weight, the seat structure must be designed to absorb dynamic extreme loads experienced during a collision. In particular, the seatback and headrest must be strong and stable to help prevent injuries to the head and neck during rear impacts.

2.2 Car Seat Structural Elements

The seat frame structure is generally formed by welding together sheet metal components. Although some examples may use aluminum alloys or materials like carbon fiber, the majority of automotive seats feature a structure made from steel or aluminum. The seat is attached to the vehicle through a rail-mounted connection system, and the base of the seat structure is positioned on these rails having an adjustment that moves the frame fore and aft named seat track.

Due to EuroNCAP, head restraint is the part used to limit the backward motion of an adult occupants' head relative to the torso. This keeps the neck from getting hurt in the event of a rear-end collision. [1]

Seatback is a part that can be rotated the entire seat back, irrespective from the seat cushion, about a pivot at the seat cushion joint. As a result, the angle of the seat back relative to the seat cushion is changed.

Side bolsters are additions that modify the shape of the seat by adapting both sides of the seat back and cushion. [1]

A recliner is a mechanical or electromechanical component that allows the adjustment of the seatback angle relative to the seat pan. It connects the seatback frame to the bottom cushion so the seat pan, it provides the ability to recline the back part forward or backward, improves both comfort and safety for the occupant. In rear collisions, the recliner mechanism can be designed to absorb crash energy. It controls deformation by plastic hinges or by torsional springs, helps to reduce seatback rotation and limits head and neck injuries.

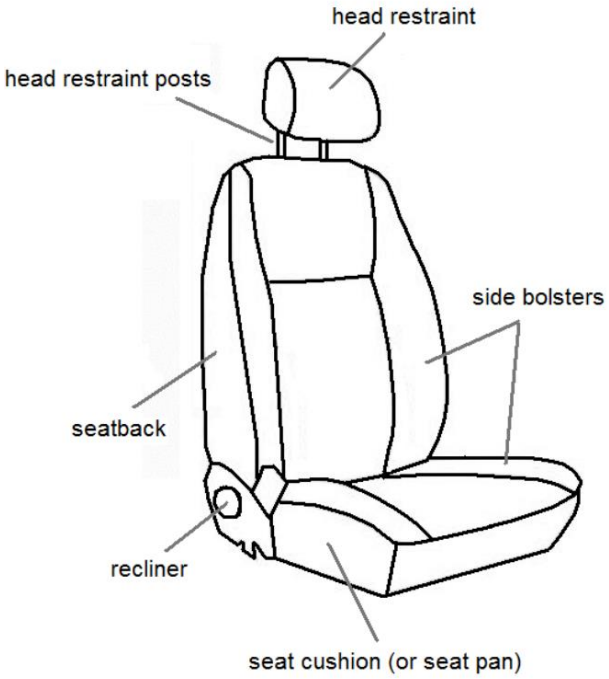

Figure 1 - Car Seat Elements [2]

The seat pan is connected to seat track and supports occupants' lower body under seat cushion. Seatback frame, is the structure that supports occupants' torso. It is the most critical part means of strength. Seatback consists of seatback frame, seatback suspension, seatback structural cross member and side brackets. A structural cross member is usually a metal bar, beam or formed sheet, which is horizontally across the seatback frame, connecting the two side vertical brackets. Cross members provide rigidity to the seatback structure, distribute loads from the seatback such as occupant force during crash, reduce

deformation under stress or impact, and serve as a mounting point for other components. All of these parts are made from sheet metal that is bent or formed in various shapes.

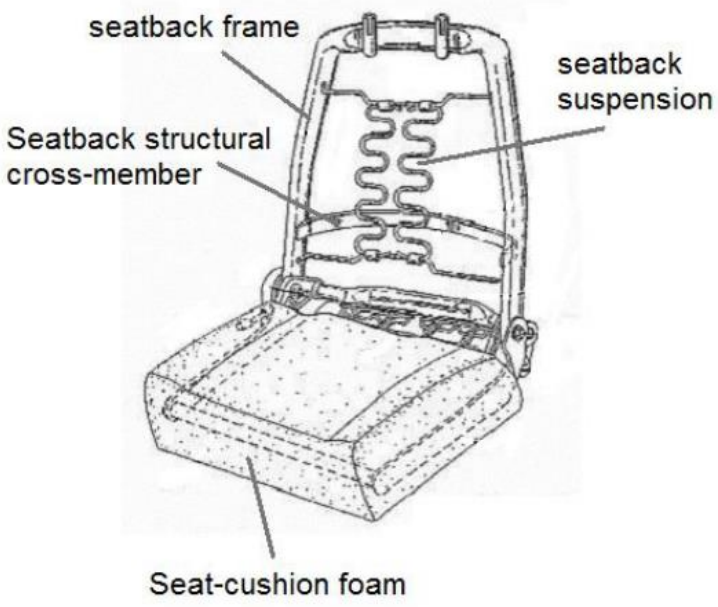

Figure 2 - Car Seat Structural Elements [2]

2.3 Car Seat Design Parameters

A number of crucial factors are included in the structural requirements for car seat design. To guarantee that the seat deforms as small as possible under typical driving and braking circumstances, it must be sufficiently rigid. In rear-end collisions, where the seatback must restrict rearward movement in a controlled manner to improve passenger safety, energy absorption capacity is particularly crucial. Another important consideration is weight optimization; while structures with lower mass improve vehicle performance and fuel economy, structural strength shouldn't be sacrificed in the process. Finally, because of the floor attachments and the recliner are subjected to heavy loads during a collision and need to be able to withstand forces, the strength of these connection points is important.

2.4 Literature Review

Using prior comprehensive research and thesis studies on vehicle seat designs, safety standards, and test procedures, a wide assessment of knowledge was carried out in the literature review section of this study. The study hopes to contribute significantly to the knowledge about car seat rear impact performance in this way.

The structural performance of seats, particularly in rear-end collisions, and their effects on occupants have been the subject of a large number of studies on seat design in terms of vehicle safety. The most serious effect of rear-end collisions, which typically happen at low to moderate speeds, is the elevated risk of injuries to the head and neck areas of car occupants. Often referred to as "whiplash," these injuries usually involve ligament damage, muscle or disc trauma, and soft tissue damage in the cervical spine [3]. The mechanisms underlying these injuries have been thoroughly studied in the literature, and a great deal of research has been done on how seatback design can lower the risk of whiplash injuries [4].

The structural characteristics of the seatback have a direct impact on how well car seats absorb the loads that arise during rear-end collisions. In order to prevent passengers from moving uncontrollably within the vehicle, the seatback frame must be able to sustain the forces that the occupants transmit during impact and stay within allowable deformation limits. Numerous investigations have been carried out in the literature to ascertain the ideal deformation limits for seatback frame design. Thiyagarajan [5] conducted a finite element analysis with the goal of structural optimization for his master's thesis, which assessed the structural behavior of an automobile seatback frame under headrest and seatback moment loads specified by the UNECE R-17 standards. The goal of the study was to make a commercially used seatback structure made of low-carbon ductile steel that was stamped and welded lighter while maintaining safety regulations and increasing production efficiency. Sheet thicknesses were designated as design variables for this purpose, and an OptiStruct software thickness optimization produced a 15.2% reduction in total mass.

The study of Thiyagarajan [5] loading scenarios were separated into two primary categories: seatback moment loading and headrest loading. The upper portion of the seatback was subjected to a moment of 530 Nm with respect to the H-point in the first stage. The deformation and stress responses of the seatback frame were then examined using a methodology similar to that of FMVSS 207 [6]. The headrest mounting points were subjected to a force couple that created a moment in the second stage. Specific aspect of these loadings is that the headrest loading was modeled separately from the seatback, which made it possible to assess the headrest component's impact on the seatback frame's stress distribution more precisely.

A nonlinear steel material model exhibiting elastic-plastic behavior was used in Thiyagaran's study [5], and the analyses were conducted using ABAQUS software. To capture stress distributions with high accuracy, a fine mesh was specifically applied to critical areas where stress concentrations were likely to occur, such as the headrest attachment points, upper cross members, and lower mounting areas of the seatback frame. Based on the analysis results, localized plastic deformations were seen in some areas of the original design, and maximum Von Mises stresses in other areas approached the material's yield strength. It was reported that after the optimization process, the maximum deformation value dropped about 11.8 mm, stresses in these specific areas were lowered, and the structure supported the loads more evenly. The design could be considered as safe because the amount of deformation stayed below the parameters specified in the test protocol. Furthermore, the mass and inertia values obtained from the deformation outputs of the model offered trustworthy information appropriate for use as input parameters in simulations of multi-body dynamics (MBD).

There are significant similarities between Thiyagarajan's study [5] and this thesis. Both studies created separate loading scenarios for the seatback frame and evaluated the loads on the seatback frame and headrest regions independently. However, the goal of this thesis was to analyze a particular design using a linear elastic material approach and correlate the analysis results with mass and inertia outputs, rather than to focus on optimization. Furthermore, CATIA V6 3DEXPERIENCE was used for the 3D modeling in this thesis, and the ANSYS Static Structural environment was used for the finite element analyses.

Viano [3] carried out another significant study evaluating how seat design affects whiplash injuries. This study looked closely at how headrest design, deformability, and seat structure stiffness affected the likelihood of whiplash injuries. In contrast to low-stiffness systems that were previously in use, Viano showed that "high-retention" seat designs, which were introduced in the mid-1990s, significantly reduced accelerations and neck forces. According to the study, excessively high seat stiffness increases the force applied to the passenger's torso, which leads to rebound effects that cause excessive neck extension. Conversely, overly soft seats raise the risk of whiplash because they may cause excessive deformation that delays contact with the headrest. Thus, the study underlined that the ideal seat design should preserve a structure that strikes a balance between stiffness and energy absorption capacity.

By reducing the distance between the head and the headrest, active head restraint systems (which automatically move forward and upward during a crash) significantly reduce neck moments, according to Viano's analysis [3]. The head's rearward displacement and duration are decreased in seats with these systems, which significantly lower neck deformation and related injuries. Therefore, in addition to seat stiffness, energy absorption capacity, controlled seatback deformation, and optimal head restraint positioning have become essential components that improve passenger safety in seat design.

Together with EDAG Engineering, the National Highway Traffic Safety Administration (NHTSA) carried out another significant study on seat design. In this project, Bridges et al. [7] used finite element analysis to create detailed models of the front seats of a 2014 Honda Accord and test them in high-severity rear impact scenarios. LS-DYNA software was used to run the simulations, and separate analyses were conducted for the manual and power seat versions. Important parts like the seatback frame, headrest connections, recliner mechanisms, and foam structure were all included in the models, which were based on real-world geometry. For both seat versions, high-fidelity FEA models with realistic geometry and material definitions were produced. The models were validated by comparing them to previous research and physical tests.

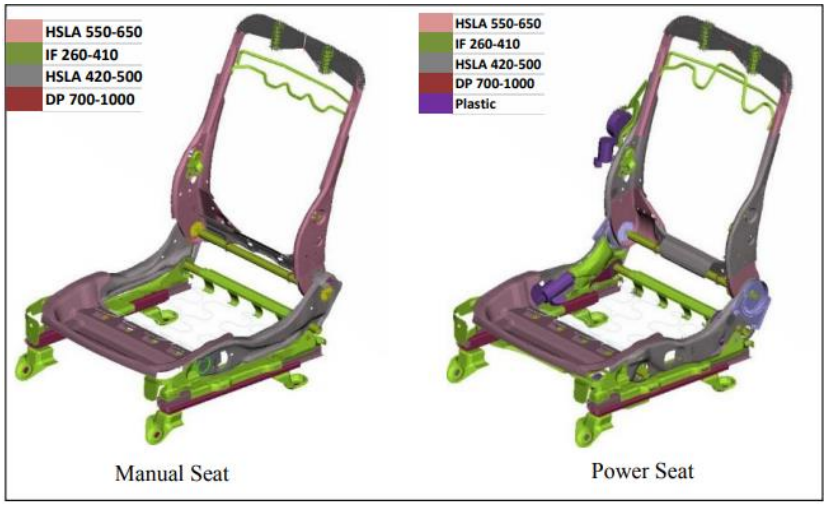

Figure 3 - Manual and Power Seat Models [7]

The study focused on examining the effects of loads transferred to the seatback during impact by modeling individual components, including the headrest connections, adjustment mechanisms, and seatback structure. The FMVSS 207 [6] requirement to apply a horizontal load to the seatback at a height of 46 cm was a crucial evaluation point.

This requirement was noted as possibly impractical because it is higher than the human torso's center of mass. Using an acceleration level of 20g, the loading conditions were established in accordance with the FMVSS 301 [8] standard. According to simulation results, the rear seat occupants may be at risk due to the high levels of deformation in the seatback frame. Therefore, in order to limit deformation, improvement strategies like thickening the seatback structure and altering the material were tested. In order to avoid unexpected collapses or structural failures that could endanger rear passengers, it was found that controlling seatback deformation was crucial. Bridges et al.'s study highlights the significance of striking a balance between structural integrity and energy absorption potential in seat frame design. It can be used as a model for studies that combine simulation and physical testing methods.

One of the most commonly used methods for evaluating the strength of a seatback frame is the FMVSS 207 [6] test procedure, which is defined by U.S. federal safety standards. According to FMVSS 207, the structural integrity of the seatback is tested by applying a horizontal load. The test is typically performed by applying the force approximately 46 cm above the H-point. However, in the literature, it is criticized that this loading height is significantly higher than the center of mass of an average adult’s upper torso, and therefore may not fully represent real-world crash scenarios [3]. This is questionable that how well FMVSS 207 test results align with realistic in-vehicle load transfer conditions.

Figure 4 - FMVSS Tests in Burnett et.al. [9]

The "Body Block" test was investigated as an alternate testing technique in the 2016 study by Viano and White [10]. In this test, a rearward load is applied while a flat, rigid block contacts the seatback at a height of roughly 35.6 cm. When the block slides upward or the seatback reclines to a 45-degree angle, the test is deemed finished. The block's flat, rigid surface only approximates the real interaction between the seat and the human back, despite the fact that this approach is frequently chosen because it is straightforward.

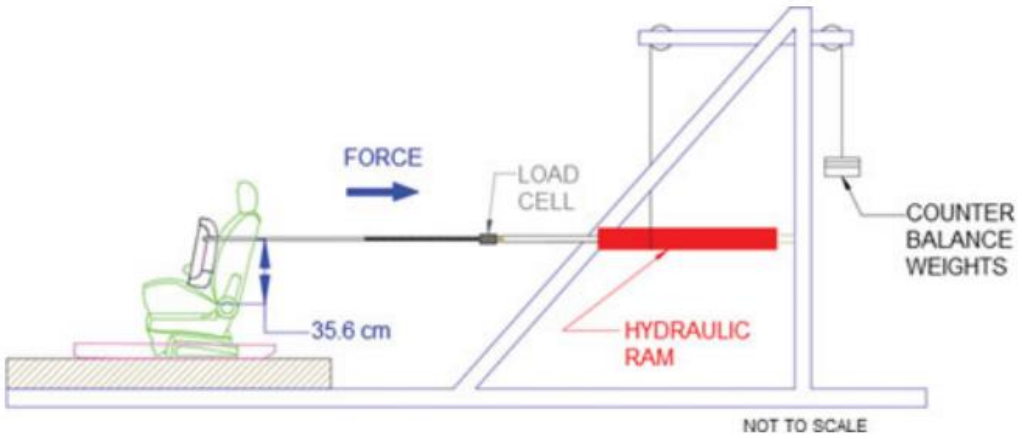

Figure 5 - Body block test setup [10]

Figure 6 - Body Block Test [9]

In the study by Burnett, Viano, and Parentau [9], a much more advanced method known as the Quasi Static Seat Test (QST) was performed using a crash test dummy, that offers more accurate simulations of the interaction between a human and the seat frame. In this

method, the load distribution on the seatback structure is more real, and the deformation measurements can directly represent passenger-seat interaction. However, this method is not advised for use in the early stages of design but rather in the final validation phases due to its high cost and complexity.

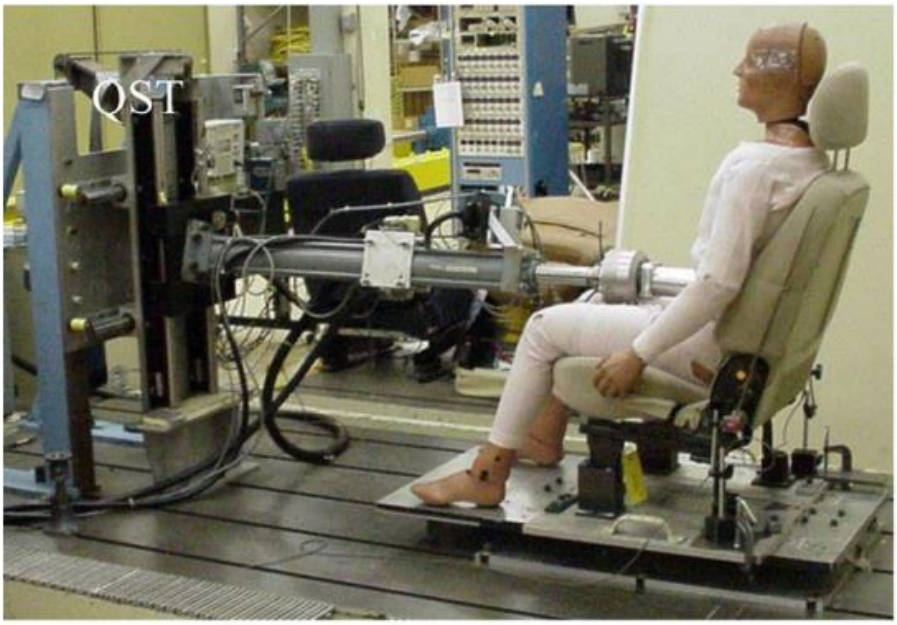

Figure 7 - Quasi-static Test Setup [9]

In contrast, a simplified model based on the SAE J826 H-point device is used to conduct the FRED II test. Because it accurately captures realistic seat-occupant interaction, this test, which is intermediately complex between the body block and QST tests, can be used for a general evaluation of seat designs.

Figure 8 - Fred II Test Setup [9]

It is clear from comparing these test procedures that the seatback's structural strength is significantly impacted by the height at which the load is applied. Adopting a standardized reference height is therefore necessary because it is challenging to directly compare test results obtained at various loading heights. A more equitable and consistent comparison of various seat designs would be possible by a loading height that precisely corresponds to the center of mass of the human upper torso.

Experiments show that different test methods should be used at different stages of the design process More sophisticated techniques like QST and FRED II offer realistic seat-occupant interaction for evaluating final safety performance, even though FMVSS 207 or its modified versions can offer fast and affordable data to inform engineering decisions in the early stages. In this regard, the seat design process benefits greatly from the use of a range of test methodologies.

The experimental research by Viano et al. [11], which was based on sled tests, is one of the studies carried out to assess seat performance in high-speed rear-end collisions. In order to compare traditional seat designs with seats that have All Belts To Seat (ABTS) systems, rear impacts at a speed of 40.2 km/h (25 mph) were simulated in these tests. The biomechanical effects of various seat designs on occupants were investigated using crash test dummies. The findings demonstrated that, in comparison to earlier models, contemporary seat designs (from model year 2000 and onward) significantly decreased neck moments and forces. Modern seats' better "pocketing" capabilities, in particular, improved the way the body and seat interacted, limiting excessive neck motion and lowering the risk of whiplash injuries.

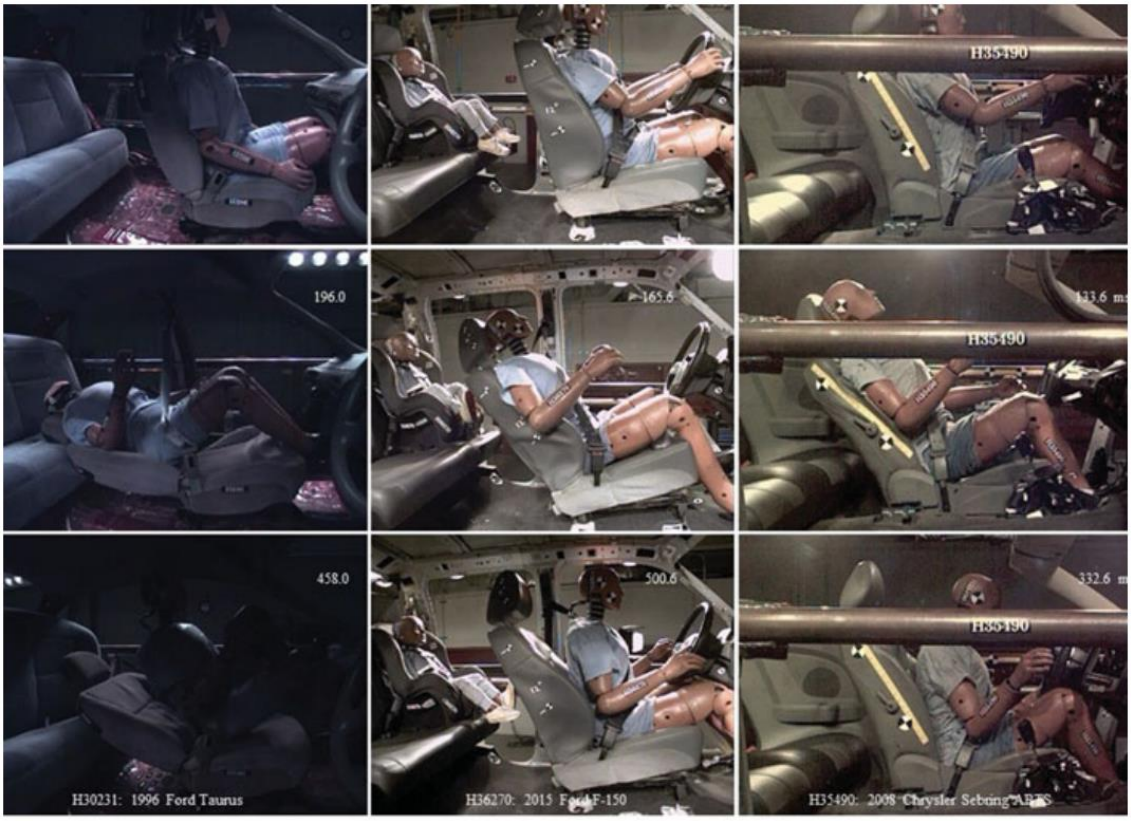

Figure 9 – Traditional seats to modern seats [11]

The goal of ABTS seat systems is to synchronize the motion of the body and the seat by integrating the entire seatbelt assembly into the seat structure itself. But according to Viano's research [11], these seats produced 13% more biomechanical responses than traditional, contemporary seats. This result was ascribed to ABTS seats' increased structural stiffness, which caused forces to be transferred from the seat to the occupant more directly. This research emphasizes how difficult it is to strike a balance between seat stiffness and occupant safety when designing seats.

In order to assess the structural strength of a passenger car seatback, Karambe et al. [12] performed finite element analyses in compliance with FMVSS 207 and ECE R-17 regulations. They used CATIA to model and ANSYS Workbench to analyze seatback components, including the upper beam, side supports, lower mounting plate, and reinforcement member, under static loading conditions. A moment of 373 Nm was applied under FMVSS 207, which led to a maximum Von Mises stress of 379 MPa and a deformation of 4.99 mm. ECE R-17 [13] reports a stress of 207 MPa and a deformation of 3.21 mm under a force of 530 N. These findings led to the implementation of structural enhancements, including thickening the profile, adding reinforcement plates, and

enlarging the upper cross-member, which decreased the maximum stress to 317 MPa and the deformation to 4.12 mm. The safety of structural designs that stay within elastic bounds in crash situations is emphasized in this study, which also identifies loads, reinforcement components, and sheet thickness as important design factors. Furthermore, its focus on direct engineering improvements rather than optimization aligns closely with the analysis approach presented in this thesis.

Research attempting to lower the whiplash effects by integrating smart systems into the seat structure is another noteworthy trend in the literature on seat design. The performance of a smart seat system with a sliding mechanism that uses a magnetorheological (MR) damper was compared to that of conventional passive anti-whiplash seats in the study by Kaya and Himmetoğlu (2024) paper published in Machines journal [14]. The developed smart seat system significantly decreased commonly used neck injury criteria like NIC (Neck Injury Criterion) and Nkm, according to simulations conducted using a human body model. This study showed that, in addition to passive structures, semi-active systems can be incorporated into seat designs to lower injury risks and provide opportunities for future automotive safety initiatives.

When paired with more conventional structure-based analytical techniques, Kaya and Himmetoğlu's study adds to a more thorough framework in seat design, even though it offers a more dynamic and biomechanical viewpoint. It was also underlined, though, that production and cost issues still limit the use of the MR damper systems in industrial applications. However, these systems are anticipated to receive increased attention in the near future due to the development of autonomous vehicles.

The structural and biomechanical performance of rear-facing seat systems designed for autonomous vehicles was the subject of another study by Yavuz and Himmetoğlu (2023) paper published in Machines journal [15]. A unique seat design with a fixed recline angle, rigid torso plates, and an energy absorber underneath the seat was suggested in the study. This design was found to lower neck forces from 600 N to 350 N in frontal impact simulations carried out at 64 km/h. Furthermore, it was stated that the design complied with safety regulations and that there was a decreased chance of harm to the head, chest, lower back, and legs. This study's importance in the literature comes from its critique of the limitations of conventional forward-facing seat designs and its suggestion of substitutes tailored for autonomus cars. Since rear-facing seats redirect crash energy differently, they necessitate a re-evaluation of conventional seat design criteria. The

system proposed by Yavuz and Himmetoğlu showed advantages in terms of deformation control due to its fixed rigid structure, but also highlighted potential limitations regarding user comfort and driving ergonomics. In this respect, the study draws attention to emerging safety requirements that may arise in future seating configurations and supports the evaluation of alternative structural scenarios.

According to international standards, one of the most well-known consumer-based assessments of how well car seats perform in low-speed rear impact situations is the whiplash test protocol created by Euro NCAP. Three impact severity levels are included in this protocol: low ($\Delta V = 16$ km/h), medium ($\Delta V = 24$ km/h), and high ($\Delta V = 32$ km/h) due to Avery et al. [16]. A BioRID II crash test dummy is usually used for the tests, and variables like head kinematics (forward and backward motion), seatback deformation characteristics, rebound behavior, and head restraint position are evaluated. Biomechanical indicators like NIC (Neck Injury Criterion), Nkm, and head-to-headrest contact timing serve as the foundation for the main evaluation criteria.

Manufacturers have been prompted to create safer seat designs by the Euro NCAP testing protocol. Design modifications made to seats tested under this protocol since the mid-2000s have included raising the headrest, decreasing the horizontal distance (backset) between the head and headrest, and creating a seatback frame that can absorb energy in a regulated way. Effective seat designs usually include a head restraint with optimal geometry and a combination of adequate stiffness and effective energy absorption capacity.

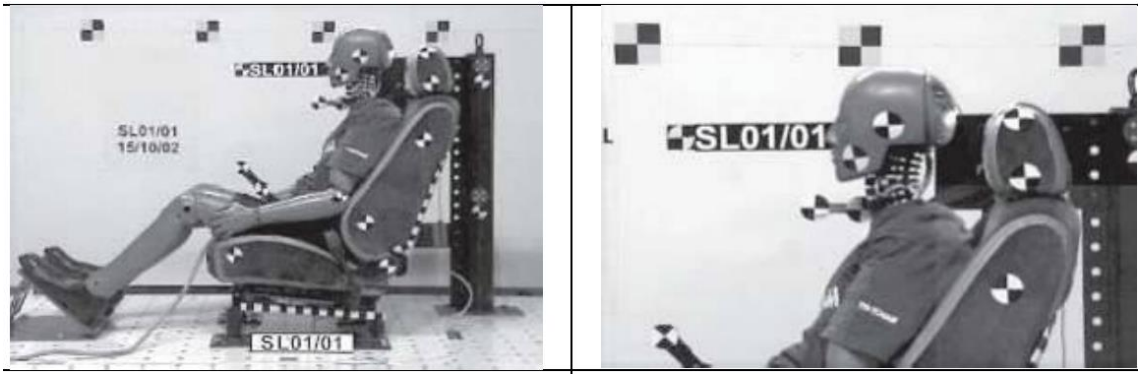

Figure 10 - EuroNCAP Test Protocol [1]

The promotion of seat design optimization for low- and medium-severity collisions as well as high-speed impacts is one of the main benefits of Euro NCAP testing. The majority of whiplash injuries happen in low-speed collisions, according to real-world

crash data. [1] Thus, a more thorough assessment of occupant safety is ensured by including low-speed scenarios in addition to high-speed tests.

Among the main laws dictating the structural design of car seats are the FMVSS 207 [6] and FMVSS 301 [8] federal safety standards in the United States. The minimum structural strength specifications for seatbacks and their attachment systems are outlined in FMVSS 207. This standard state that seats must not deform excessively when subjected to specific static and quasi-static loads. By exerting a horizontal force on the upper part of the seatback, the test procedure assesses the seat's durability.

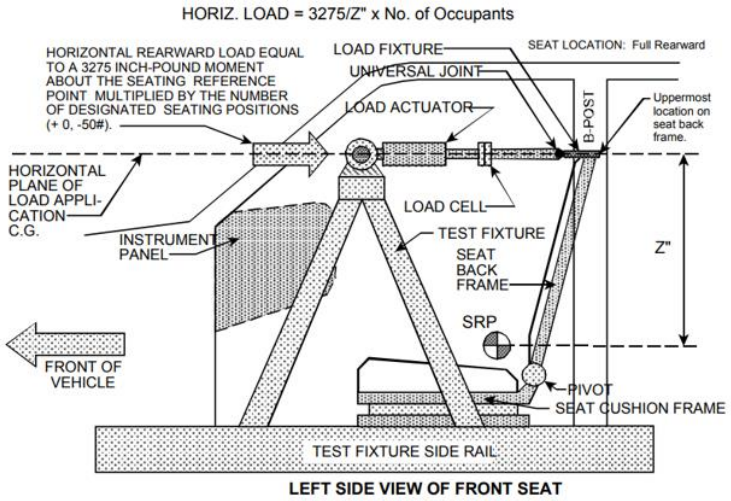

Figure 11 - FMVSS 207 test [6]

FMVSS 207 is a vital safety criterion evaluating the integrity of the attachment points, bending strength of the seatback, and ability of the seat to be returned to its starting point. These criteria state that seats cannot separate from the vehicle structure in the case of a collision and must only allow limited deformation up to a specified angle [6].

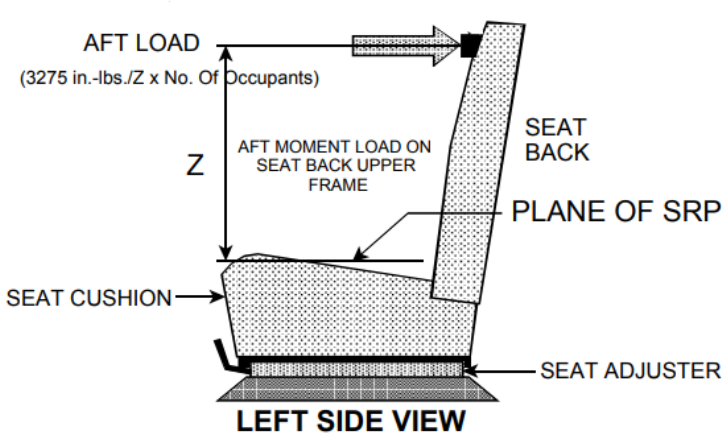

Figure 12 - FMVSS 207 [6]

Although FMVSS 301 does not specifically address seat structures, it focuses on maintaining the integrity of the fuel system in rear-end collisions. But the test's crash scenario, where a 1,361 kg deformable barrier hits the car at 80 km/h, also demonstrates how much the seatbacks and other in-car parts deform. Therefore, FMVSS 301 provides crucial information about the energy-absorbing capacity and durability of seatback frames in an indirect manner. If the impact causes seat deformation or fuel leakage, the test is considered unsuccessful. This highlights how crucial it is that seatback structures be robust enough to withstand severe rear-end collisions.

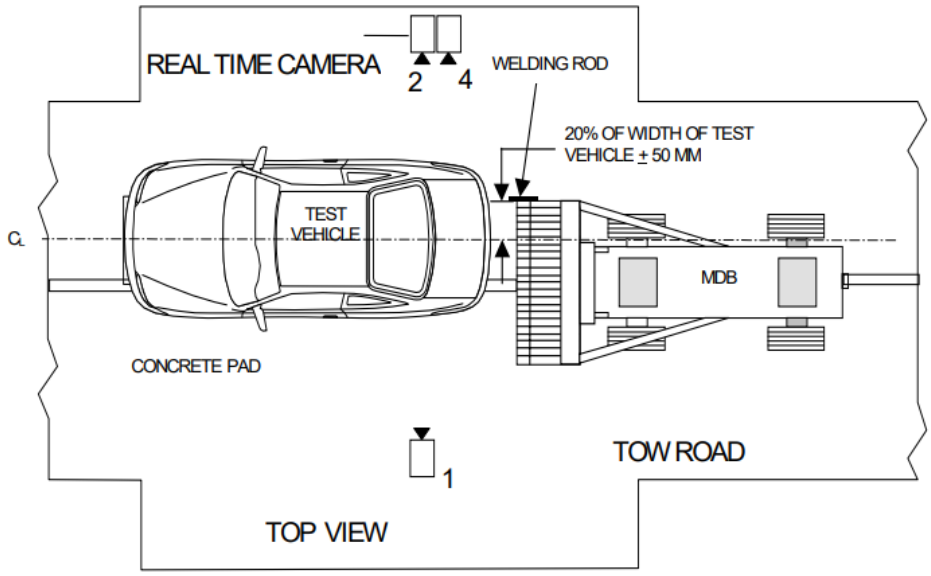

Figure 13 - FMVSS301 [8]

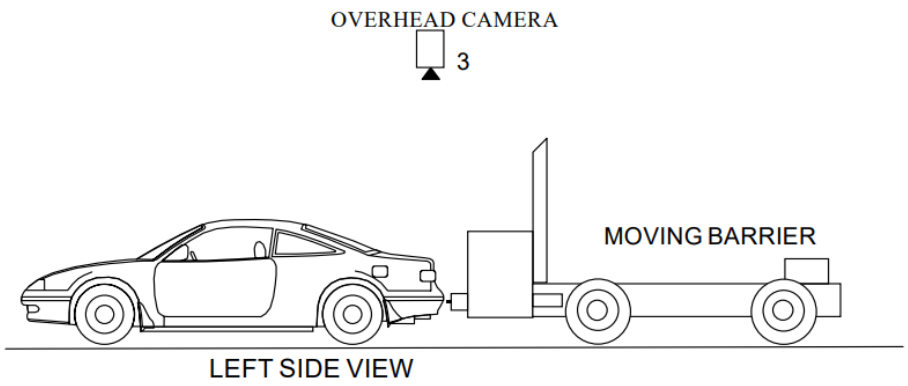

Figure 14 - FMVSS301 [8]

The ECE R-17 [13] standard is developed to evaluate the crash safety and structural integrity of passenger car seats in Europe. Its main goal is to determine the attachment security and deformation limits of components such as seatbacks and head restraints under specific loading conditions. During the test, a horizontal force of 530 N is applied to the seatback, and the resulting deformation is expected to be less than a predefined threshold, typically 50 mm. The seat must remain solid during the test, and force is applied uniformly across the seatback using a pressure plate. This standard is frequently used in the literature to evaluate characteristics like energy absorption capacity and seatback bending strength. ECE R-17 force conditions are shown to directly affect seatback design, the thickness of reinforcement plates, the stiffness of side profiles, and the geometry of the seatback cross-member, that affects deformation behavior. For procedures involving structural analysis and ergonomic design, ECE R-17 is considered an essential engineering standard in this regard.

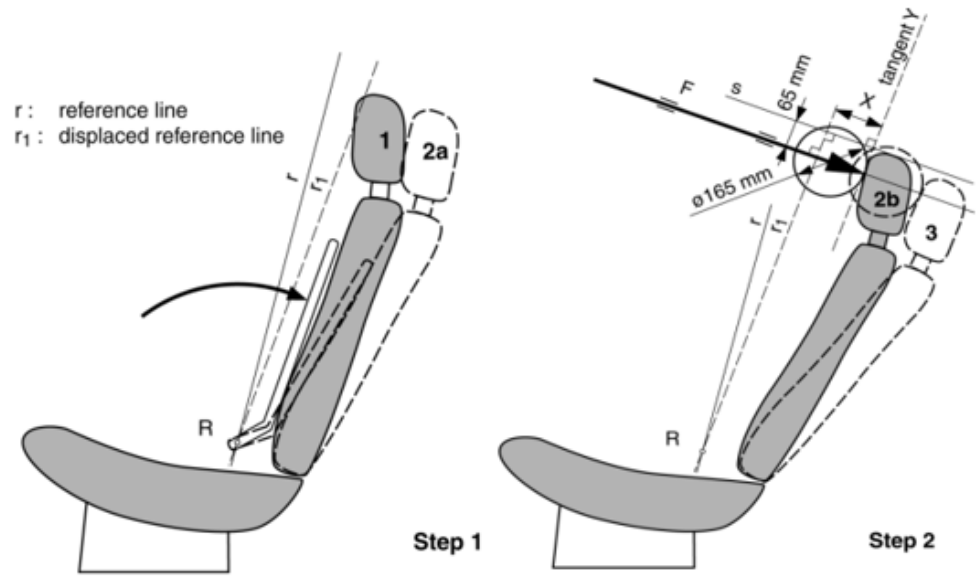

Figure 15 - ECE R17 [13]

Beyond safety performance, these standards influence seat design because they are essential in determining the loading scenarios used in structural analysis. FMVSS guidelines shape parameters such as the magnitude, direction, and application height of the force applied to the seatback. FMVSS 207 and 301 provide a technical framework for simulation inputs to ensure the precision and relevance of structural analyses.

3. MATERIAL AND METHOD

3.1 Car Seat 3D Model

In this research, finite element analysis (FEA) was used to look at how the structure of car front seats reacts to rear-end collisions. A software program called CATIA V6 3DEXPERIENCE was used for the modeling, and the ANSYS Static Structural environment was used for the analyses. The main goal was to make sure that the seat structure does not deform excessively while obtaining the best mass and inertial properties from the system.

In the beginning stages of designing the seat frame in 3D, measurements from a real car seat, product catalogs were used.

Figure 16 - Seat measurement in laboratory

3-dimensional modeled seat frame includes seatback frame, seatback suspension, head restraint posts, head restraint frame, seatpan frames, seat pan suspension, mounting brackets and a solid recliner body and necessary joints as shown below.

Figure 17 - Car seat frame model

Polyurethane foam material for the seat cushion and headrest was included to precisely determine their contribution to the total mass and inertia properties after finalizing the seat geometry by structural analyses.

Figure 18 - Car seat model with cushion

The seatback frame in this work was built on a 17° recline angle. This angle was chosen in line with the factory-default configuration of a normal passenger car seat, also frequently found in rear seats. In the study by Latchford et al. [4], changing the angle of

the seatback from 20° to 30° during rear-end collision tests had a big effect on the loads on the neck. However, these angles were chosen for testing so that impact scenarios could be generalised and different occupant positions could be simulated. In real life, manufacturers of cars tend to choose angles that are narrower, between 15° and 18°, to keep comfort and ergonomics in check. Also, in literature, Bridges et al. [7] chose a recline angle of 18° for their studies on seat modelling. Taking this into account, the 17° recline angle used in this study not only matches the shape of most production seats, but it also gives a good representation of how the seat's structure works. This 17° recline angle also represents the recline angle of rear seats whose recliners are fixed.

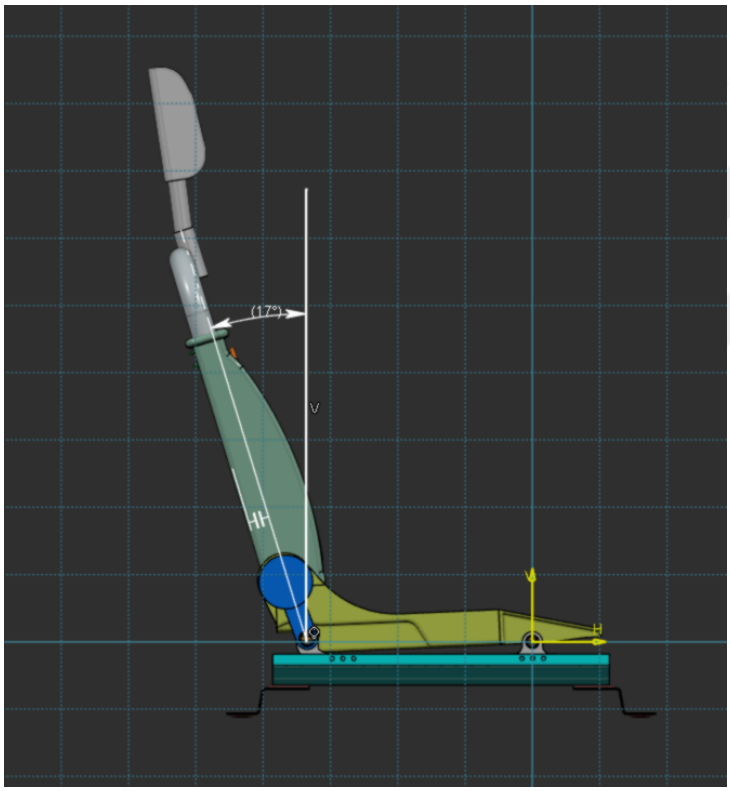

Figure 19 - Seatback angle

3.2 Material Properties

The material properties and results were determined for the structural frame parts are all assigned as structural steel. For the mass and inertia, the head restraint frame is assigned as polyamide, and polyurethane foam is used in seat cushioning.

S355 structural steel, a common high-strength low-alloy steel used in automotive and structural applications, was used to model all metal frame parts in this study. A European

Standard called EN 10025-2 [17] describes this material. It is called "Hot rolled products of structural steels/Part 2: Technical delivery conditions for non-alloy structural steels."

In this group of steels, S355 is found. The letter "S" stands for "structural." From 0 to 16 mm thick, the number 355 shows the material's lowest yield strength in MPa. This grade of steel is good for structures that are welded, bolted, or riveted together because it has a good balance of mechanical performance and ease of manufacture. The type of this steel may vary due to chemical composition, however the yield strength, ultimate tensile strength, percent elongations are close.

Table 1 - S355JR Steel Mechanical Properties

Yield Strength	355 MPa
Ultimate Tensile Strength	470-630 Mpa
%Elongation	20%
Young's Modulus	210 GPa
Poisson's Ratio	0.28
Density	7800 kg/m^3

Since foam has a very nonlinear behavior that would make simulations harder to run, the structural strength and deformation resistance of the foam components are left out of this study on purpose. Thiyagarajan's study [5] on the other hand, clearly included polyurethane foam elements inside the finite element models, as shells to reflect their stiffness and possible contribution to the rigidity of the seat structure under applied loads. Thiyagarayan underlined how the foam supports the seat structure and its ability to affect general deformation and stress distribution.

Table 2 - ISO 5999:2013 – Flexible Cellular Polymeric Materials – Specification for Polyether-Type Polyurethane Foam

Yield Strength	0.9 - 4.5 MPa
Ultimate Tensile Strength	0.43 - 3 Mpa
%Elongation	50-100%
Young's Modulus	15 - 151 MPa
Poisson's Ratio	0.3 - 0.4

Density	160 kg/m^3

Unlike Thiyagarajan's comprehensive approach, this thesis decided to simplify the analysis method by focusing just on the response of the metal frame under loading conditions, so considering the foam as simply a mass contributor without structural interaction.

Aluminum alloy used in analysis of recliner-equiped seatbacks has the mechanical properties below in ANSYS material database.

Table 3 - Aluminum Alloy used in ANSYS database

Yield Strength	280 MPa
Ultimate Tensile Strength	310 Mpa
%Elongation	25%
Young's Modulus	71 GPa
Poisson's Ratio	0.33
Density	2770 kg/m^3

3.3 Boundary Conditions

3.3.1 Fixed Seatback Analysis Boundry Conditions

Since the aim of this study is related seatback deformations, the seatback frame structure was the main object of static structural analysis.

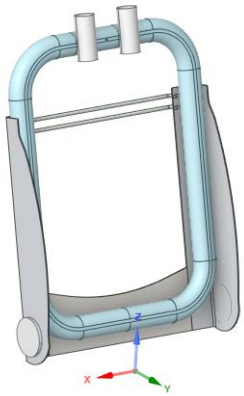

Figure 20 - Seatback frame structure analysis model

In the first part of the analysis, an area of 40 mm radius was modelled as fixed support at the recliner, because of the contact area was designed by using 80 mm diameter recliner body. Bonded contacts have been used to simulate welding conditions between the other components.

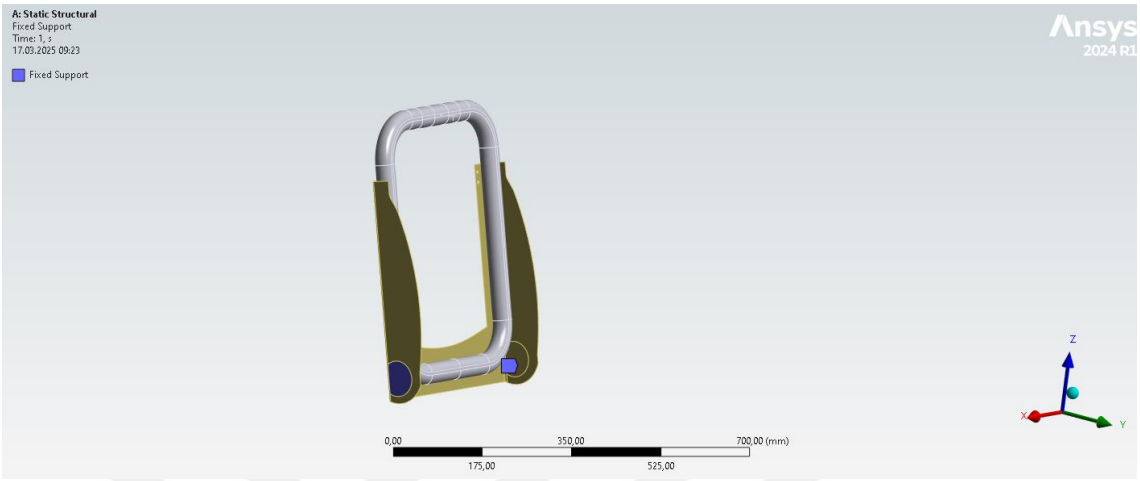

Figure 21 - Fixed support

In order to compare the fixed seat analyses with those of recliner-equipped versions (in which recliner can be deformable), a second version of fixed seat analyses are performed. In this second version, the fixation areas are the same for both fixed seat analyses and recliner-equipped seat analyses. In this second version, fix support area had 30 mm diameter as shown in figure.

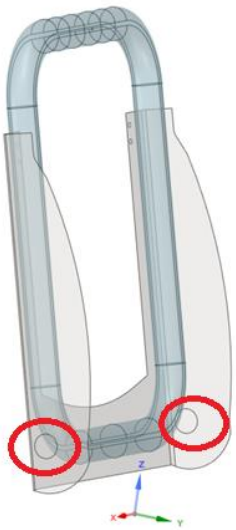

Figure 22 - Smaller fix area

3.3.2 Seatback with Bending Recliner Analysis Boundary Conditions

In order to observe how much the seatback deformation could be reduced if a recliner was used in the seat structure to absorb energy through plastic deformation when necessary, different types of recliners were included in the structural analyses. Two recliner types were modeled; one to observe bending effects, and the other for torsional effects. The bending recliner model is shown in the figure.

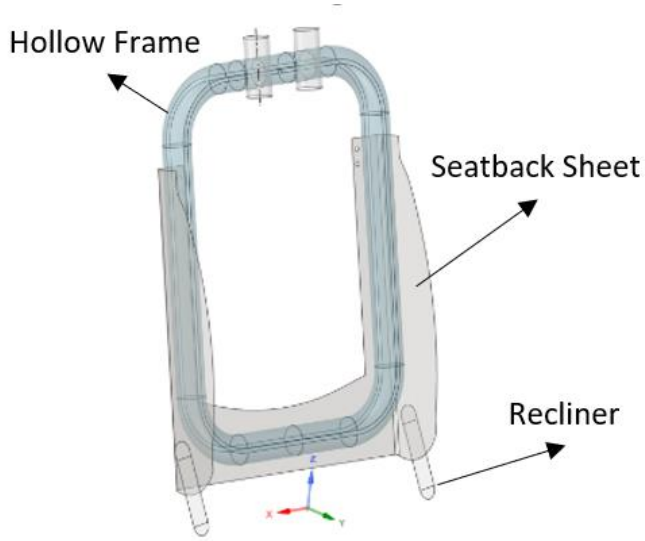

Figure 23 – Analysis model and recliner

In this setup, a fixed support was applied to the lower end of the bending recliner, which is intended to be connected to the seatpan.

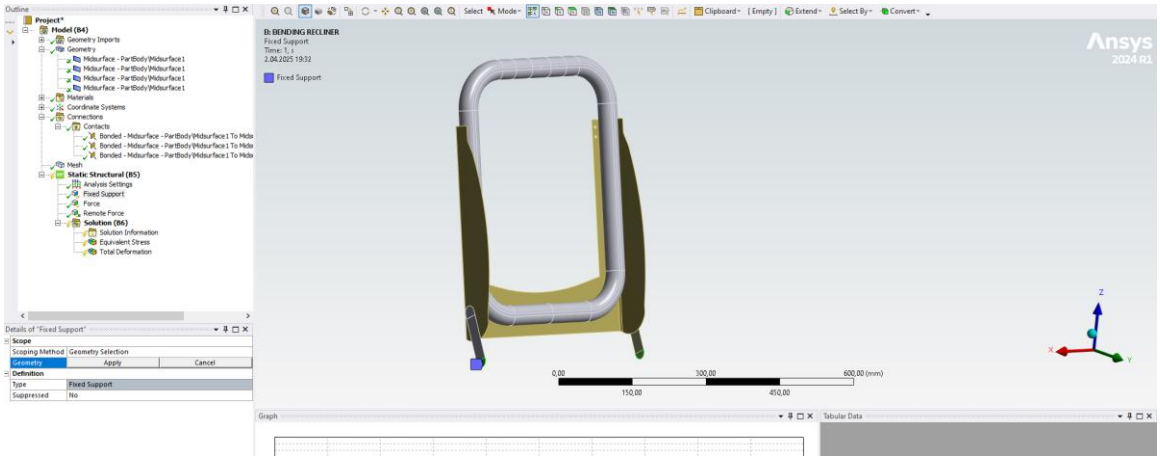

Figure 24 - Boundary conditions for recliner model

In the 2D analyses, the thickness of the beam was varied to obtain multiple results.

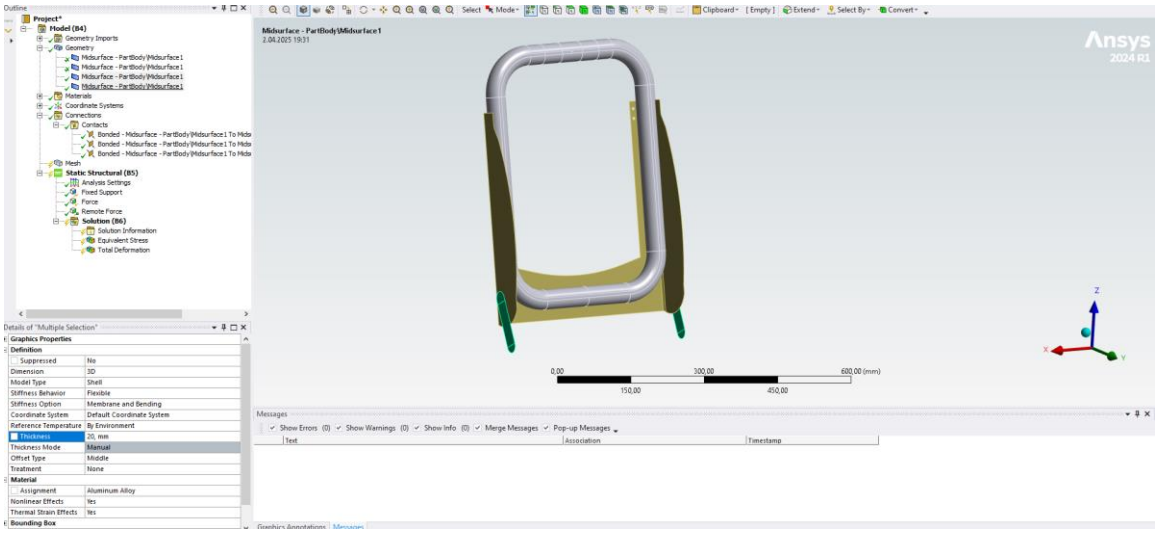

Figure 25 – Recliner thickness adjustment

3.3.3 Seatback with Torsional Recliner Analysis Boundary Conditions

In order to see how much deformation occurs on seatback using with torsional recliners, a bar is modeled to both sides of seatback. The model of the torsional recliner is shown in the picture, analysed as a 3D body, the bar's diameter and length were changed to get different results.

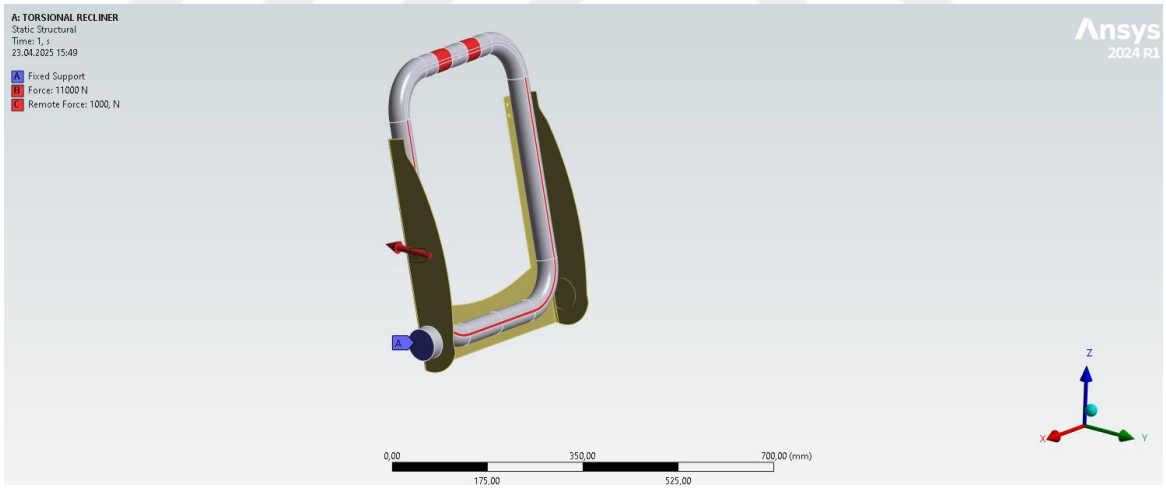

Figure 26 - Torsional recliner boundary conditions

3.4 Load Conditions

In this study, the loading scenarios were defined based on internationally recognized test standards such as FMVSS 207, FMVSS 301, and ECE R-17, along with the 26 high severity real-world crash data-based study by Edwards et al. [18]. These criteria have different uses and force magnitudes and application sites differ as well. Thus, the loading

strategy in this work was made to include these variations while ensuring structural realism.

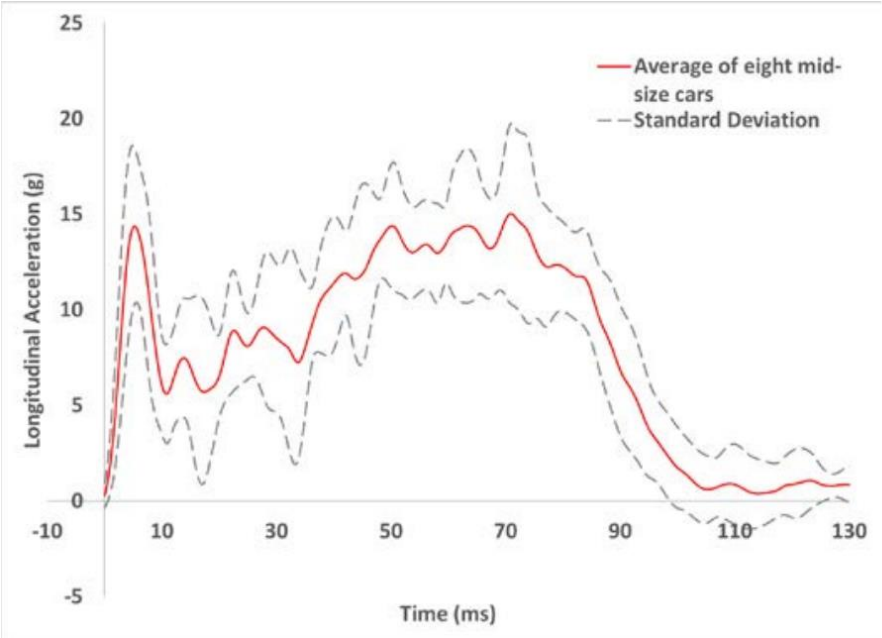

Figure 27 – Longitudinal acceleration averaged from 8 midsize cars in the FMVSS 301R test used to obtain the sled pulse [18]

While the FMVSS 301 criterion mostly evaluates fuel system integrity during rear-end collisions, the rear impact scenario it uses also offers understanding of the dynamic performance of seats under crash load. The vehicle accelerates roughly 15g when a 1,361 kg deformable barrier strikes it at 80km/h. The force the human back applies to the seatback during impact can be calculated using this acceleration.

In this context, based on the study by Edwards et al. [18], the force applied to the seatback for a 75 kg occupant under 15g peak acceleration was calculated as:

$$F = m \times a$$

$$= 75kg \times \left(15 \times \frac{9.81m}{s^2}\right) = 11000\ N$$

Within the scope of this study, this force was applied to the seatback as a distributed force. In this way, the realistic crash condition emphasised by FMVSS 301 and the loading approach described by FMVSS 207 were combined, making sure that the structure was loaded in balance.

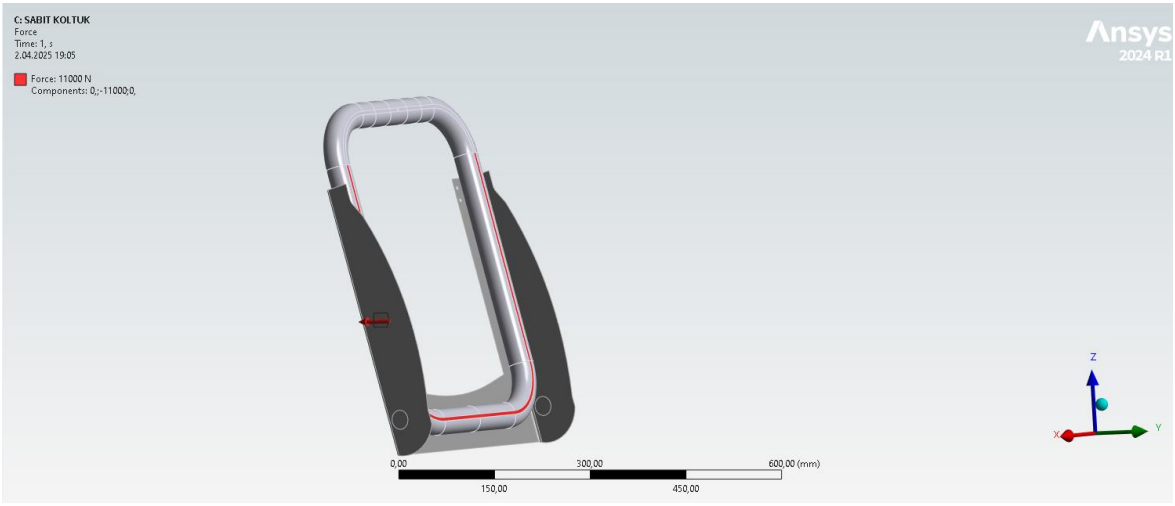

Figure 28 – The application of the load of occupant's torso

In order to get a better idea of the moment caused by the head moving forward and upward relative to the seatback during a rear impact, an extra 1,000 N of force was applied to the area where the headrest attaches. Assuming the average human head weighs about 4.5–5.0 kg, and considering a 15g acceleration:

$$F = m \,.\, a$$

$$= 5kg \times \left(15 \times \frac{9.81m}{s^2}\right) = 735\ N$$

This value was rounded to 1,000 N in this study to ensure a more conservative approach and to strengthen the moment transfer.

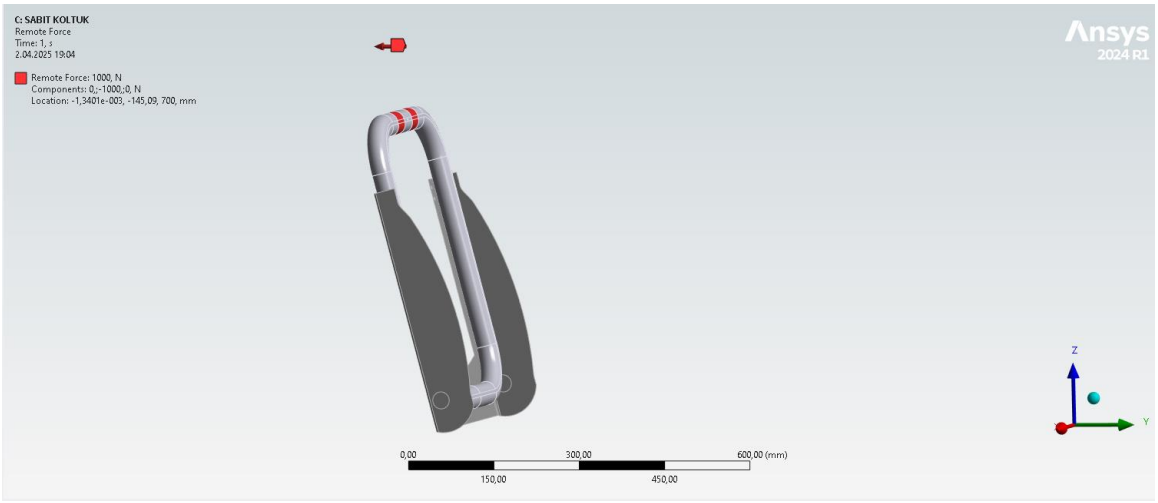

Figure 29 - The application of the occupant's head

The application point was defined at the headrest support structure, and since the force was applied at a distance from the seatback, it was modeled to create a rotational moment.

Because of this loading strategy, the force that the body mass exerts on the seatback and the head's movement relative to the seat could be simulated separately. This made it possible to get a full picture of how the seat structure works in a rear-end collision. Because of this, the load levels used in the simulations were set according to both standards and literature.

After the static structural analysis, during dynamic simulations phase, it has seen that the distribution of load needs to be divided over the seatback frame profile, to balance the moment of inertial effects. Based on the divided load distribution approach the body force applied to the seatback during rear impact was modified to better reflect biomechanical behavior.

At first, the inertial force from the person's upper body was modelled as a single load of 11,000 N acting on the seatback structure, a second remote force of 1,000 N was used to simulate the head, then it was decided that dividing the applied force along the vertical length of the seatback profile would make the simulation more realistic. Because the lower torso has less inertial load than the upper torso during rear impacts. This is because of how the body's mass and acceleration are distributed.

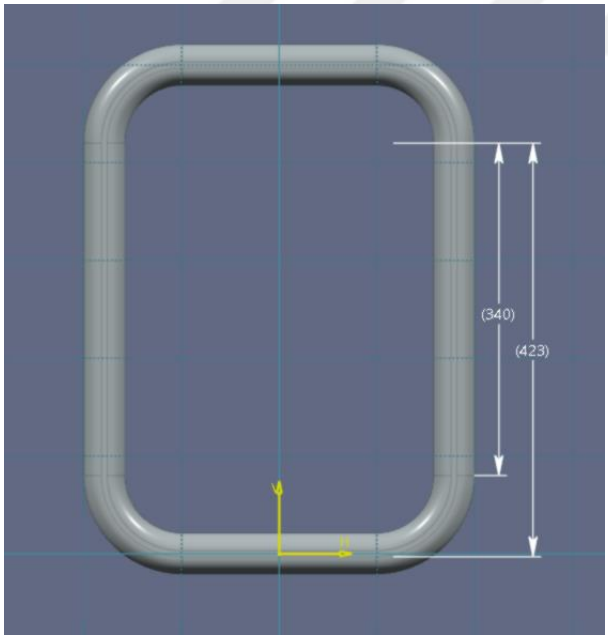

Figure 30 - Two body force calculation

So, the seatback's hollow tubular structure was geometrically split into two parts, one 340 mm long (the upper part) and the other 83 mm long (the lower part). Then, the total force of 11,000 N was split up among the segments based on their lengths.

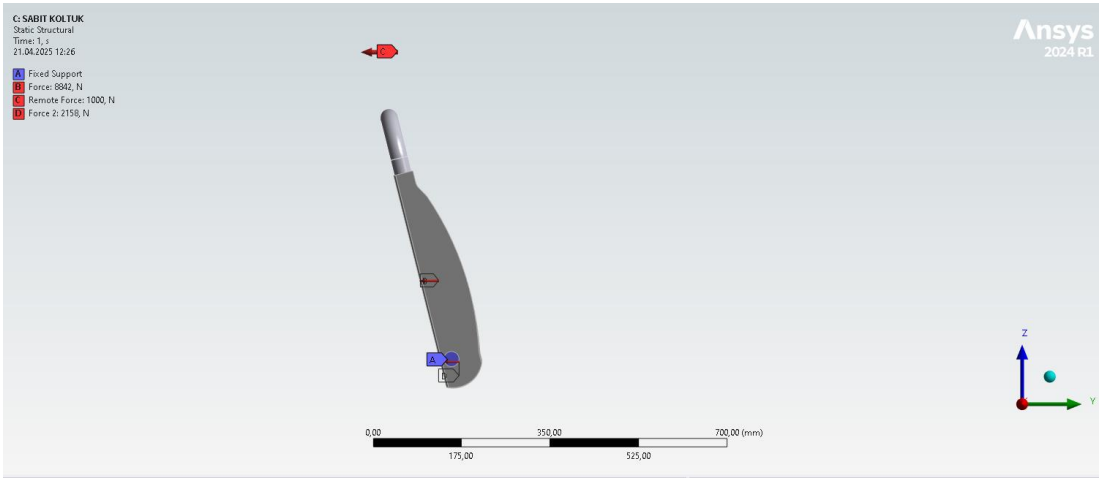

Figure 31 - The application of two body force to fixed seat

According to this segmentation:

- A force of 8,842 N was applied to the upper segment (annotated as B in the figure),
- A force of 2,158 N was applied to the lower segment (annotated as D in the figure),
- The head force (1,000 N) continued to be applied as a remote load at the headrest connection region (annotated as C).
- The fixed support annoted as A in the figure.

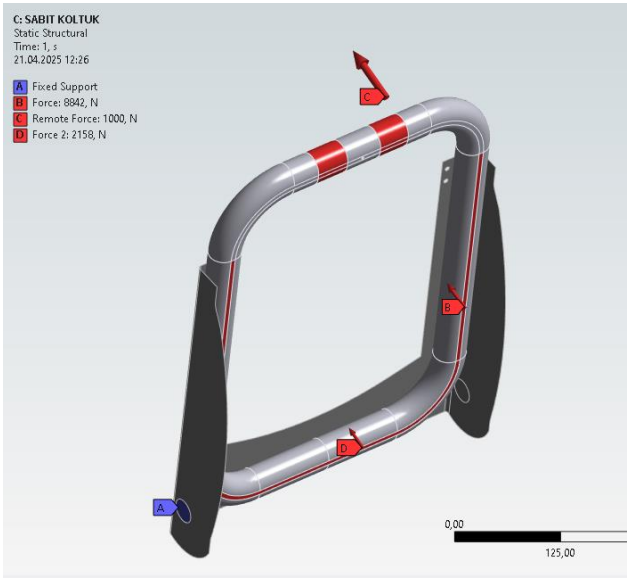

Figure 32 - Distribution of the loads

By adding another force on the part of the upper torso region, this load distribution strategy better showed how the body reacts to rear impacts.

3.5 Meshing

The meshing method used in this thesis was to let the ANSYS software make the mesh automatically, and then it was checked for quality to make sure it was suitable for analysis. The automatically generated mesh was checked and found to be acceptable in terms of quality in Figure 33 and element distribution, as shown in Figure 34.

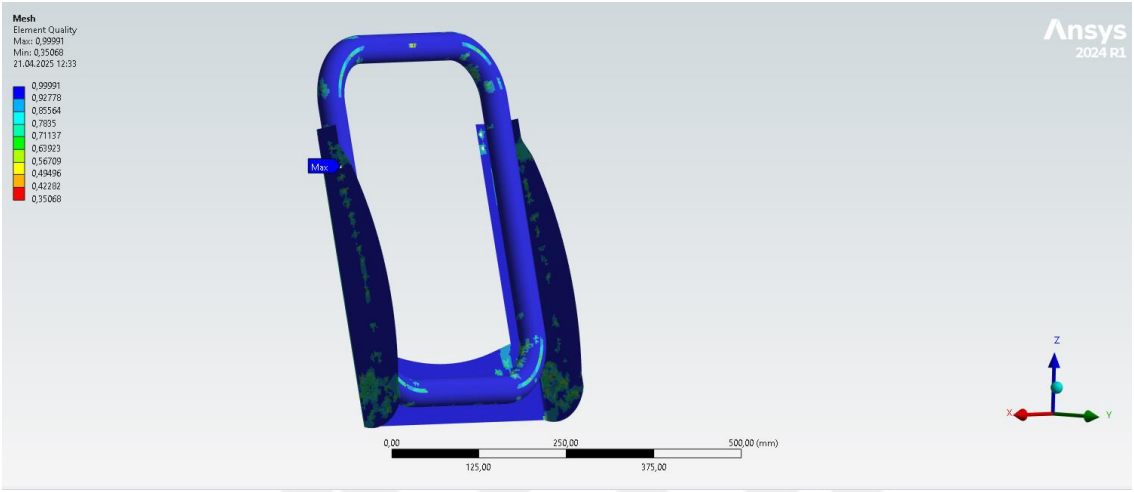

Figure 33 - Overall mesh quality

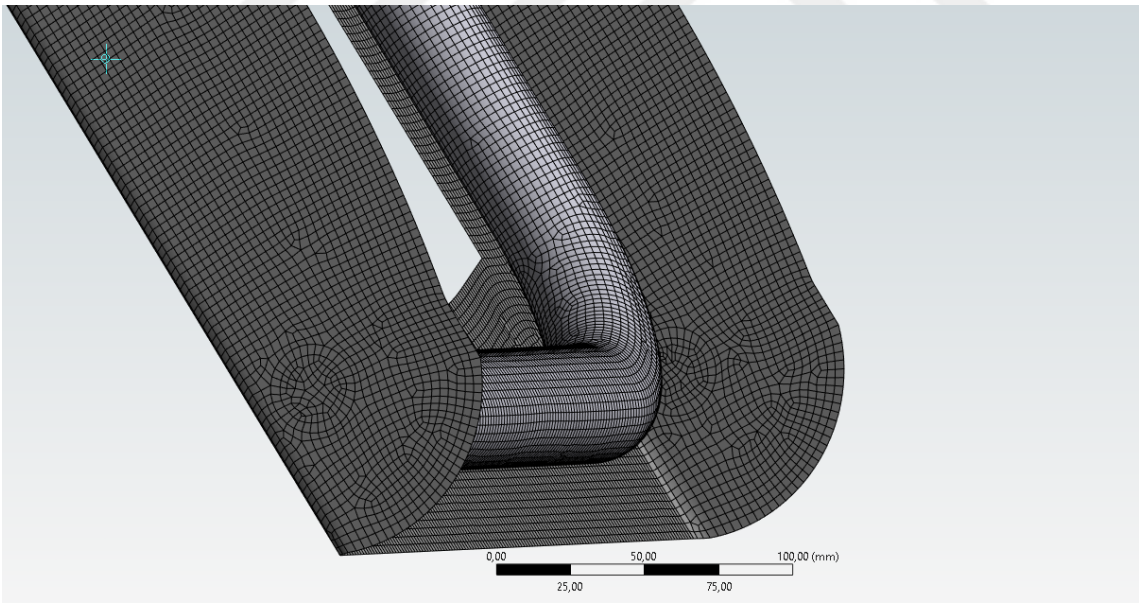

Figure 34 - Fixed support mesh area

Because sheet metal parts have very low thickness values, a full 3D analysis would need an extremely fine mesh, which would take a lot longer to compute. Because of this, the shape of the model was perfect for a 2D analysis method. In this case, the midsurface tool

was used to extract the midsurface, and the next steps were carried out as 2D shell elements.

Figure 35 - Meshed model for 2D analysis

The parameters for sheet thickness were changed directly in the software settings to get good results and evaluate them. The bending recliner model in Figure 36, which was also made as a 2D structure, was made in the same way.

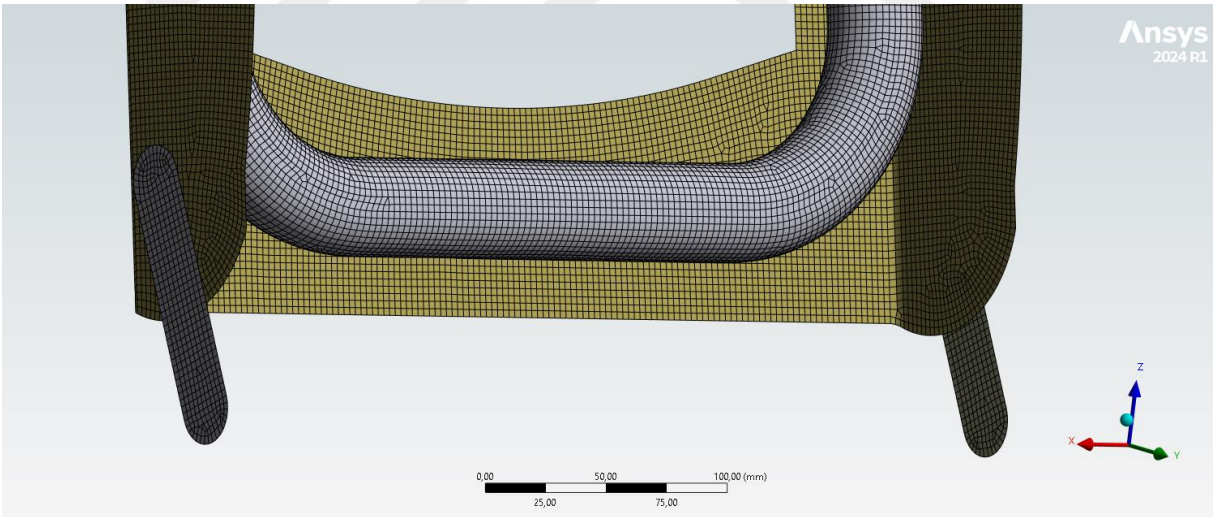

Figure 36 - 2D bending recliner mesh details

On the other hand, a 3D modeled bar was used for the torsional recliner model. By changing the bar's diameter and length, this made it possible to directly change the mesh density.

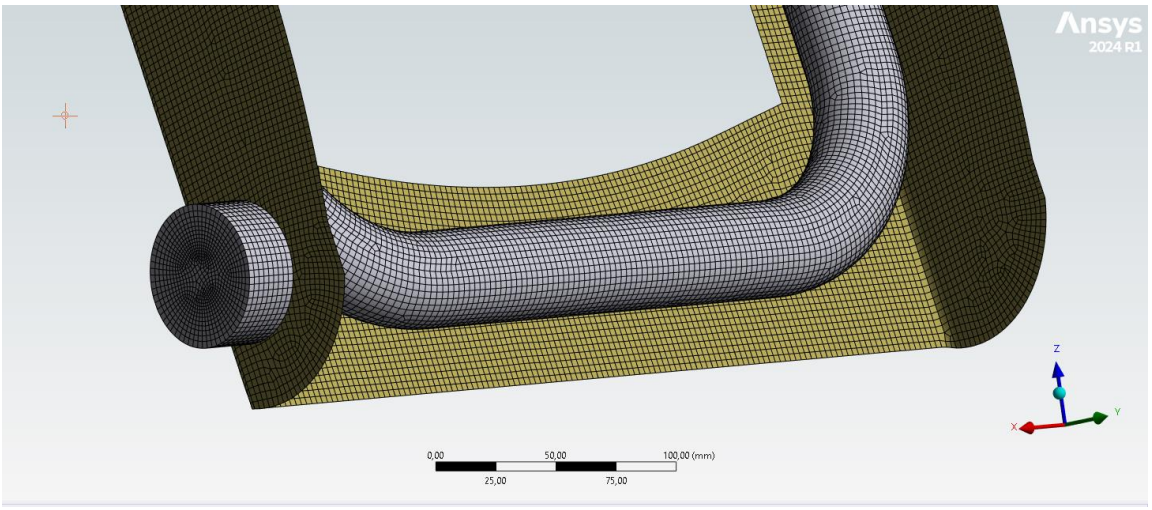

Figure 37 - Mesh details of torsional recliner

This made it possible to precisely manage mesh elements and improve the efficiency of the computations.

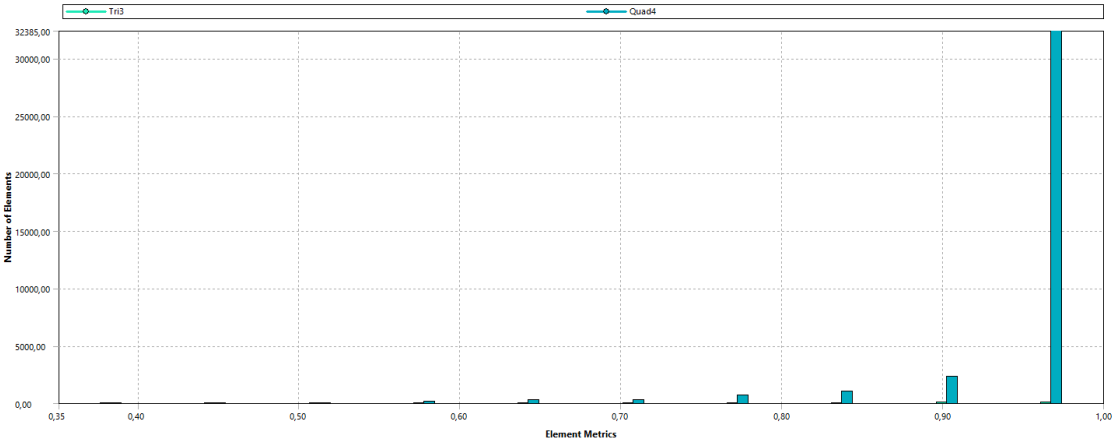

Figure 38 - Mesh quality

Average element quality is shown above as 0.967, which is enough to get correct results.

4. RESULTS AND DISCUSSION

4.1 Fixed Seatback Analysis Results

4.1.1 Fixed Seatback with Ø 80 mm Fix Area Analysis Results

The first analyses results were from fixed seatback with 80 mm diameter fixed support are as boundary condition, seatback sheet having 2 mm thickness, hollow frame having 1 mm thickness. In case of S355 steel material useage, plastic and elastic deformation were expected.

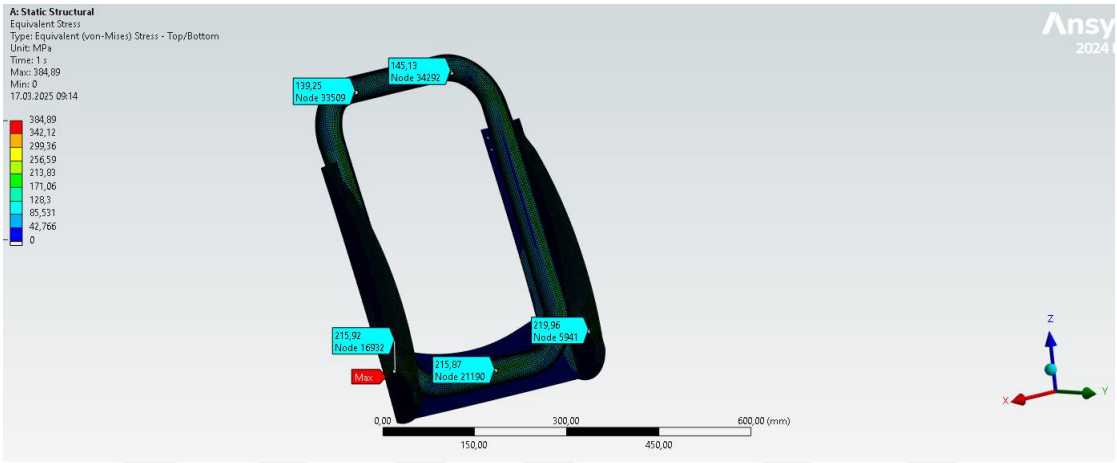

Figure 39 - Fixed seatback with Ø 80 mm fix area stress result

The total deformation value obtained as 2.95 mm, which is allowable due to the standards, but plastic deformation expected.

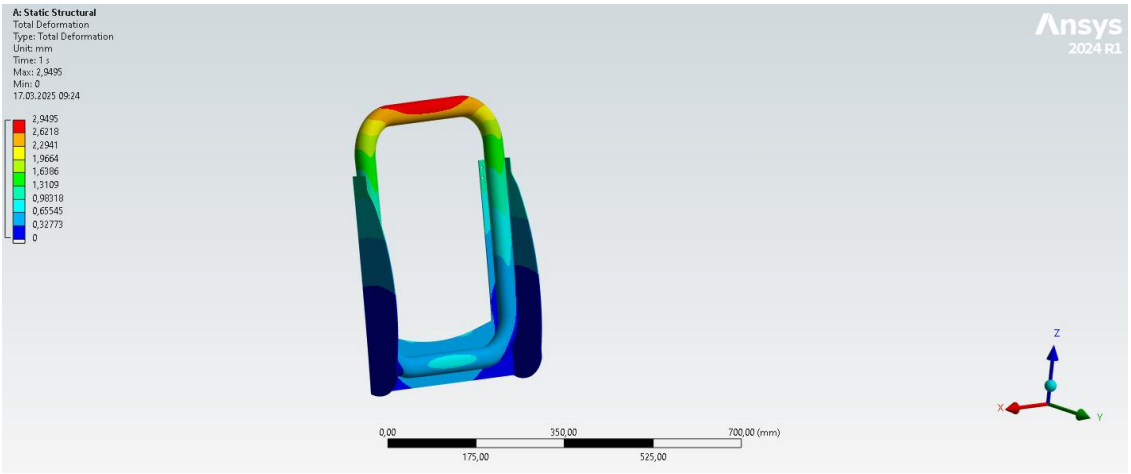

Figure 40 - Fixed seatback with Ø 80 mm fix area deformation result

After these results, fix area is lowered to compare the fixed seat analyses with recliner-equipped versions.

4.1.2. Fixed Seatback with Ø30 mm Fix Area Analysis Results

Fixed seatback with 30 mm diameter fixed support are as boundary condition, seatback sheet having 2 mm thickness, hollow frame having 1 mm thickness have been analyzed.

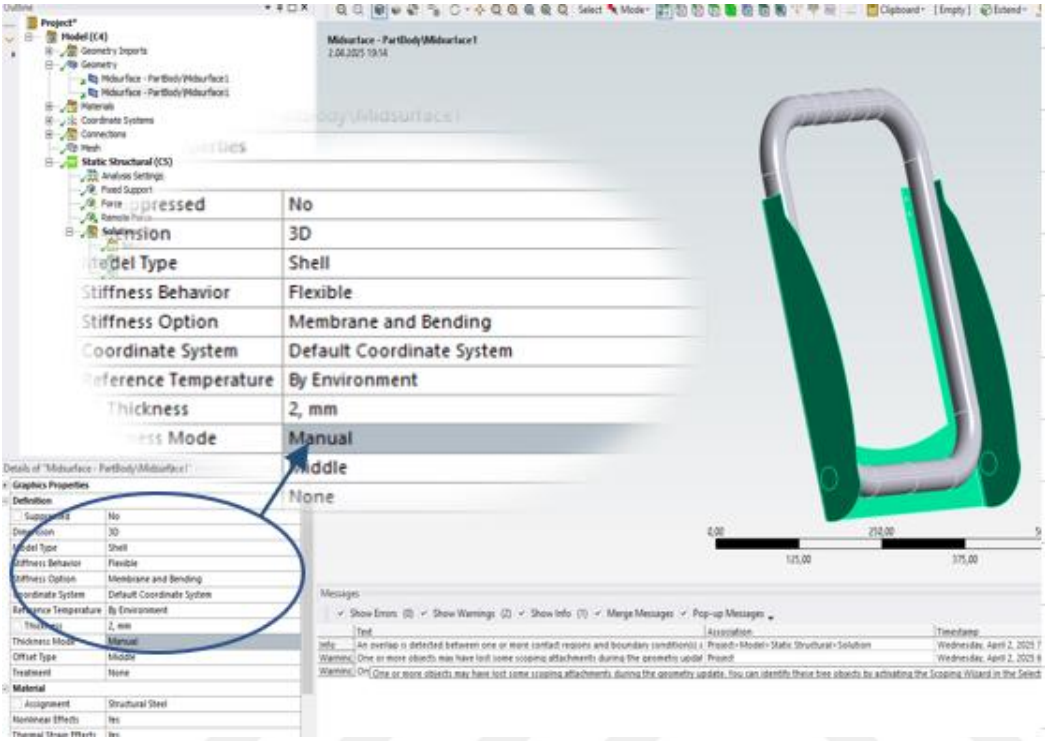

Figure 41 - 2 mm sheet thickness adjustment

After reducing the connection diameter from 80 to 30 mm, the analysis was repeated without altering the contacts between other components. When analyzed with a sheet thickness of 2 mm, stresses very close to the UTS limit were observed.

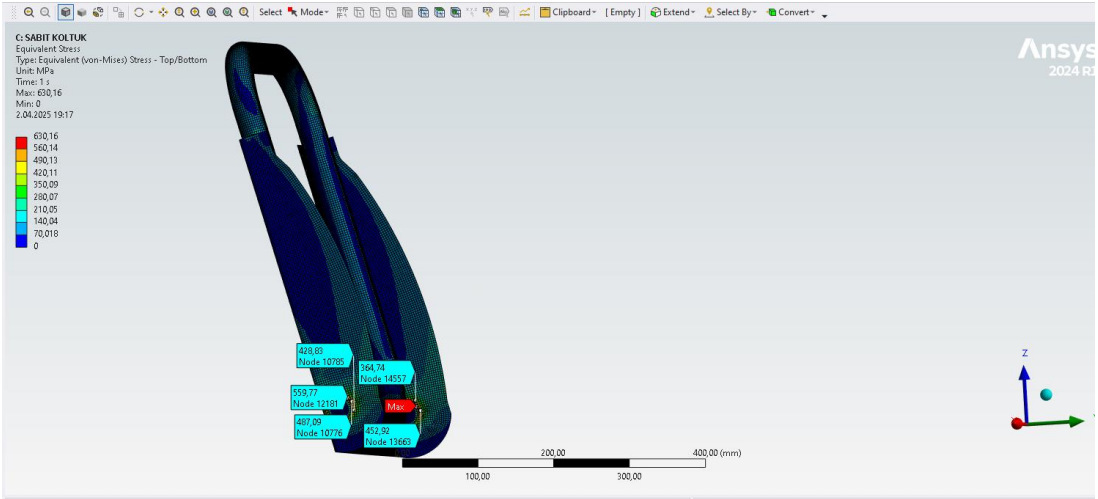

Figure 42 - Fixed seatback with Ø30 mm fix area stress results

The total deformation was increased as well.

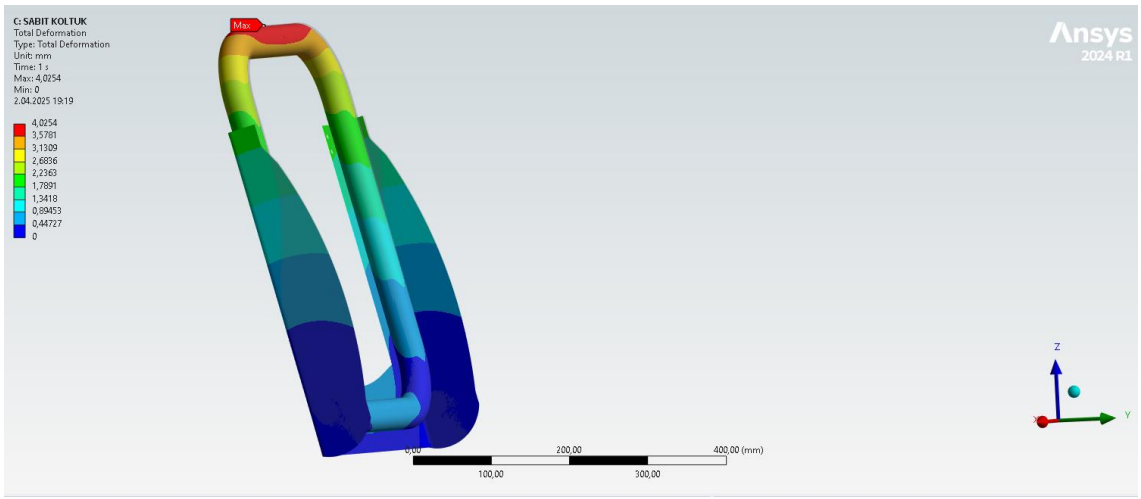

Figure 43 - Fixed seatback with Ø30 mm fix area deformation results

Since the obtained results indicated that the seatback exceeded the yield strength limits for S355 steel, even when joints causing stress concentrations were avoided, the analyses were repeated with the sheet thickness increased to 3 mm.

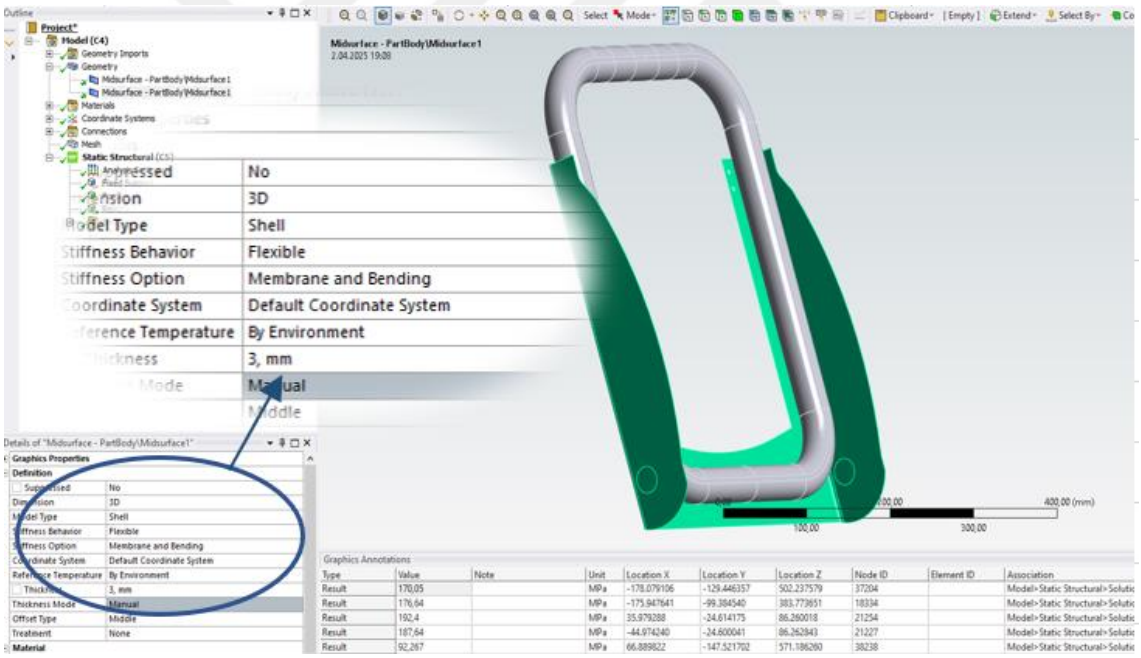

Figure 44 - 3 mm sheet thickness adjustment

In all analyses, the hollow profile thickness was kept constant at 1 mm as below.

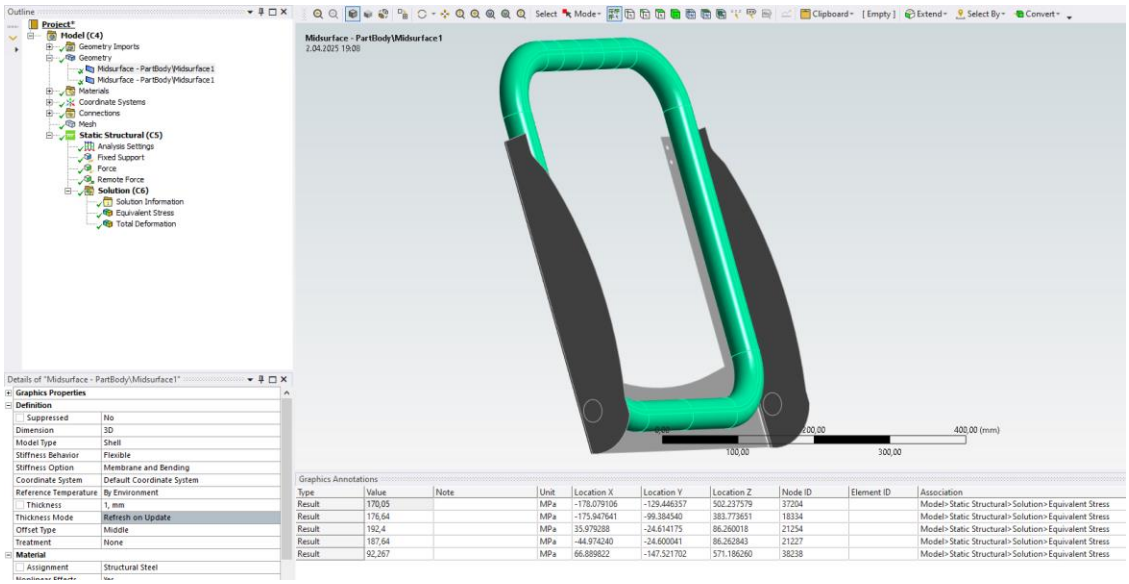

Figure 45 - Hollow frame profile thickness adjustment

In this case, the obtained results indicate that the seat will not undergo plastic deformation under the applied load. The Figure 46 below shows the maximum stress value as 385 MPa, however this maximum point was a singular point, around that point the values were below 355 MPa, which means no yielding.

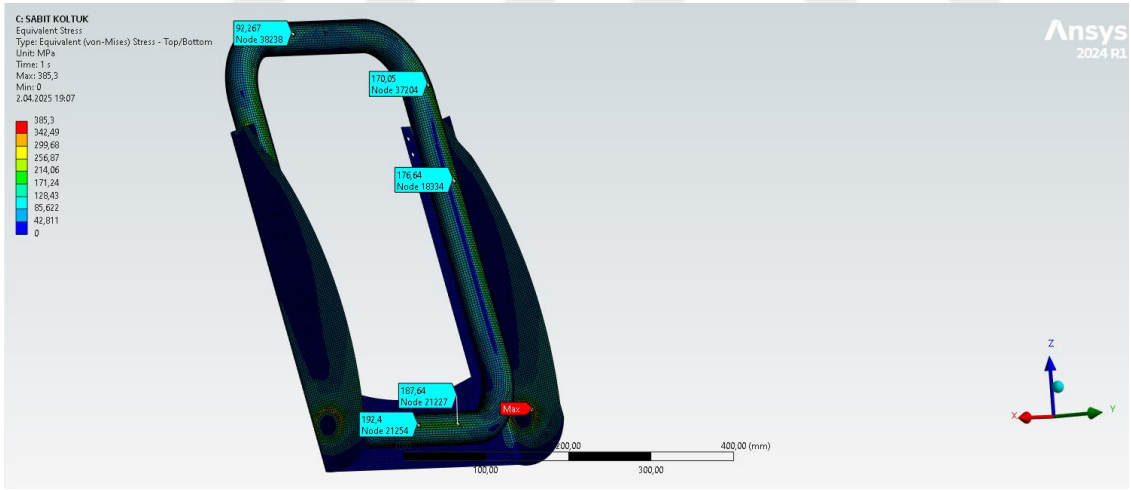

Figure 46 - 3 mm sheet stress results

The total deformation is decreased to 2.8 mm shown in Figure 47.

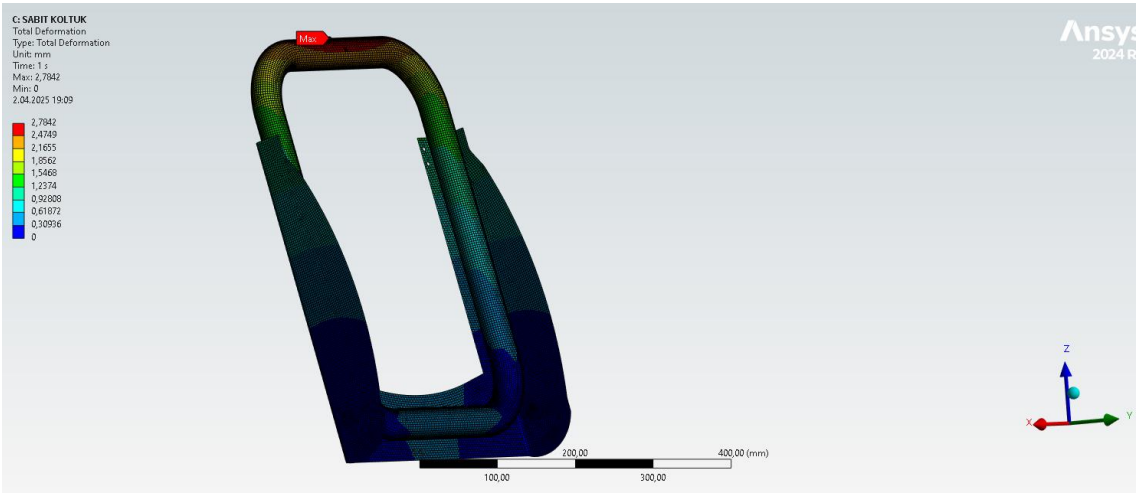

Figure 47 - 3 mm sheet deformation results

4.1.3. Fixed Seatback with Ø 30 mm Fix Area and Two Body Force Analysis Results

In the updated loading condition, considering that the upper torso experiences higher accelerations in a rear-end crash compared to lower body, splitting the load proportionaly changed the stress concentration patterns and deformation.

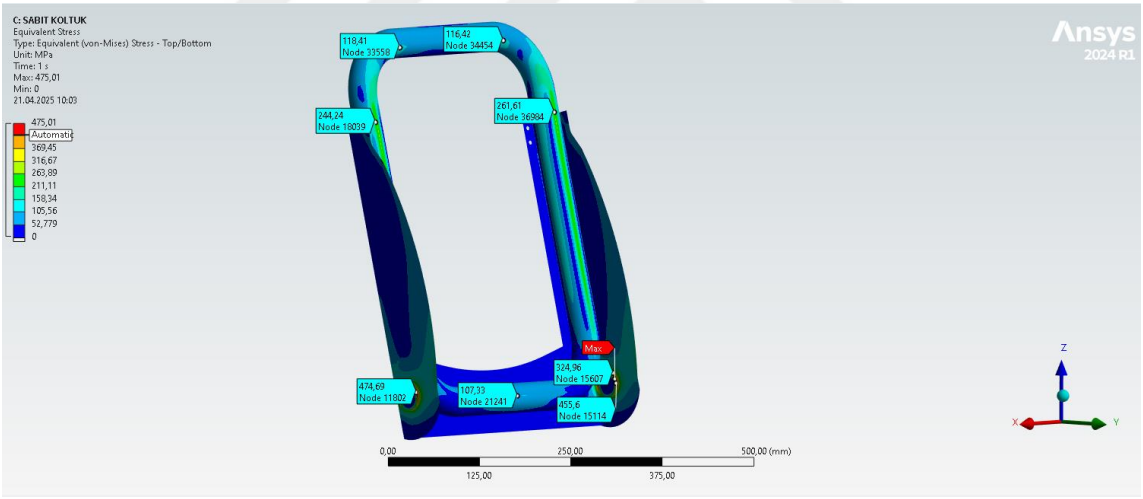

Figure 48 - Fixed seatback with Ø 30 mm fix area and two body force stress results

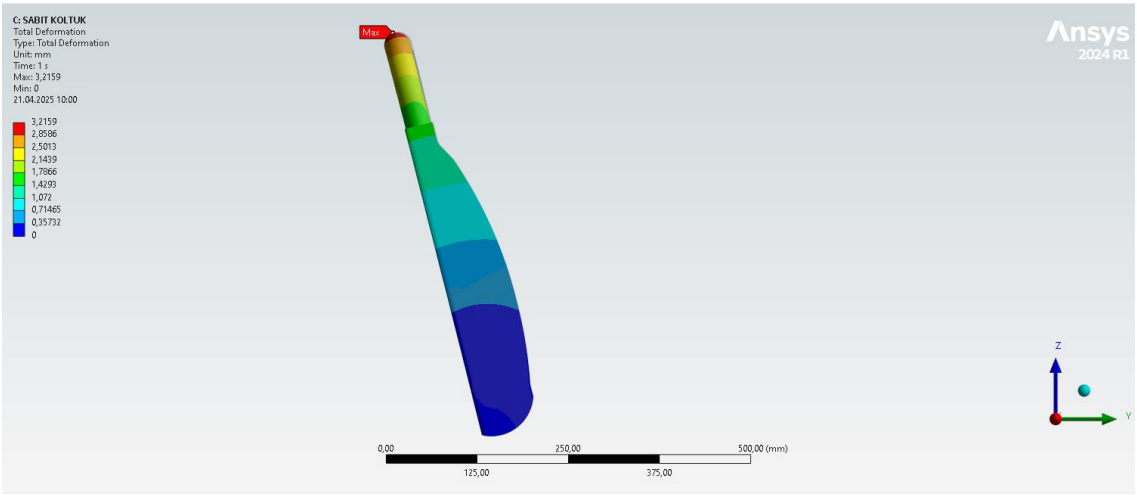

Figure 49 - Fixed seatback with Ø 30 mm fix area and two body force deformation results

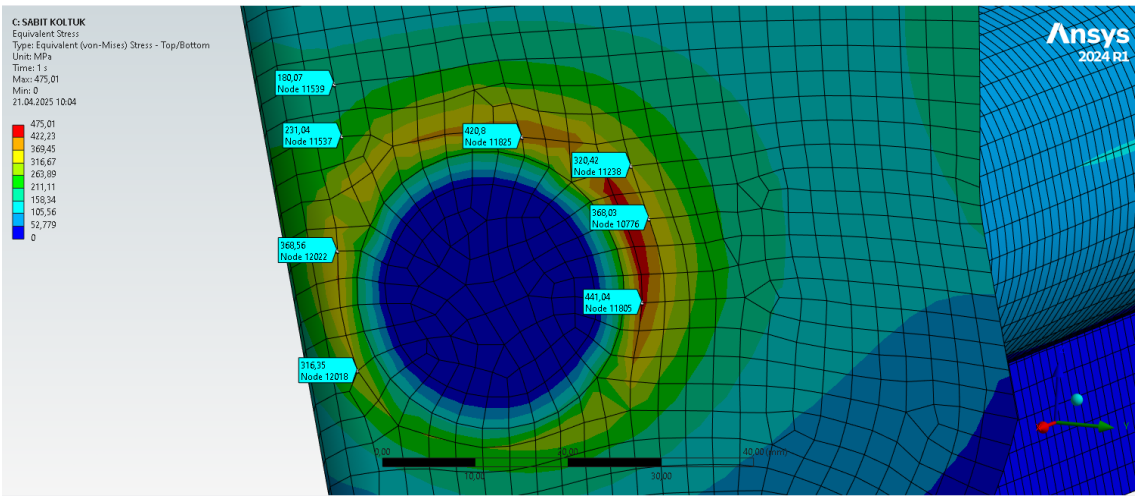

Figure 50 - Average value calculation nodes

Due to singular points obtained in joint regions, 475 MPa value is not a reliable value. Since average value need to be calculated to determine real maximum stress levels, the calculations below have been made.

$$\sigma = \frac{420.8+320.4+368+441}{4} = 387\ MPa$$

4.2 Seatback with Bending Recliner Analysis Results

The same loads applied to the fixed seat model were also applied to the bending recliner-equipped model with a 2 mm thick seatback sheet. In the initial setup, the seatback was made of 2 mm thick sheet metal, and a 20 mm thick aluminum alloy rod was assigned as the bending-type recliner.

Graphics Properties	
Definition	
Suppressed	No
Dimension	3D
Model Type	Shell
Stiffness Behavior	Flexible
Stiffness Option	Membrane and Bending
Coordinate System	Default Coordinate System
Reference Temperature	By Environment
Thickness	20, mm
Thickness Mode	Manual
Offset Type	Middle
Treatment	None
Material	
Assignment	Aluminum Alloy
Nonlinear Effects	Yes
Thermal Strain Effects	Yes
Bounding Box	

Figure 51 - Aluminum alloy application

The results were obtained Figure 52 below.

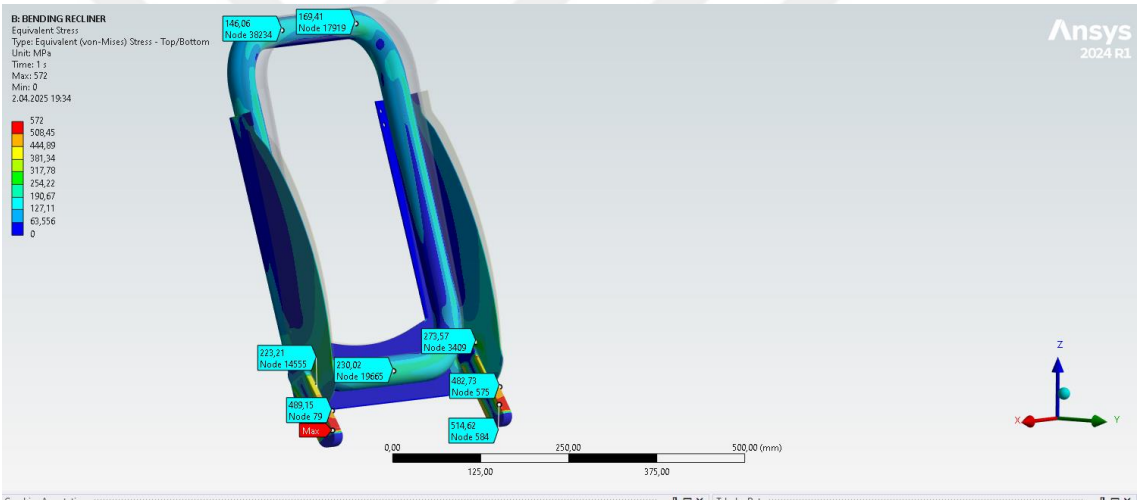

Figure 52 - Aluminum sheet analysis equivalent stress result

The maximum stress value was 572 Mpa, and the intensity was on the bending recliner body, which means the recliner yields first as desired. However, these values were extremely high on standard aluminum alloy recliner bar. It could have resulted in the failure of the aluminum bar.

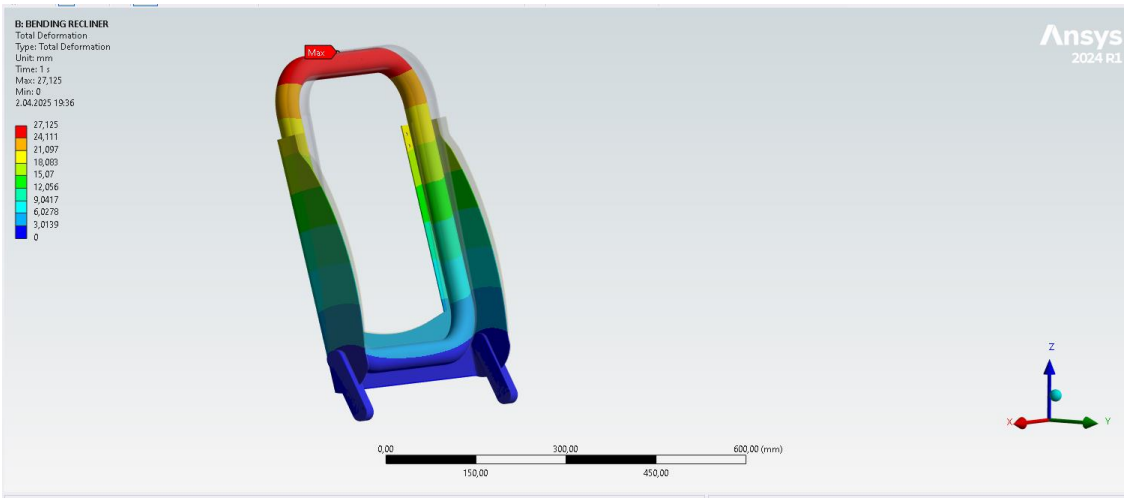

Figure 53 - Aluminum sheet deformation result

Total deformation value was determined to be 27.12 mm in Figure 53.

Since this deformation was considered very high, the same configuration was tested using a 30 mm diameter recliner. It was observed that the stress values decreased from around 500 MPa to approximately 360 MPa shown below.

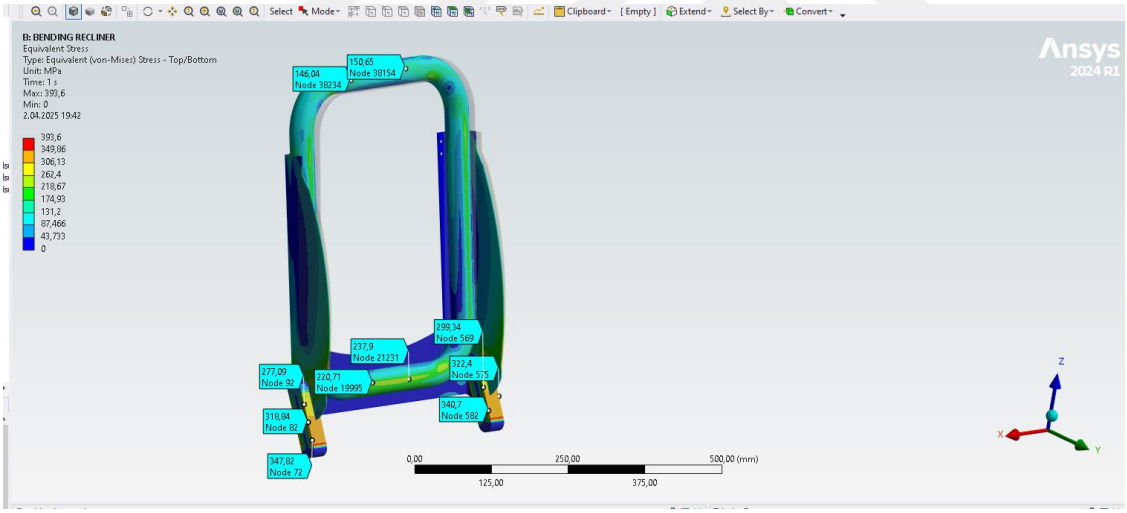

Figure 54 - 30 mm recliner thickness analysis stress result

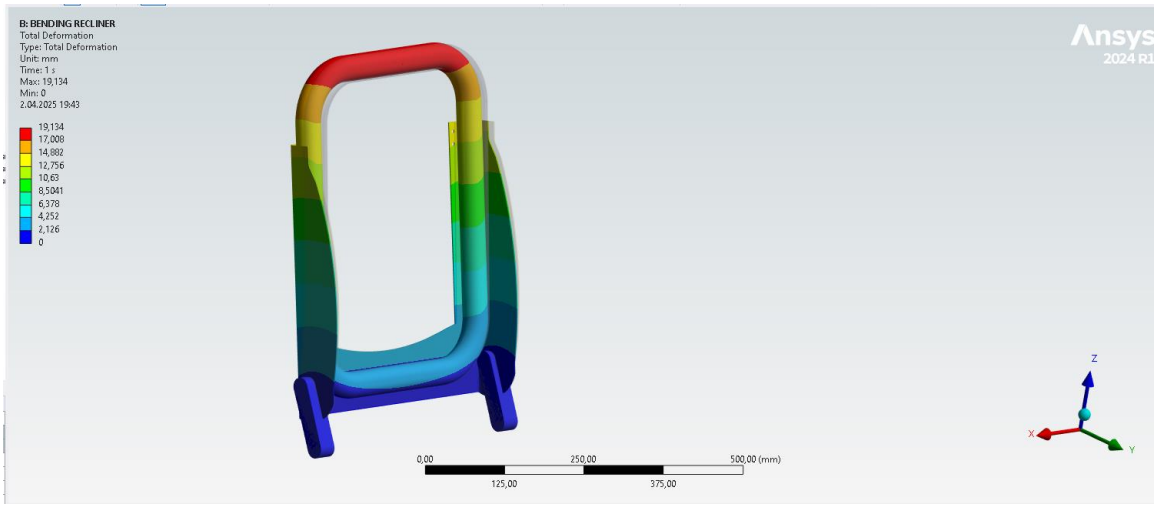

Figure 55 - 30 mm recliner thickness analysis deformation result

The total deformation was reduced from 27 mm to approximately 19 mm.

After this, when the seatback sheet thickness was increased to 3 mm while keeping the recliner bar diameter constant at 30 mm, the analysis showed that the total deformation was reduced to around 18.3 mm.

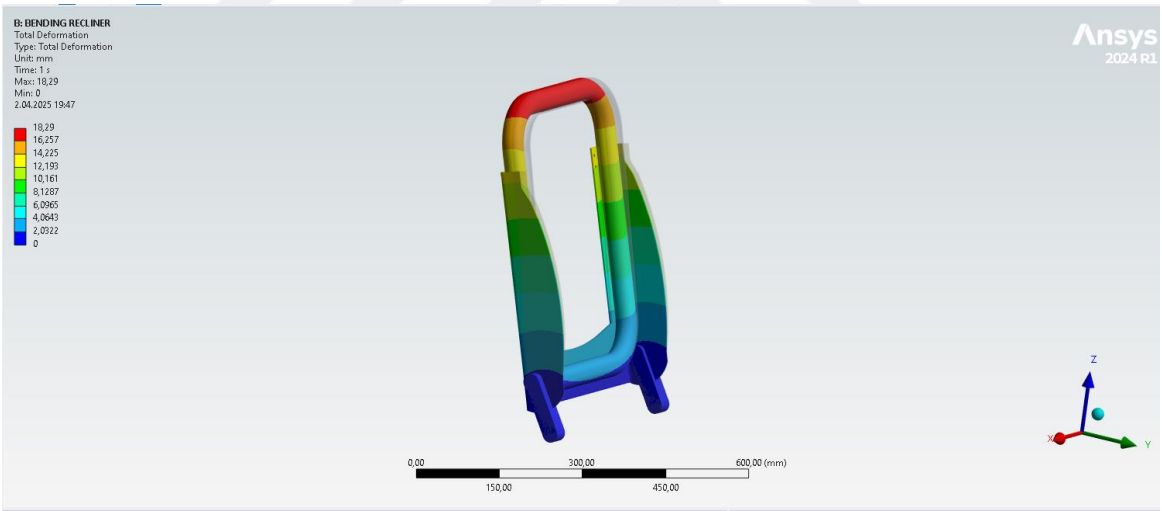

Figure 56 – 3 mm sheet thickness aluminum recliner total deformation result

However, this adjustment did not result in a significant improvement in stress distribution shown below Figure 57, maximum stress value reduced only 17 Mpa. In both conditions yielding would occur.

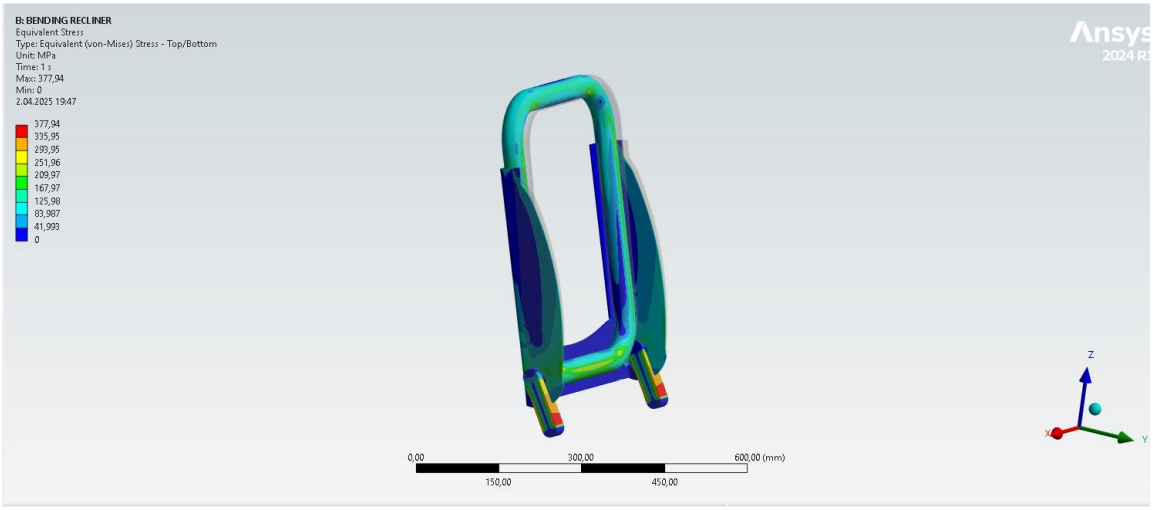

Figure 57 - 3 mm sheet thickness aluminum recliner equivalent stress result

Since it was necessary to reduce the total deformation, the recliner material was changed back to steel again and the analysis was repeated. However, as previous sheet thickness change did not create a significant improvement, the seatback sheet thickness was reduced back to 2 mm in order to avoid increasing the total mass.

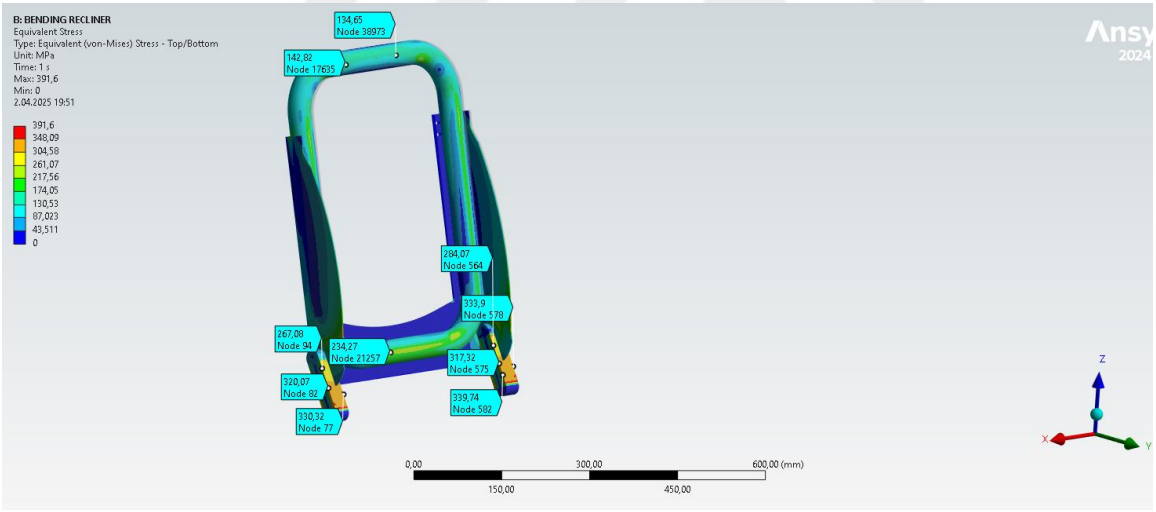

Figure 58 – 2 mm sheet thickness steel recliner 30 mm recliner bar stress result

Eventhough the maximum value shown 391 Mpa in figure, stress values intensely observed on the 30 mm steel recliner was approximately 340 MPa.

With this configuration, the total deformation was reduced from 19 mm to 9.3 mm.

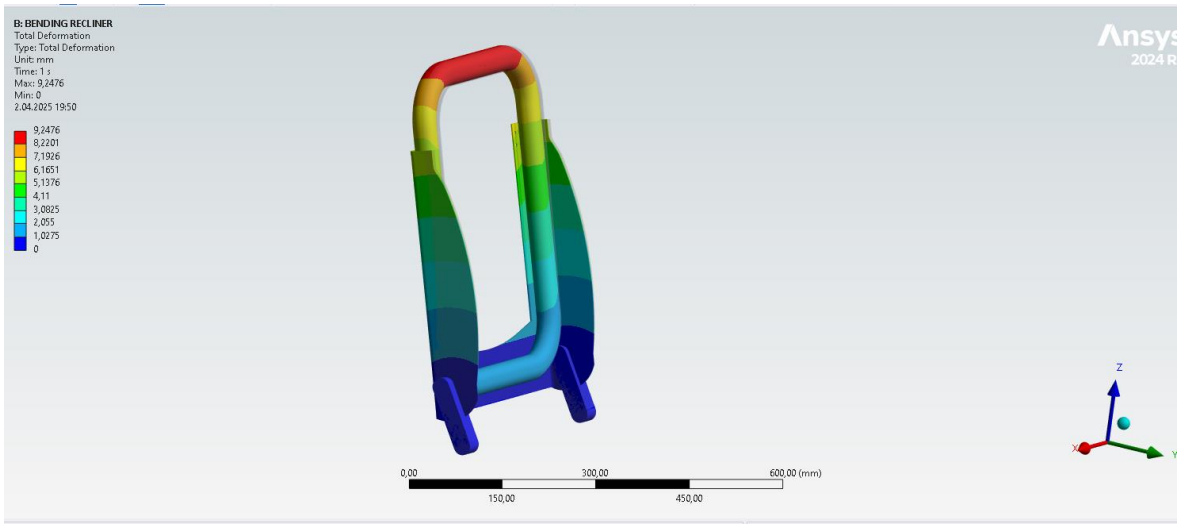

Figure 59 - 2 mm sheet thickness steel recliner 30 mm recliner bar deformation result

When the seatback sheet thickness was kept at 2 mm and the recliner thickness was reduced to 20 mm, it was observed that the stress on the steel recliner increased.

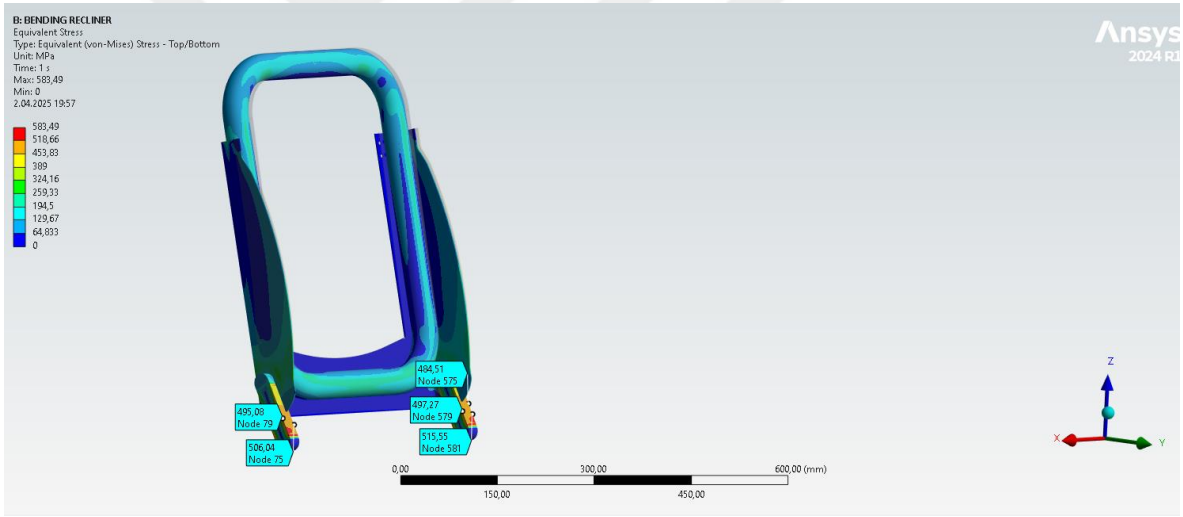

Figure 60 - 2 mm sheet thickness steel recliner 20 mm recliner bar stress result

However, the total deformation decreased significantly, from approximately 27 mm to around 12 mm, in case of using steel seatback sheet instead of aluminum.

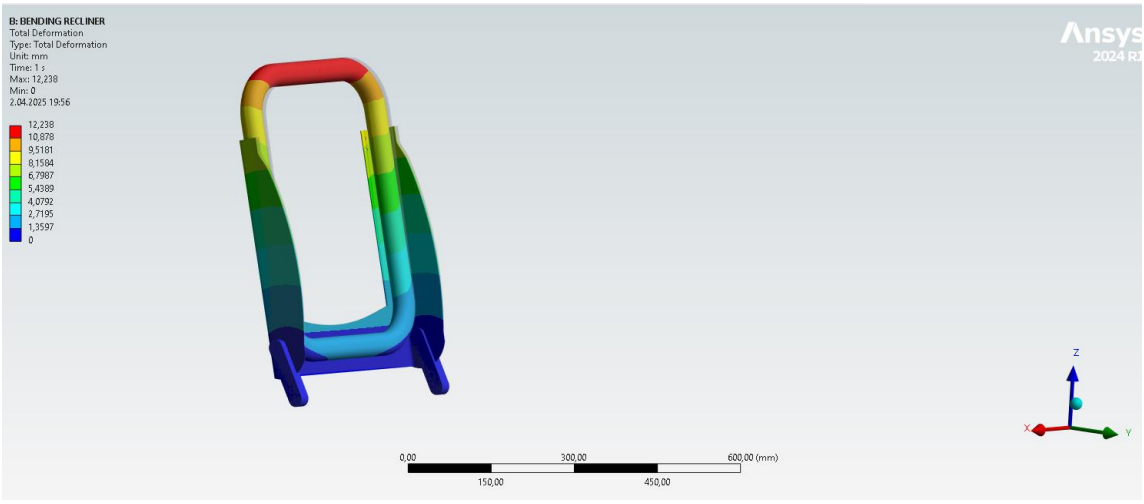

Figure 61 - 2 mm sheet thickness steel recliner 20 mm recliner bar deformation result

As in the seatback structure, if S355 structural steel is also to be used for the recliner, the stress levels observed on the 30 mm recliner approached the yield strength of the material. This resulted in insufficient plastic deformation, which was originally intended for the recliner component. Therefore, the recliner thickness was updated to 25 mm, and the same steel material was assigned. The aim was to maintain the resulting stress values above 355 MPa but below 630 MPa.

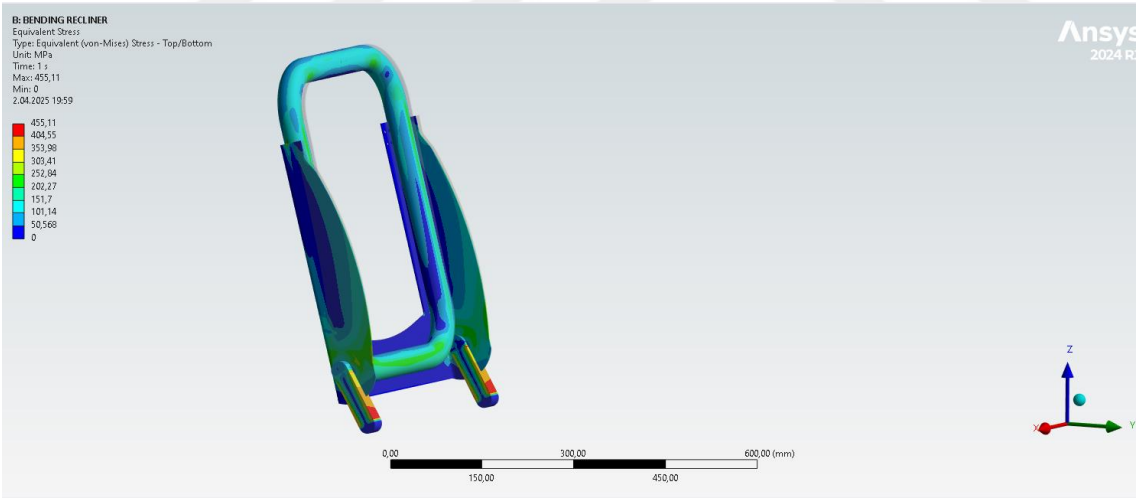

Figure 62 - 2 mm sheet thickness steel recliner 25 mm recliner bar stress result

In this case, the resulting stress value between 400-450 MPa was considered acceptable.

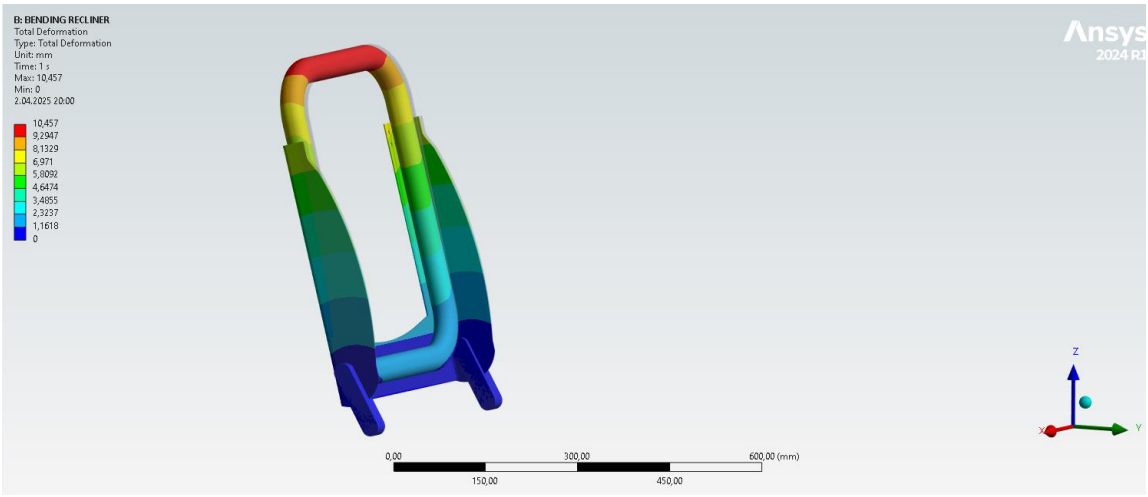

Figure 63 - 2 mm sheet thickness steel recliner 25 mm recliner bar deformation result

The total deformation was determined as 10.5 mm.

4.3 Seatback with Torsional Recliner Analysis Results

Since the 30 mm thick steel bending recliner used in the previous section was measured to have a mass of approximately 850 grams, the torsional recliner model was also modeled as a solid cylinder with the same mass and attached to the seatback from the same surface (30mm diameter). However, the analysis results showed stress levels exceeding 900 MPa on the seatback sheet, indicating a risk of structural failure.

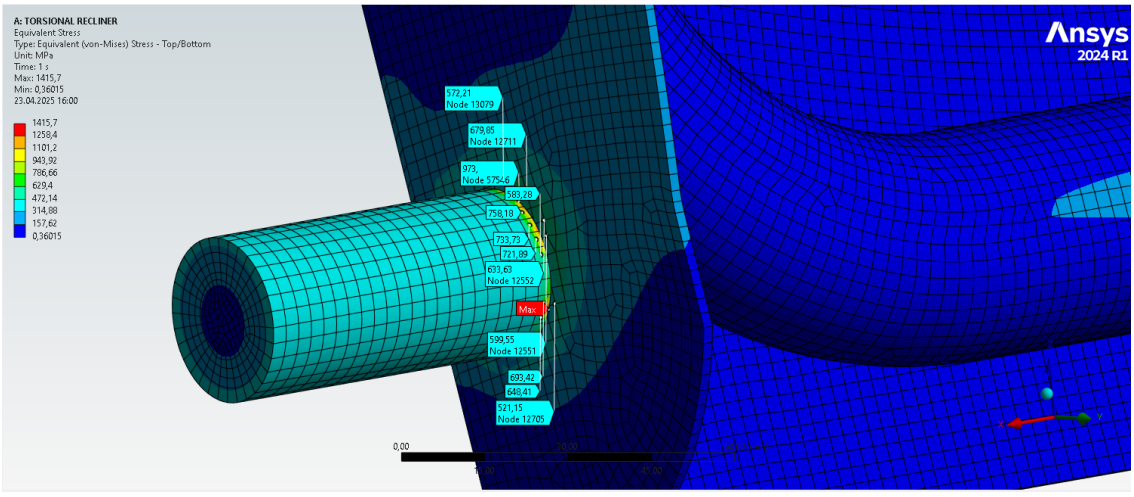

Figure 64 - Stress values of 26 mm length torsional recliner nodes

When the mass was kept constant but the diameter of the torsional recliner was doubled (60mm) length became 26 mm, thereby increasing the surface area connected to the

seatback, the resulting stress values were reduced to maximum 300 Mpa that would not cause seatback failure.

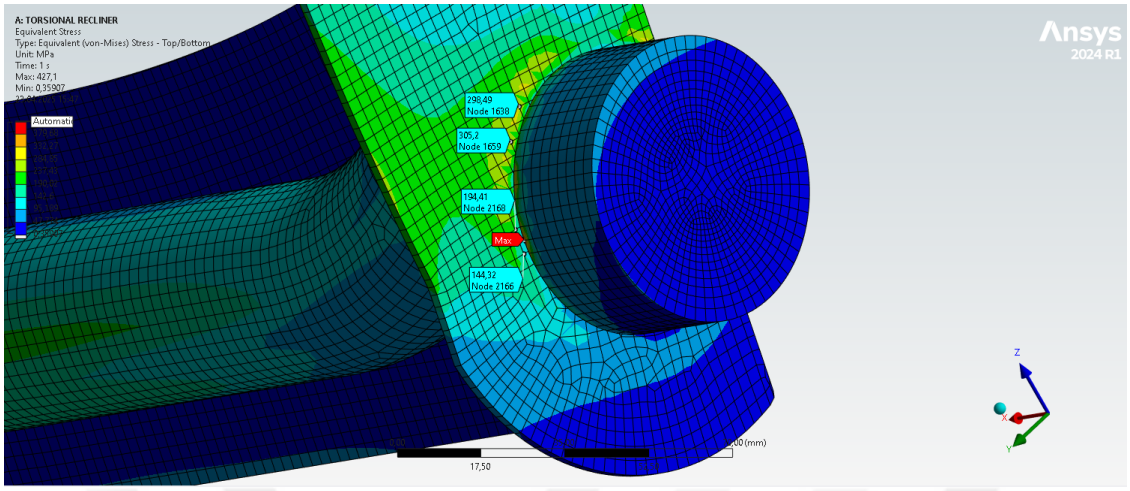

Figure 65 - Stress values of 60 mm diameter torsional recliner nodes

In the torsional recliner analysis, when the aim was to ensure that the stress would develop purely as torsion within the recliner, it was observed that higher stress occurred on the seatback sheet compared to the recliner. This output contradicts the primary objective of allowing plastic deformation in the recliner while keeping the seatback in elastic limits. Although total deformation values around 3.2 mm were recorded, this level of deformation would be no different than rigidly fixing the seatback through a wide surface area, failing to provide the desired localized energy absorption.

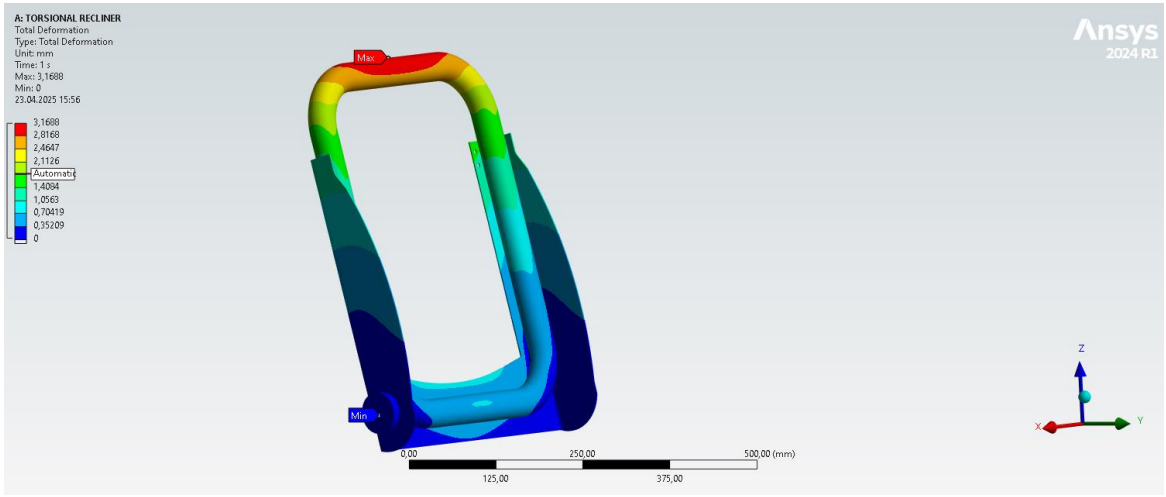

Figure 66 – Deformation values of 12 mm length torsional recliner

Then the length of the torsional recliner was reduced by half (12 mm) without changing its diameter, the total deformation decreased to 3.16, also the stress on the seatback was slightly decreased to 280 MPa same region.

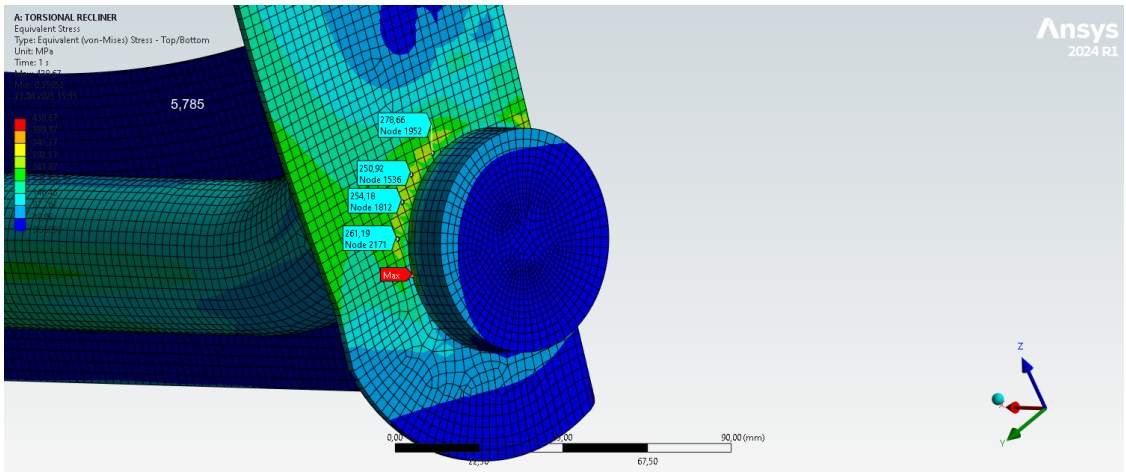

Figure 67 - Stress values of 12 mm length torsional recliner nodes

This indicates that shortening the recliner does not significantly improve its ability to localize deformation or reduce structural loads on the seatback.

4.3.1 Torsional Recliner with Ø 60 mm Diameter and Two Body Force Analysis Results

In the last analysis, a seatback with torsional recliner has 12 mm legth is analysed by two body force.

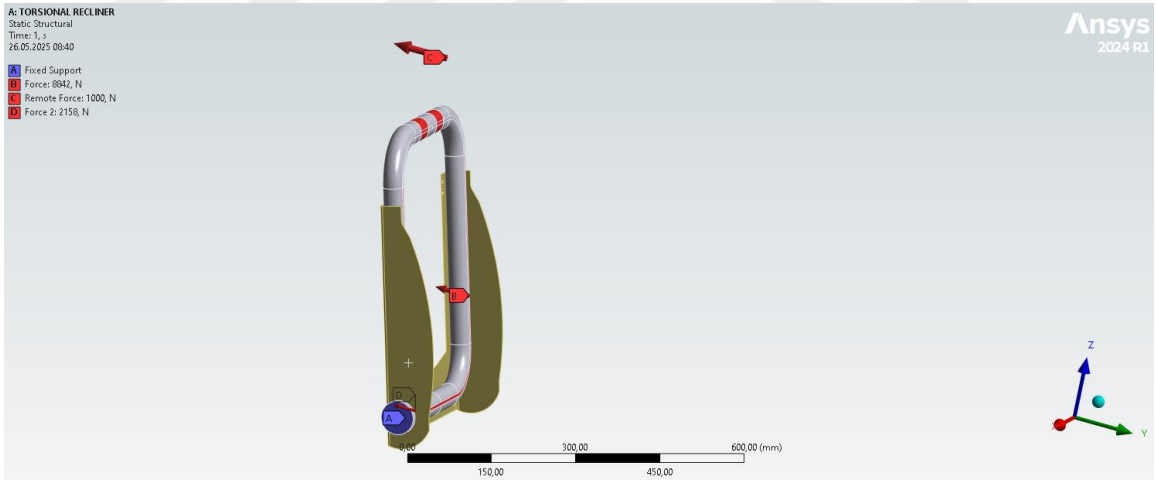

Figure 68 - The application of two body force to seat with torsional recliner

The total deformation is decreased to 2.8 mm, and the maximum stresses became around 240 Mpa after checking the singular points caused by 2D and 3D analysis model used together.

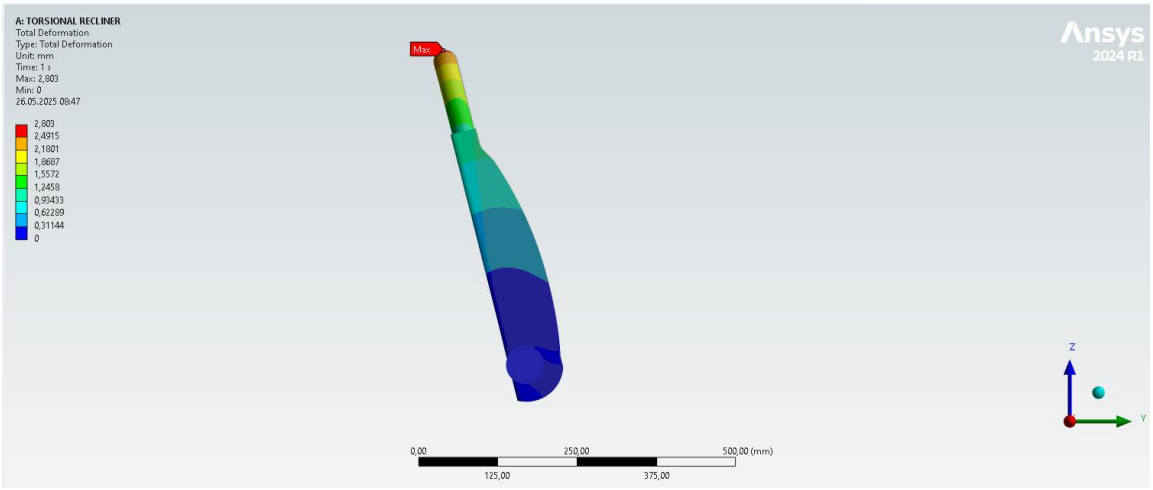

Figure 69 - The deformation results of two body force applied torsional recliner

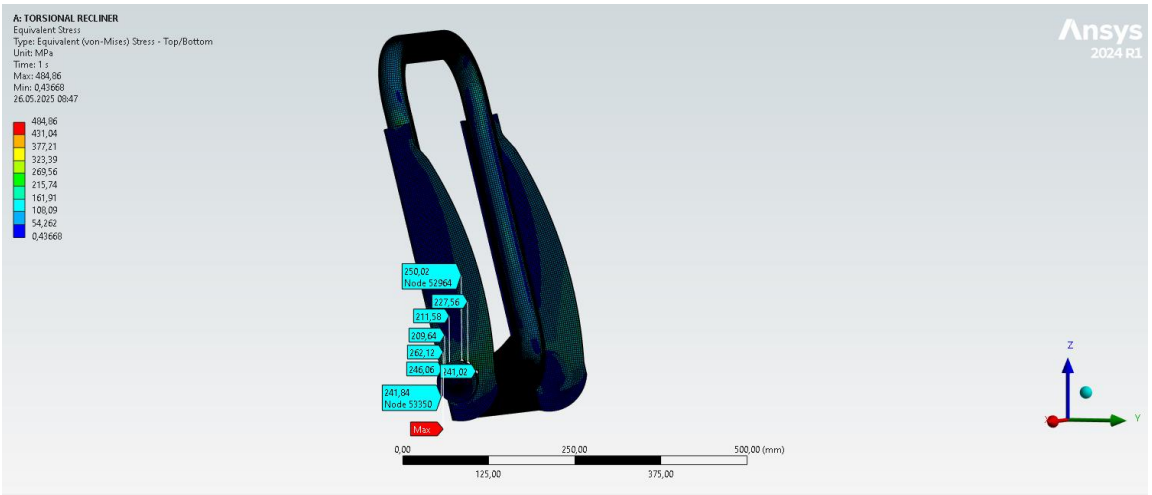

Figure 70 - The deformation results of two body force applied torsional recliner

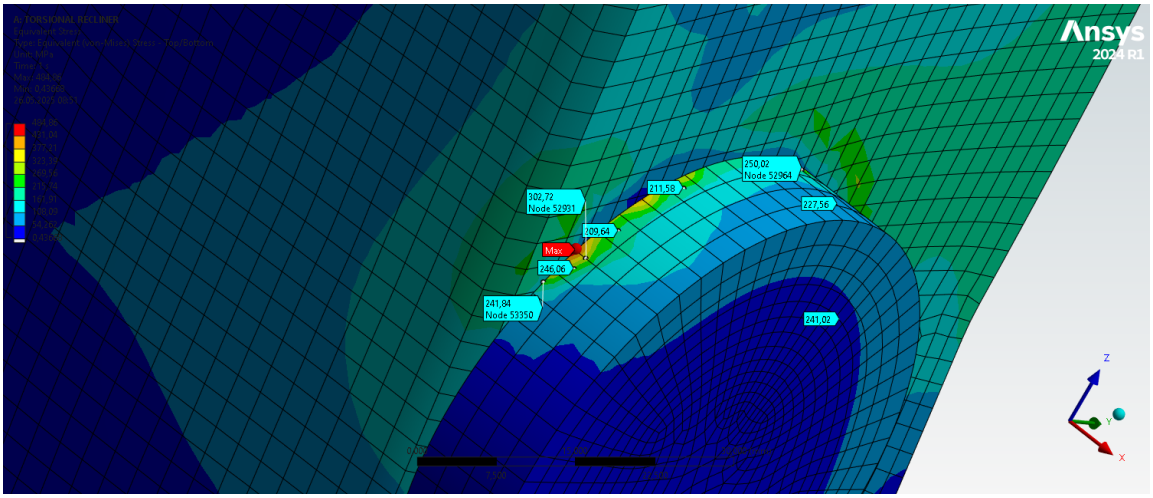

Figure 71 - The stress results of two body force applied torsional recliner and singular points

4.4 LS-Dyna Analysis Results

ANSYS Static Structural tool offers analysis of the stress distribution and deformation behaviour of the seatback under static loading, and its capacity to reflect the dynamic character of actual rear-end collisions is limited. ANSYS LS-DYNA tool in the other hand, is an explicit finite element solver, and made to deal with nonlinear, time-dependent crash scenarios involving complex contact interactions and high strain rates. This type of dynamic simulation is essential to understand how the seatback responds throughout the entire crash event—not just at its peak deformation. By incorporating mass properties, velocity inputs, and body forces, LS-DYNA complements static analysis results and allows for more realistic predictions of structural behavior under impact.

The dynamic analyses are considered as recliner has a velocity, and seatback subjected to occupants' weight by two body parts as 60.3 kg and 14.7 kg, and a head force as shown in figure below as 5 kg.

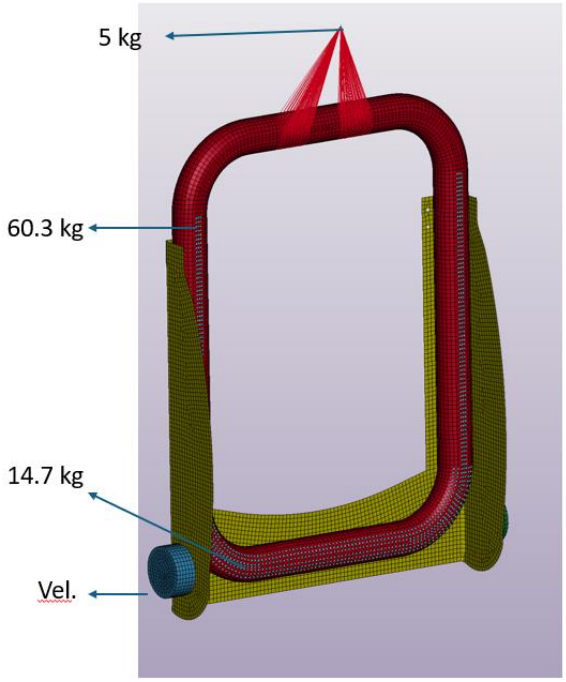

Figure 72 - LS-DYNA analysis model

The velocity profile in the Y-direction was applied to replicate the crash pulse observed in FMVSS 301 rear-impact conditions as shown in Figure 27.

The velocity profile is applied along Y direction, which is the direction of movement.

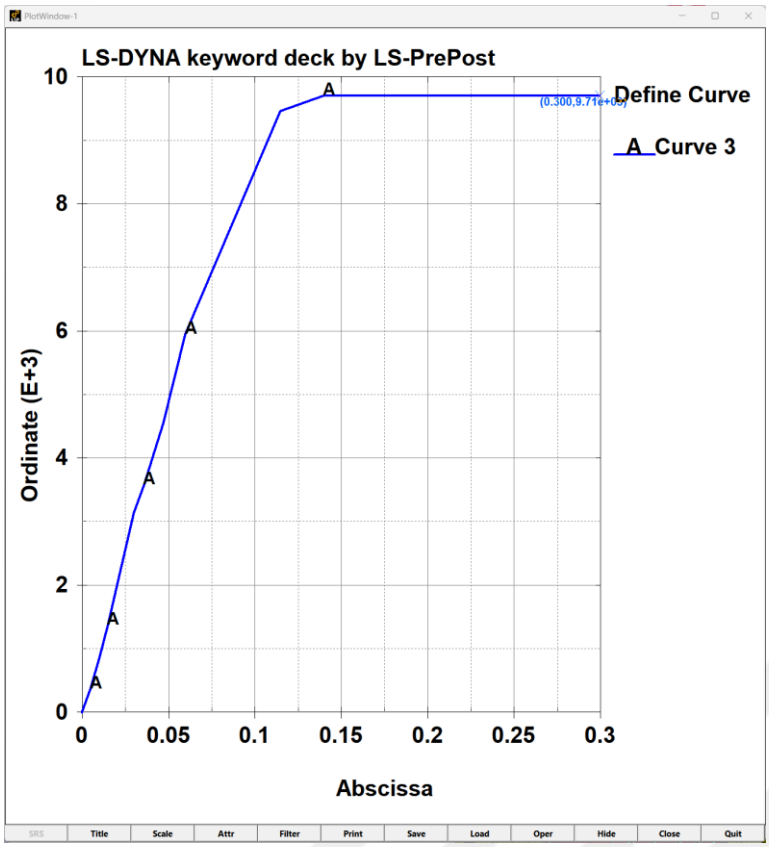

Figure 73 – Velocity profile in Y axis

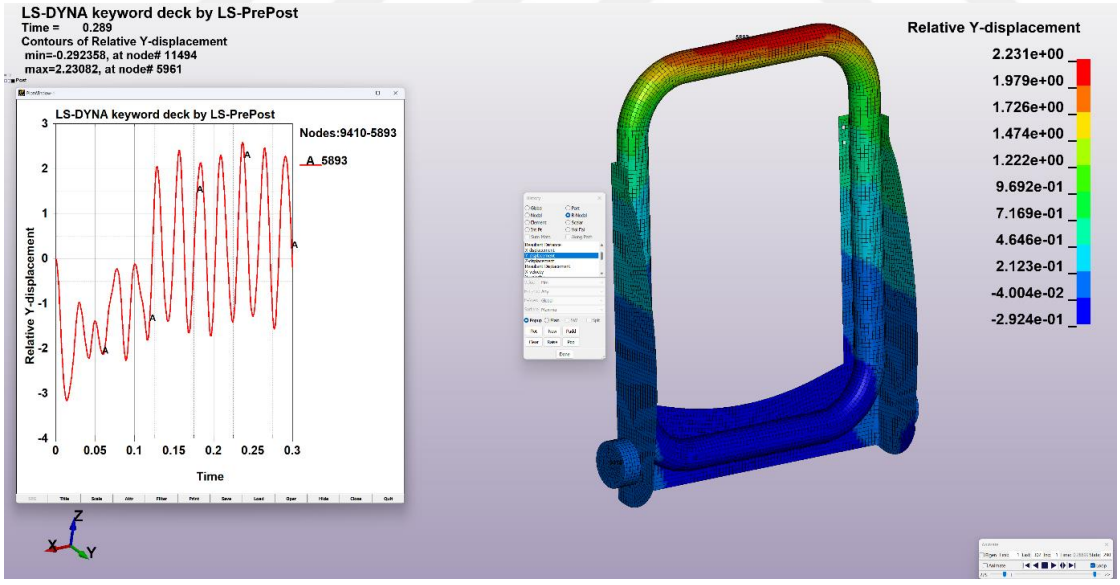

Figure 74 – Seatback dynamic displacement results in Y axis

The results which plotted as relative Y displacements, provide insight into how the seat structure responds dynamically under crash loading and validate the effectiveness of mass-inertia parameters derived from static analysis. In this case, with 60 mm diameter

recliner and 3 mm seatback sheet, displacement in Y axis to time graph shows the relative displacement oscillates between 2.2 mm to -2.9 mm.

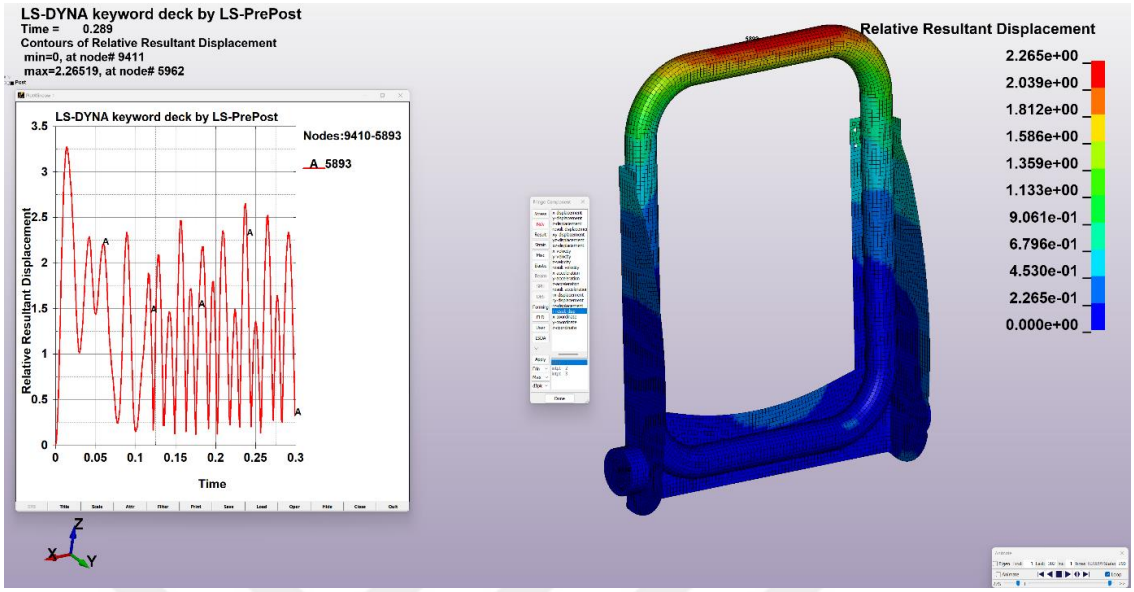

Figure 75 - Seatback dynamic relative displacement results

4.5 Discussion

When evaluating the results, the reported maximum stress value should be interpreted by averaging the stress values around the concentration, excluding the singular point, to obtain a more representative von Mises stress.

Additionally, if the maximum stress values exceed the yield strength, the total deformation provided by the analysis includes both elastic and plastic deformation values.

When the results are reviewed, the table below can be the output of this analyses period.

The higher total deformation observed in the case of the aluminum recliner body, compared to the steel version, can be explained by mechanical properties. Aluminum alloys typically have a significantly lower Young's modulus (about 70 GPa) than structural steels such as S355 (about 210 GPa). Young's modulus defines a material's stiffness; a lower modulus means the material deforms more under the same load.

Table 4 - Analysis results summary

Seatback Sheet Thickness	Recliner Type	Recliner Material	Recliner Dimensions	Maximum Stress (MPa)	Total Deformation (mm)
2 mm	None	-	-	370	2.95
2 mm	None	-	-	600	4
3 mm	None	-	-	340	2.8
3 mm*	None	-	-	387	3.2
2 mm	Bending	Aluminum	20 mm	500	27.12
2 mm	Bending	Aluminum	30 mm	360	19
3 mm	Bending	Aluminum	30 mm	340	18
2 mm	Bending	Str Steel	30 mm	340	9.3
2 mm	Bending	Str Steel	20 mm	520	12
2 mm	Bending	Str Steel	25 mm	400	10
2 mm	Torsional	Str Steel	30 mm	900	10.4
2 mm	Torsional	Str Steel	60 mm**	300	3.2
2 mm	Torsional	Str Steel	60 mm***	280	3.16
3 mm	Torsional	Str Steel	60 mm****	240	2.8

*two body force applied, ** 26 mm length of torsional bar, ***12 mm length of torsional bar, ****12 mm length and two body force applied

As a result, under identical loading conditions, the aluminum recliner undergoes more elastic deformation than its steel, even if both materials remain within their elastic limits. While aluminum offers advantages in terms of weight reduction, its lower rigidity leads to larger deformations, making it less favorable in structural applications where stiffness and minimal displacement are critical, like seatback recliner mechanisms during rear impact scenarios.

When the length of the torsional bar is increased while keeping the diameter constant, the moment arm becomes larger. This results with increase in deformation observed on the seatback sheet. According to the results, it is evident that torsional effects contribute more significantly to energy absorption; however, in order to minimize the stress transferred to the seatback sheet, it is preferable to incorporate bending deformation mechanisms within the recliner structure as well.

To obtain results that better reflect real-world performance, future designs should incorporate more realistic geometries that are simultaneously subjected to both torsional and bending loads. Such configurations would enable greater energy absorption while also offering improved control over seatback displacement during rear impact scenarios. Developing and analyzing these hybrid designs can provide more effective structural responses and enhance passenger safety.

4.6 Outputs for Dynamic Impact Analyses Study

In this study, due to the load distribution and fix conditions, the most realistic analyses results belong to fourth analyses case with 3mm sheet seatback frame and two divided body force effect. In real scenario with no recliner, the seatback sheet deforms plastically under 15g rear impact conditions, extreme deformations not acceptable. Due to 3.2 mm deformation being reasonable, the mass and inertia values are given for that seatback design.

Table 5 - Mass and inertia results of final model

Configuration	Mass (kg)	Inertia X ($kg*m^2$)	Inertia Y ($kg*m^2$)	Inertia Z ($kg*m^2$)
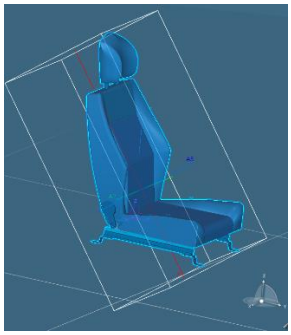 Overall Car Seat	16,682	1,571	1,443	1,069
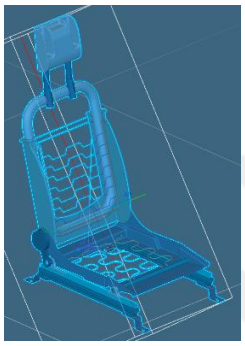 Car Seat Frame	15,271	1,416	1,316	0,978
 Seatback	7,707	0,476	0,643	0,184
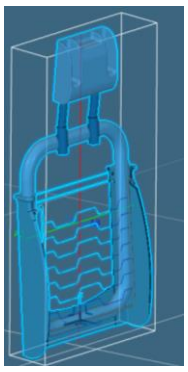 Seatback Frame	6,717	0,423	0,57	0,16

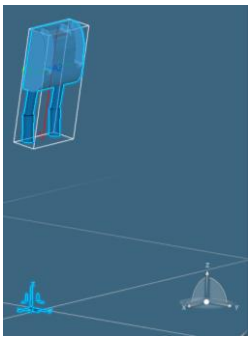 Headrestraint Frame	1,371	0,007	0,011	0,0.05
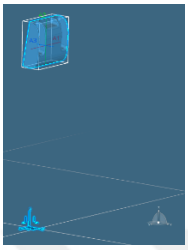 Headrestraint Top	1,169	0,003	0,006	0,004
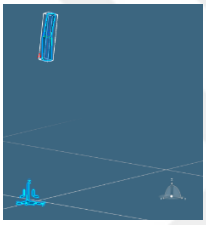 Headrest Post	0,101	0,00021	0,00021	0,000021
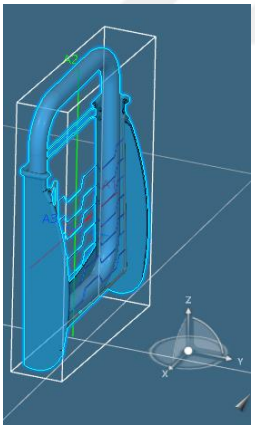 Seatback w/o HR	5,346	0,139	0,285	0,153
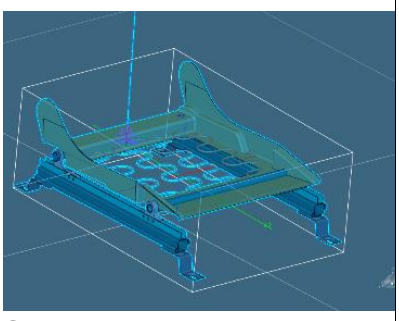 Seatpan Frame	7,292	0,197	0,236	0,414

4.7 Multi Body Dynamic Analyses

In order to evaluate the seat component behavior due to time multi-body dynamic simulations were conducted using MSC Nastran. Based on the mass and inertia values obtained from static structural analyses, the seat system was modeled as a set of interconnected rigid bodies representing the seatback, headrest, and seatpan. These components were connected using joints and boundary constraints, and a crash pulse based on FMVSS 301 test data was applied to simulate a rear-end collision scenario. Resulting motions are calculated over time, and this allowed to see a realistic representation of how the seat structure deformation and response to occupant inertia during impact. This dynamic approach complements static FEA by capturing kinematic effects such as headrest motion, seatback rotation, and energy absorption behavior during the crash.

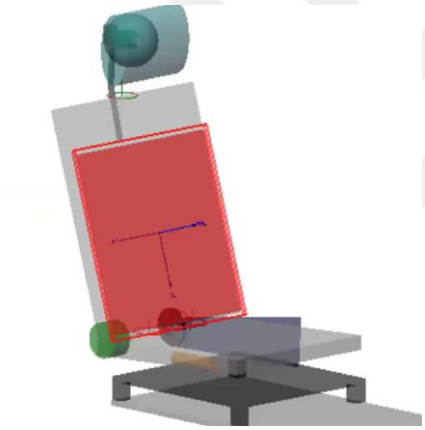

Figure 76 – MSC Nastran model

In this study, a rear-impact crash event was modeled by applying a sled acceleration pulse to the seatpan, simulated the vehicle's backward motion during a collision. The seatback was connected to the seatpan through a rotational joint with a defined recliner stiffness of 22,000 N.m/deg, represented a fixed recliner condition.

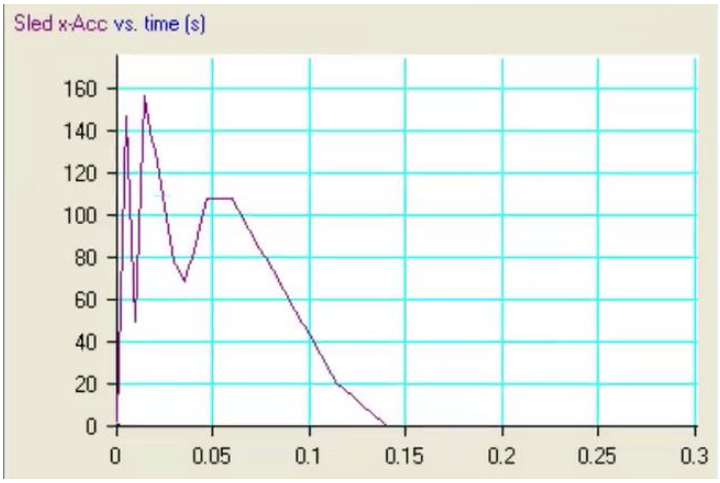

Figure 77 - The acceleration profile applied to seatpan

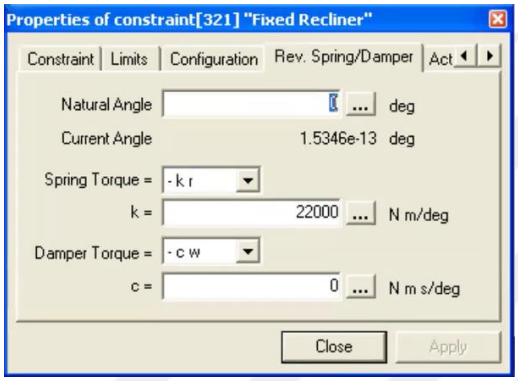

Figure 78 - Application of the stiffness value for recliner body

A multi-body system was built in MSC Nastran, where the head, upper torso, and seatback masses were applied as distributed loads as shown in Figure 79. The reference point displacement has defined to represent headrest motion. This point was tracked to observe the seatback's response under dynamic loading.

The damper torque was defined as zero, and the graph in Figure 80 – Dynamic deflection results over timeshown dynamic deflection results over time without damping effects.

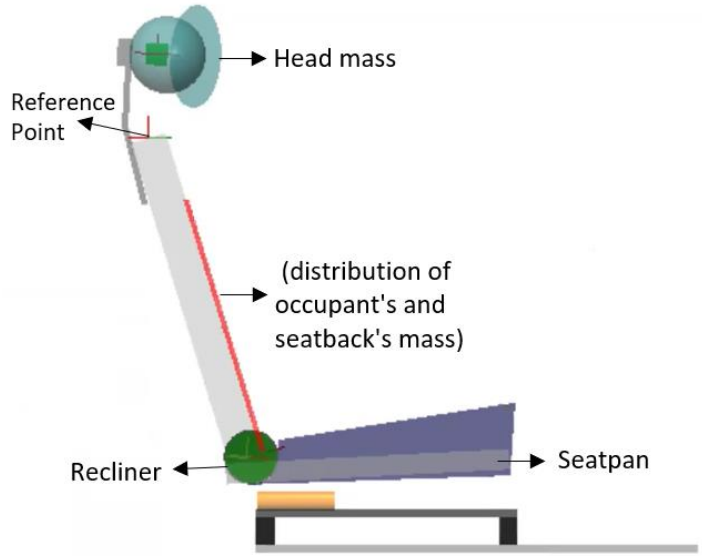

Figure 79 – Details of the dynamic analysis model

The results showed periodic oscillations and increasing lateral displacement over time, with maximum Y deflections reach around -3 mm. These results help quantify the deformation behavior of the seatback and support the assessment of energy absorption capacity and occupant safety during rear-end crashes.

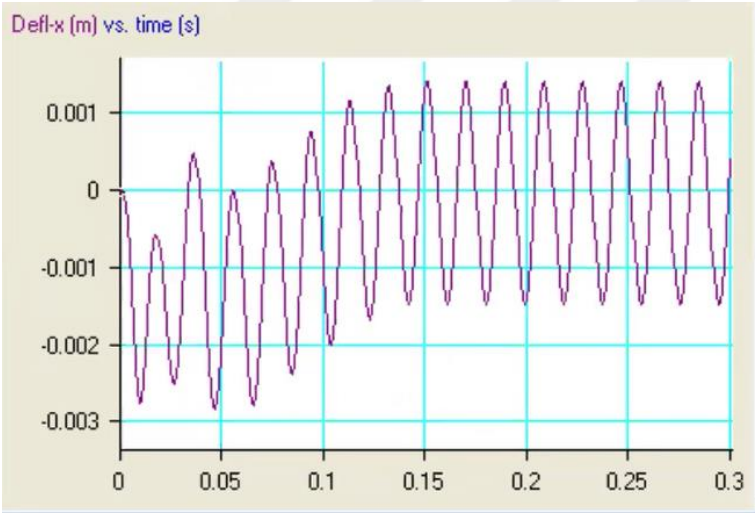

Figure 80 – Dynamic deflection results over time

5. CONCLUSION

This thesis aimed to design and evaluate the structural performance of a car seat under rear-end collision conditions. Various static and dynamic analysis methods were applied to better understand how different design choices, such as sheet thickness, recliner type, and material affect the seat's ability to absorb crash energy and limit deformation.

The analysis showed that the seatback structure made from S355 steel and equipped with an appropriate recliner can successfully stay within acceptable deformation limits under crash loads. Dynamic simulations in LS-DYNA and MSC Nastran helped to visualize how the seat structure behaves during the full crash duration, not just at peak loading.

A major outcome of this study is the determination of accurate mass and inertia values for the seatback, headrest, and overall seat assembly. These values were calculated through detailed 3D modeling and validated under realistic loading conditions. They can serve as reliable input data for multi-body dynamic crash simulations in future research and development projects. This makes the results valuable not only for evaluating seat strength but also for supporting further studies in occupant safety modeling.

In conclusion, the methodology and results presented in this thesis can provide a helpful reference for engineers and researchers working on safe and efficient seat designs, especially in the early design and simulation phases of vehicle safety development.

6. REFERENCES

[1] European New Car Assessment Programme (Euro NCAP). The Dynamic Assessment of Car Seats for Neck Injury Protection Testing Protocol, Version 3.1; Euro NCAP: Brussels, Belgium, 2011.

[2] Himmetoglu, S. OMÜ443 Principles of Vehicle Crash Safety Lecture Notes. Hacettepe University, Mechanical Engineering Department, 2021

[3] Viano, D.C. (2008). Seat Design Principles to Reduce Neck Injuries in Rear Impacts. *Traffic Injury Prevention*, 9(6), 552–560. DOI: 10.1080/15389580802381939.

[4] Latchford, J., Chirwa, E.C., Chen, T., & Mao, M. (2005). The relationship of seat backrest angle and neck injury in low-velocity rear impacts. *Proceedings of the Institution of Mechanical Engineers, Part D: Journal of Automobile Engineering*, 219, 1293–1302.

[5] Thiyagarajan, Prasanna balaji, "Non-Linear Finite Element Analysis And Optimization For Light Weight Design Of An Automotive Seat Backrest" (2008). All Theses. 469.

[6] NHTSA. Federal Motor Vehicle Safety Standard No. 207, "Seating Systems"; Laboratory Test Procedure TP-207-09; U.S. Department of Transportation, National Highway Traffic Safety Administration: Washington, DC, USA, 1992.

[7] Bridges, W., Ganesan, V., Jayakumar, P., Davies, J., & Paramasuwom, M. (2019, July). Front seat modeling in rear impact crashes: Development of a detailed finite-element model for seat back strength requirements (Report No. DOT HS 812 737). Washington, DC: National Highway Traffic Safety Administration

[8] U.S. Department of Transportation. Laboratory Test Procedure for FMVSS 301R: Fuel System Integrity—Rear Impact; TP-301R-02; National Highway Traffic Safety Administration (NHTSA), Office of Vehicle Safety Compliance: Washington, DC, USA, 2007.

[9] Burnett, R.A.; Viano, D.C.; Parenteau, C.S. Quasi-static methods to evaluate seat strength in rear impacts. *Traffic Injury Prevention* **2023**, 24, 218–223. DOI:10.1080/15389588.2022.2140280

[10] Viano, D.C.; White, S.D. Seat strength in rear body block tests. Traffic Injury Prevention, 2016, 17(5), 502–507. DOI: 10.1080/15389588.2015.1111513

[11] Viano, D.C., & Parenteau, C.S. (2018). Occupant Responses in Conventional and ABTS Seats in High-Speed Rear Sled Tests. *Traffic Injury Prevention*, 19(sup2), S111–S118. DOI: 10.1080/15389588.2018.1490719

[12] Karambe, M. D.; Karmankar, A. V.; Yenarkar, Y. L. Stress analysis of seat backrest of car. Int. J. Mech. Eng. & Rob. Res. 2013, 2(4), 443–448.

[13] United Nations Economic Commission for Europe. Uniform Provisions Concerning the Approval of Vehicles with Regard to the Seats, Their Anchorages and Any Head Restraints (UN Regulation No. 17), Revision 6. E/ECE/324/Rev.1/Add.16/Rev.6; E/ECE/TRANS/505/Rev.1/Add.16/Rev.6. United Nations: Geneva, 2020.

[14] Kaya, A.G.; Himmetoglu, S. *Semiactive Car-Seat System for Rear-End Collisions*. *Machines* 2024, *12*(8), 530.

[15] Yavuz, S.; Himmetoglu, S. Development of a Restraint System for Rear-Facing Car Seats. Machines 2023, 11(12), 1076.

[16] Avery, M.; Giblen, E.; Weekes, A. Euro NCAP Whiplash Test Procedure – A New Consumer Seat Rating Programme. Thatcham Research, UK, 2008

[17] European Committee for Standardization (CEN). EN 10025-2: Hot Rolled Products of Structural Steels – Part 2: Technical Delivery Conditions for Non-Alloy Structural Steels. Brussels: CEN, 2019

[18] Edwards, M.A.; Brumbelow, M.L.; Trempel, R.E.; Gorjanc, T.C. Seat Design Characteristics Affecting Occupant Safety in Low- and High-Severity Rear-Impact Collisions. Insurance Institute for Highway Safety, USA, 2019. Proceedings of IRCOBI Conference, Florence, Italy.

APPENDIX

Mass and Inertia Outputs

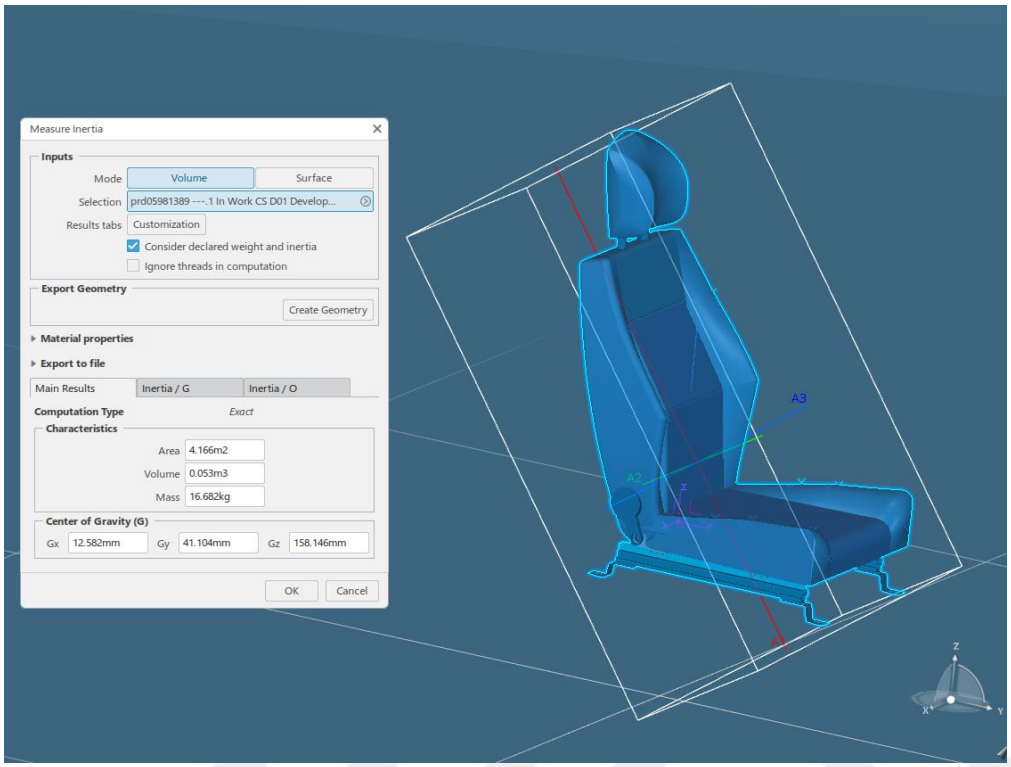

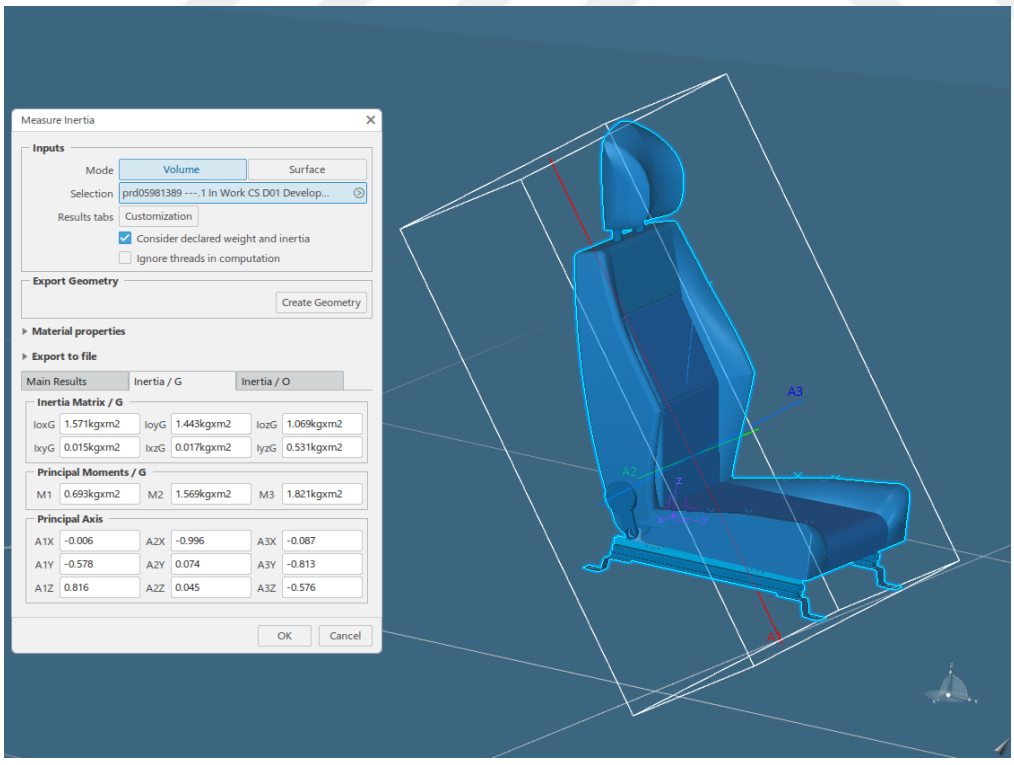

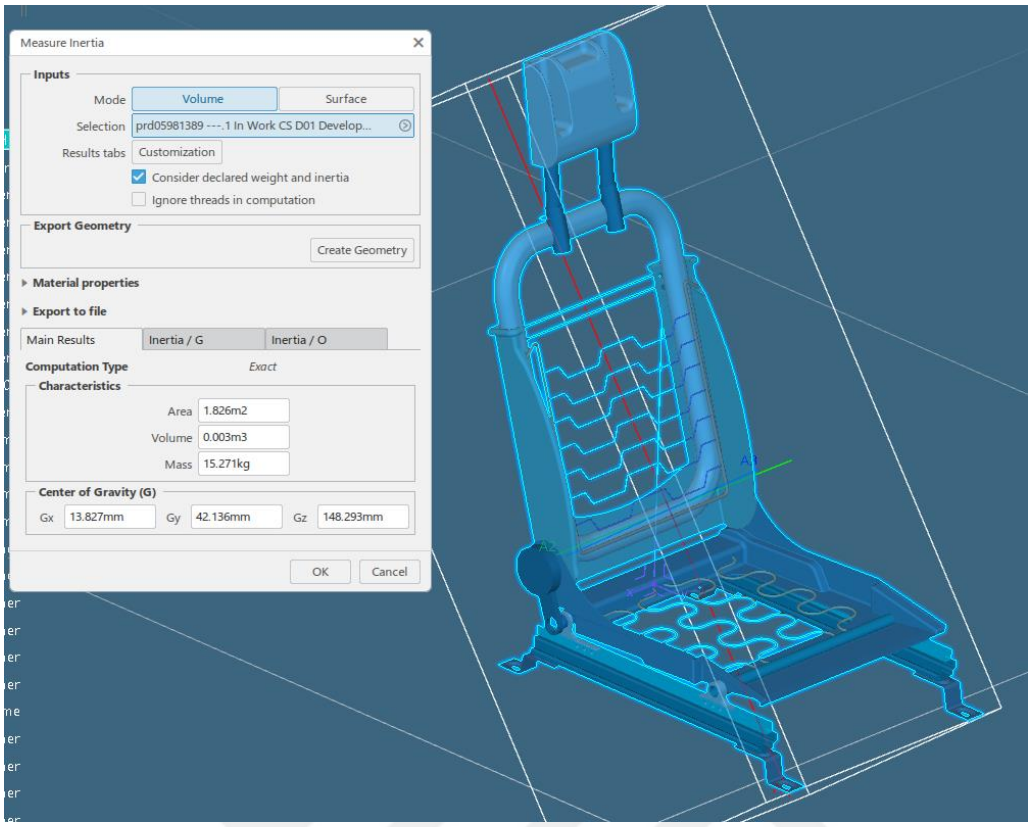
Measure Inertia
Inputs
Mode
Volume
Surface
Selection
prd05981389 ---.1 In Work CS D01 Develop...
Results tabs
Customization
Consider declared weight and inertia
Ignore threads in computation
Export Geometry
Create Geometry
Material properties
Export to file
Main Results
Inertia / G
Inertia / O
Computation Type
Exact
Characteristics
Area 1.826m2
Volume 0.003m3
Mass 15.271kg
Center of Gravity (G)
Gx 13.827mm
Gy 42.136mm
Gz 148.293mm
OK
Cancel

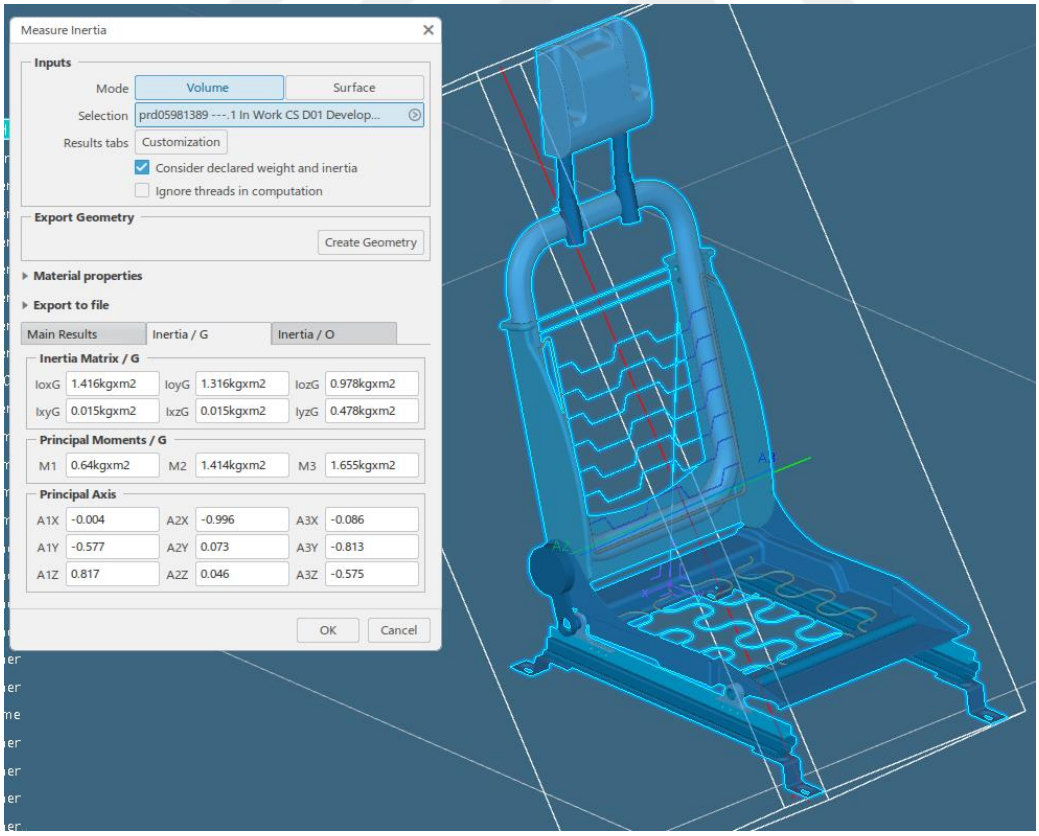
Measure Inertia
Inputs
Mode
Volume
Surface
Selection
prd05981389 ---.1 In Work CS D01 Develop...
Results tabs
Customization
Consider declared weight and inertia
Ignore threads in computation
Export Geometry
Create Geometry
Material properties
Export to file
Main Results
Inertia / G
Inertia / O
Inertia Matrix / G
IoxG 1.416kgxm2
IoyG 1.316kgxm2
IozG 0.978kgxm2
IxyG 0.015kgxm2
IxzG 0.015kgxm2
IyzG 0.478kgxm2
Principal Moments / G
M1 0.64kgxm2
M2 1.414kgxm2
M3 1.655kgxm2
Principal Axis
A1X -0.004
A2X -0.996
A3X -0.086
A1Y -0.577
A2Y 0.073
A3Y -0.813
A1Z 0.817
A2Z 0.046
A3Z -0.575
OK
Cancel

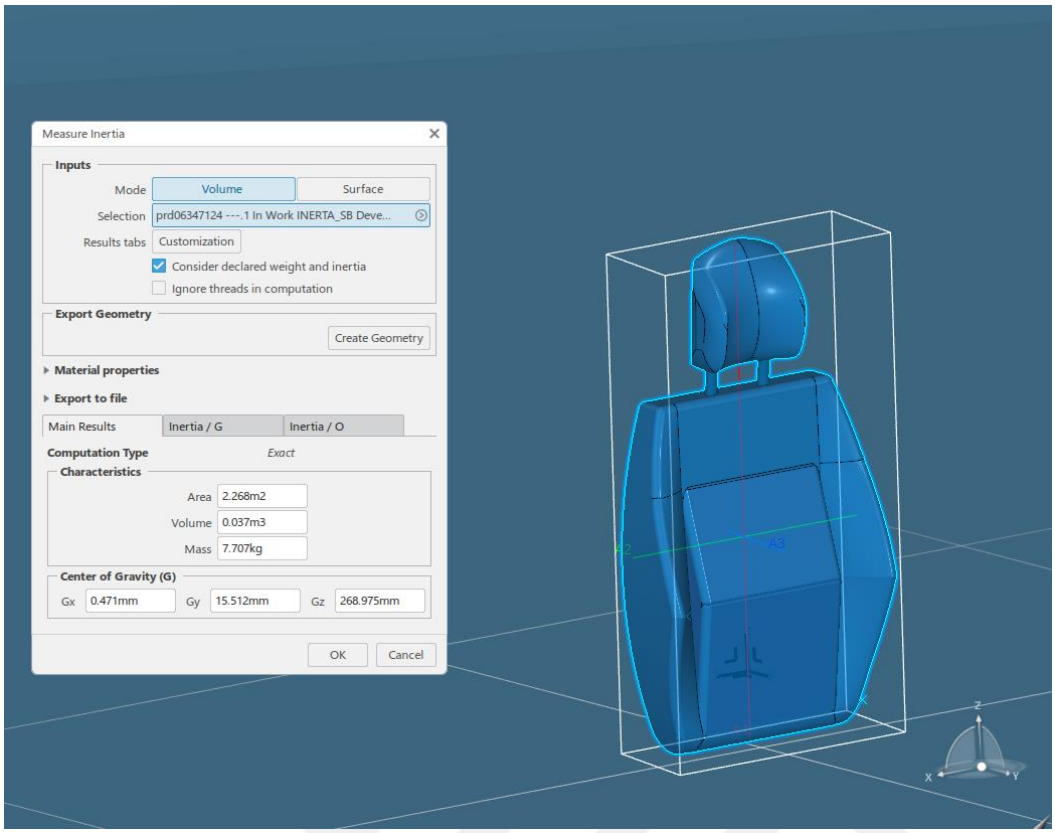
Measure Inertia
Inputs
Mode
Volume
Surface
Selection
prd06347124 ---.1 In Work INERTA_SB Deve...
Results tabs
Customization
Consider declared weight and inertia
Ignore threads in computation
Export Geometry
Create Geometry
Material properties
Export to file
Main Results
Inertia / G
Inertia / O
Computation Type
Exact
Characteristics
Area
2.268m2
Volume
0.037m3
Mass
7.707kg
Center of Gravity (G)
Gx
0.471mm
Gy
15.512mm
Gz
268.975mm
OK
Cancel

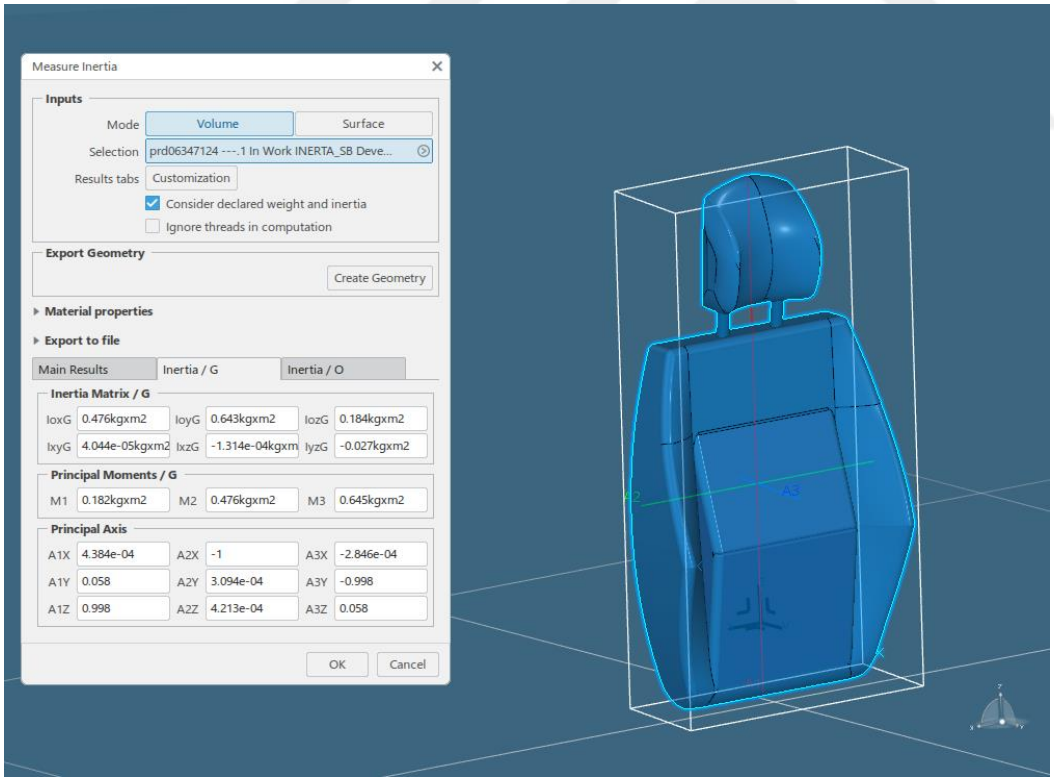
Measure Inertia
Inputs
Mode
Volume
Surface
Selection
prd06347124 ---.1 In Work INERTA_SB Deve...
Results tabs
Customization
Consider declared weight and inertia
Ignore threads in computation
Export Geometry
Create Geometry
Material properties
Export to file
Main Results
Inertia / G
Inertia / O
Inertia Matrix / G
IoxG
0.476kgxm2
IoyG
0.643kgxm2
IozG
0.184kgxm2
IxyG
4.044e-05kgxm2
IxzG
-1.314e-04kgxm
IyzG
-0.027kgxm2
Principal Moments / G
M1
0.182kgxm2
M2
0.476kgxm2
M3
0.645kgxm2
Principal Axis
A1X
4.384e-04
A2X
-1
A3X
-2.846e-04
A1Y
0.058
A2Y
3.094e-04
A3Y
-0.998
A1Z
0.998
A2Z
4.213e-04
A3Z
0.058
OK
Cancel

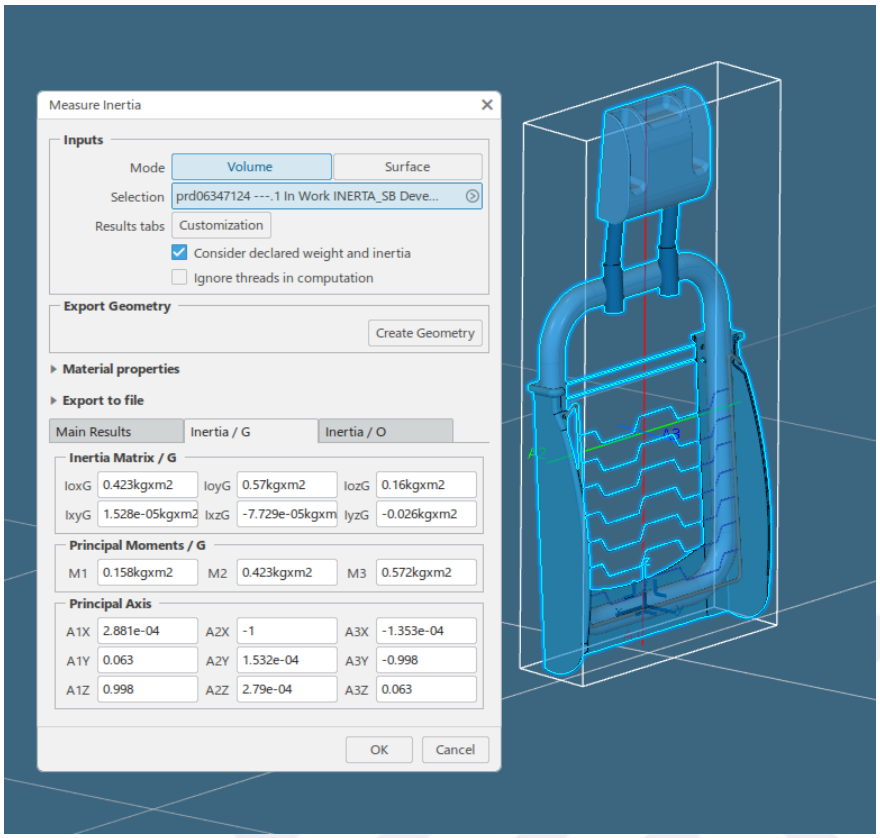
Measure Inertia
Inputs
Mode
Volume
Surface
Selection
prd06347124 ---.1 In Work INERTA_SB Deve...
Results tabs
Customization
Consider declared weight and inertia
Ignore threads in computation
Export Geometry
Create Geometry
Material properties
Export to file
Main Results
Inertia / G
Inertia / O
Inertia Matrix / G
IoxG 0.423kgxm2
IoyG 0.57kgxm2
IozG 0.16kgxm2
IxyG 1.528e-05kgxm2
IxzG -7.729e-05kgxm
IyzG -0.026kgxm2
Principal Moments / G
M1 0.158kgxm2
M2 0.423kgxm2
M3 0.572kgxm2
Principal Axis
A1X 2.881e-04
A2X -1
A3X -1.353e-04
A1Y 0.063
A2Y 1.532e-04
A3Y -0.998
A1Z 0.998
A2Z 2.79e-04
A3Z 0.063
OK
Cancel

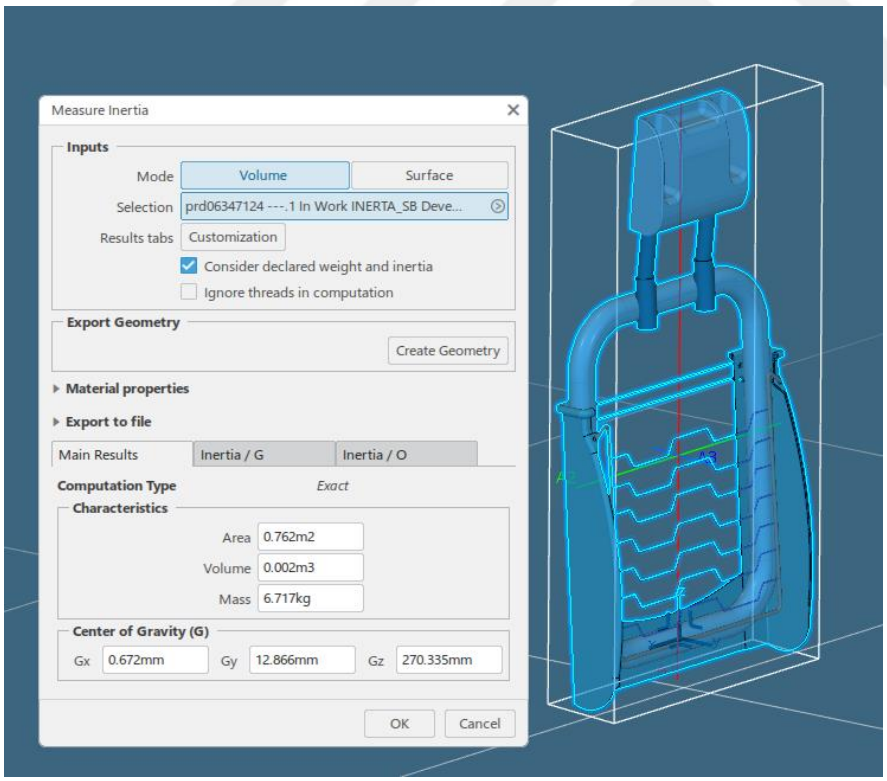
Measure Inertia
Inputs
Mode
Volume
Surface
Selection
prd06347124 ---.1 In Work INERTA_SB Deve...
Results tabs
Customization
Consider declared weight and inertia
Ignore threads in computation
Export Geometry
Create Geometry
Material properties
Export to file
Main Results
Inertia / G
Inertia / O
Computation Type
Exact
Characteristics
Area 0.762m2
Volume 0.002m3
Mass 6.717kg
Center of Gravity (G)
Gx 0.672mm
Gy 12.866mm
Gz 270.335mm
OK
Cancel

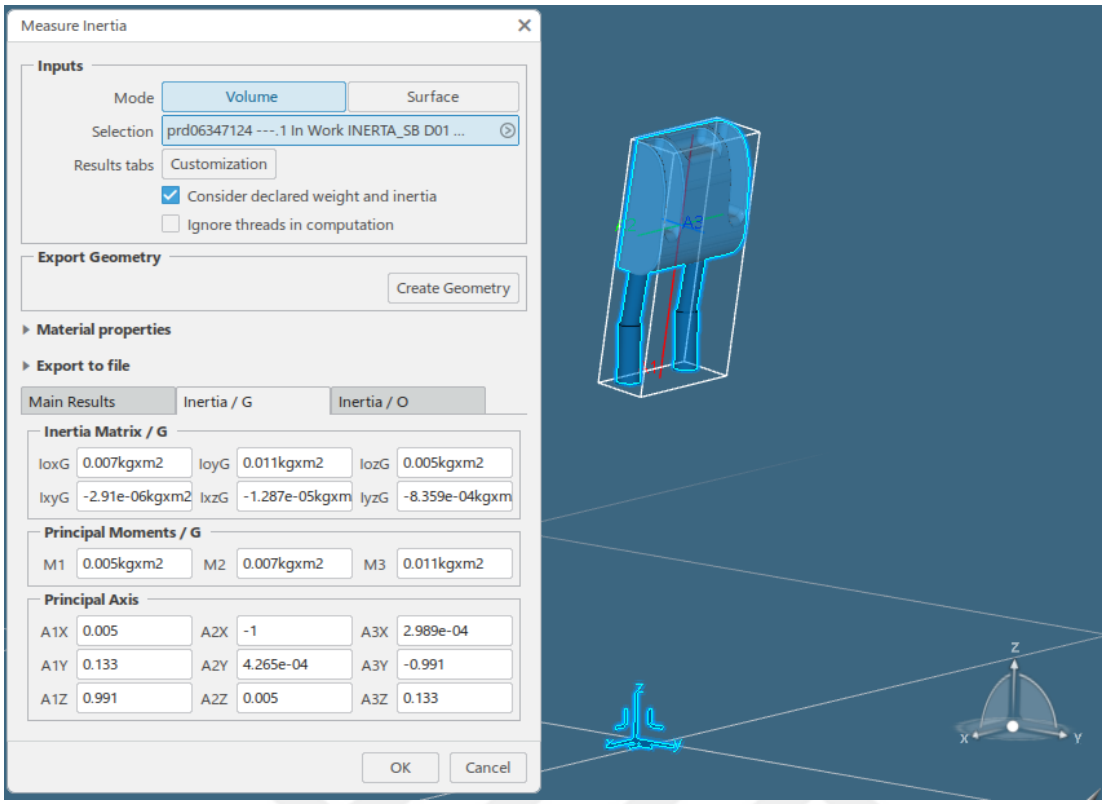
Measure Inertia
Inputs
Mode
Volume
Surface
Selection
prd06347124 ---.1 In Work INERTA_SB D01 ...
Results tabs
Customization
Consider declared weight and inertia
Ignore threads in computation
Export Geometry
Create Geometry
Material properties
Export to file
Main Results
Inertia / G
Inertia / O
Inertia Matrix / G
IoxG 0.007kgxm2
IoyG 0.011kgxm2
IozG 0.005kgxm2
IxyG -2.91e-06kgxm2
IxzG -1.287e-05kgxm
IyzG -8.359e-04kgxm
Principal Moments / G
M1 0.005kgxm2
M2 0.007kgxm2
M3 0.011kgxm2
Principal Axis
A1X 0.005
A2X -1
A3X 2.989e-04
A1Y 0.133
A2Y 4.265e-04
A3Y -0.991
A1Z 0.991
A2Z 0.005
A3Z 0.133
OK
Cancel

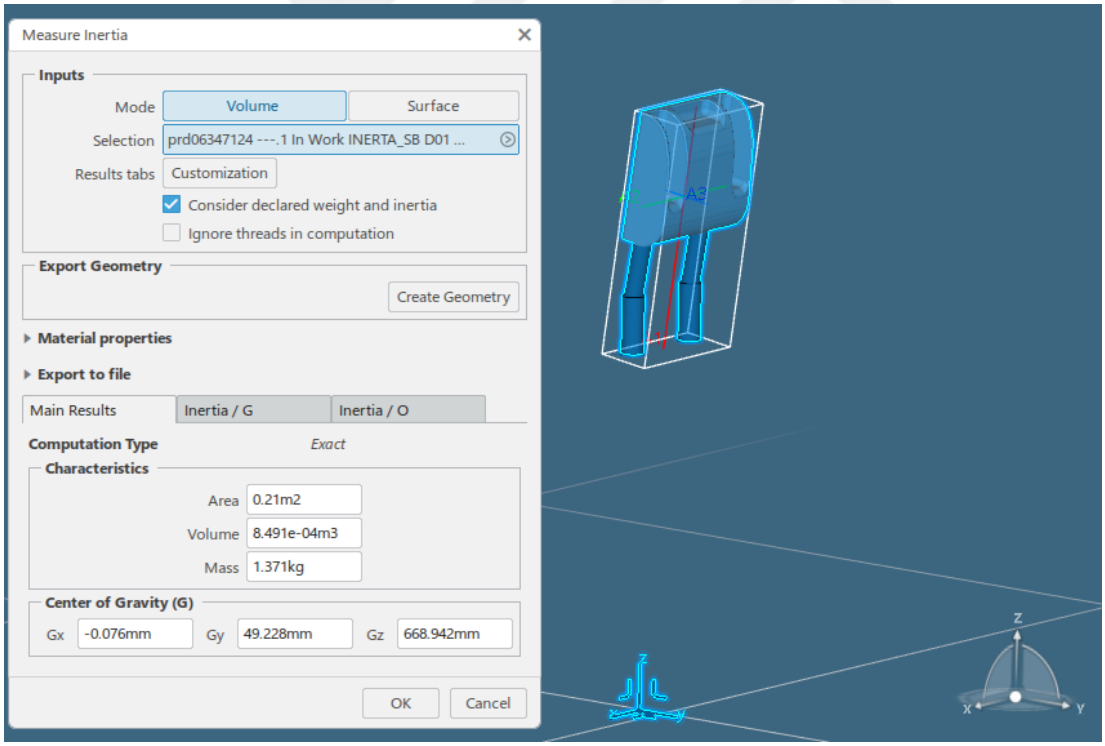
Measure Inertia
Inputs
Mode
Volume
Surface
Selection
prd06347124 ---.1 In Work INERTA_SB D01 ...
Results tabs
Customization
Consider declared weight and inertia
Ignore threads in computation
Export Geometry
Create Geometry
Material properties
Export to file
Main Results
Inertia / G
Inertia / O
Computation Type
Exact
Characteristics
Area 0.21m2
Volume 8.491e-04m3
Mass 1.371kg
Center of Gravity (G)
Gx -0.076mm
Gy 49.228mm
Gz 668.942mm
OK
Cancel

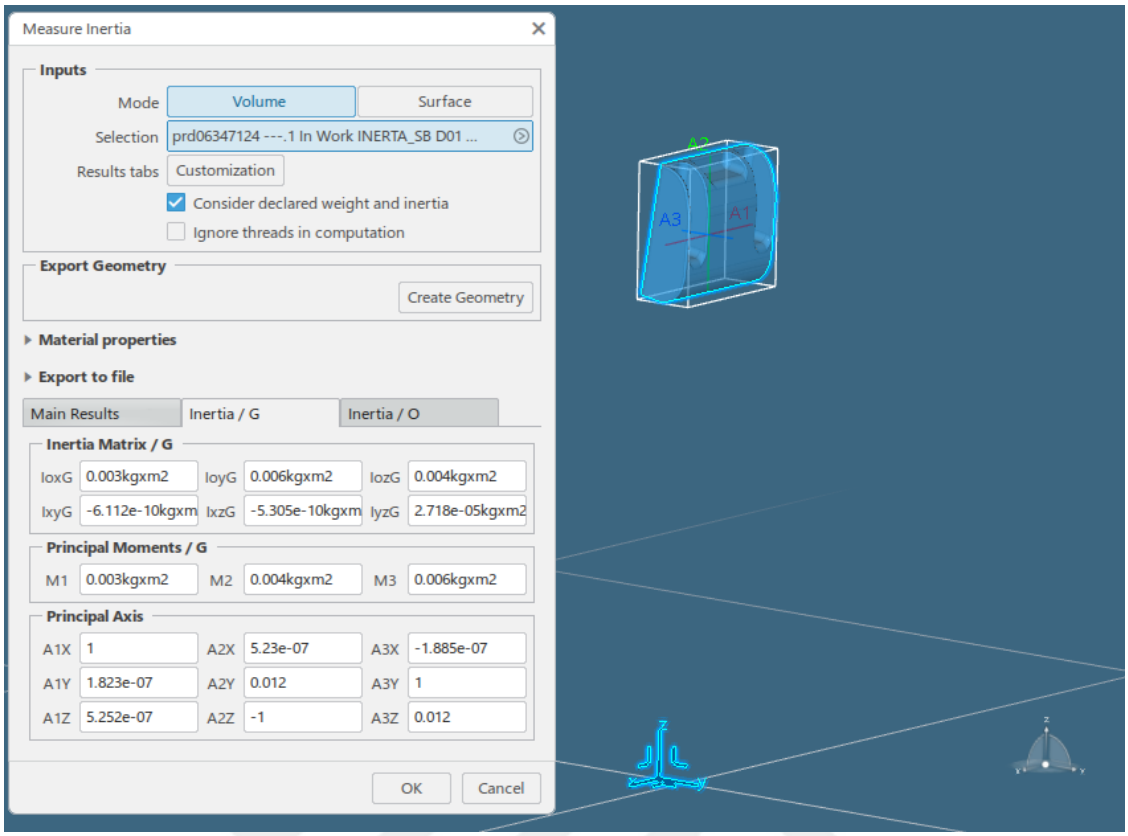
Measure Inertia
Inputs
Mode
Volume
Surface
Selection
prd06347124 ---.1 In Work INERTA_SB D01 ...
Results tabs
Customization
Consider declared weight and inertia
Ignore threads in computation
Export Geometry
Create Geometry
Material properties
Export to file
Main Results
Inertia / G
Inertia / O
Inertia Matrix / G
IoxG 0.003kgxm2
IoyG 0.006kgxm2
IozG 0.004kgxm2
IxyG -6.112e-10kgxm
IxzG -5.305e-10kgxm
IyzG 2.718e-05kgxm2
Principal Moments / G
M1 0.003kgxm2
M2 0.004kgxm2
M3 0.006kgxm2
Principal Axis
A1X 1
A2X 5.23e-07
A3X -1.885e-07
A1Y 1.823e-07
A2Y 0.012
A3Y 1
A1Z 5.252e-07
A2Z -1
A3Z 0.012
OK
Cancel
A3
A1

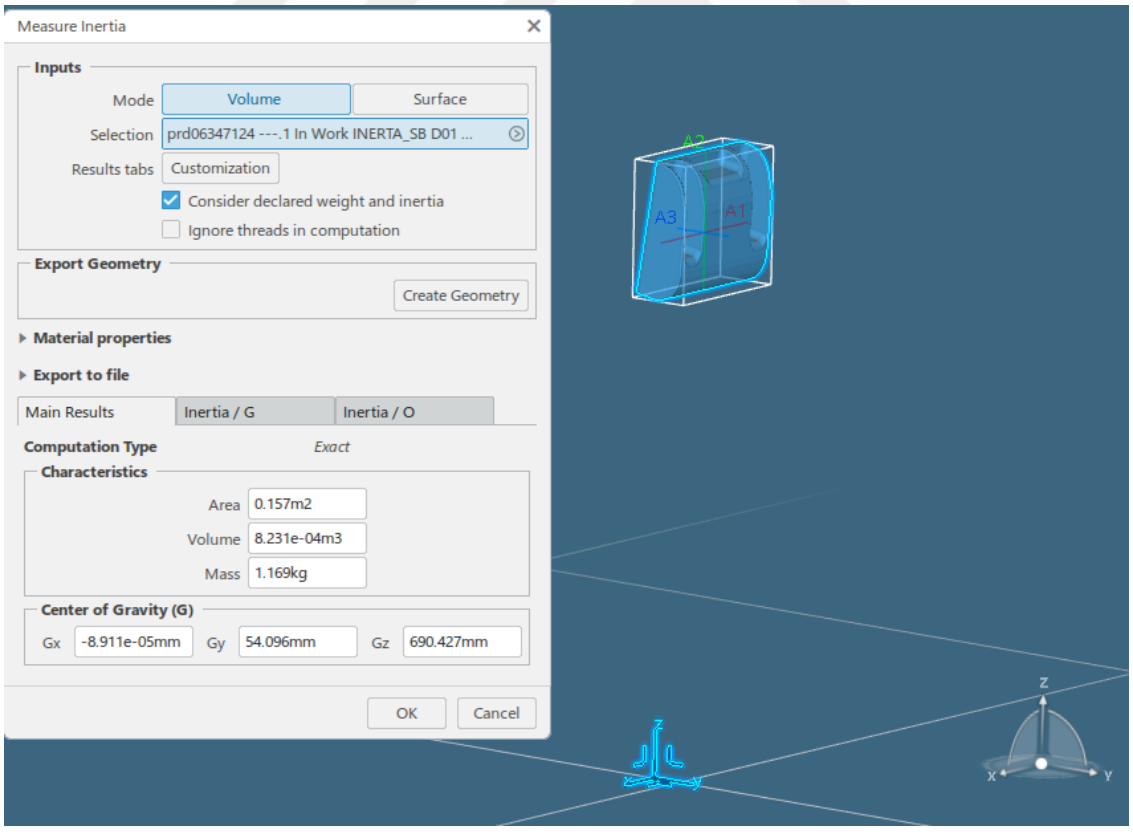
Measure Inertia
Inputs
Mode
Volume
Surface
Selection
prd06347124 ---.1 In Work INERTA_SB D01 ...
Results tabs
Customization
Consider declared weight and inertia
Ignore threads in computation
Export Geometry
Create Geometry
Material properties
Export to file
Main Results
Inertia / G
Inertia / O
Computation Type
Exact
Characteristics
Area 0.157m2
Volume 8.231e-04m3
Mass 1.169kg
Center of Gravity (G)
Gx -8.911e-05mm
Gy 54.096mm
Gz 690.427mm
OK
Cancel
A3
A1
Z
X
Y

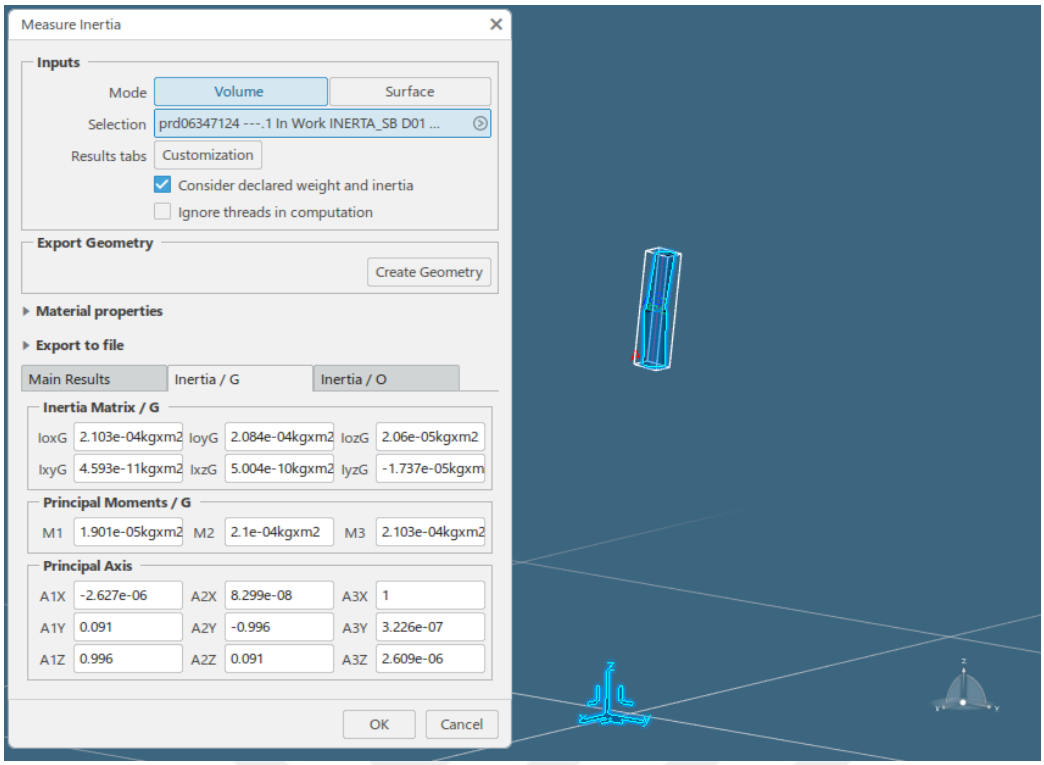
Measure Inertia
Inputs
Mode
Volume
Surface
Selection
prd06347124 ---.1 In Work INERTA_SB D01 ...
Results tabs
Customization
Consider declared weight and inertia
Ignore threads in computation
Export Geometry
Create Geometry
Material properties
Export to file
Main Results
Inertia / G
Inertia / O
Inertia Matrix / G
IoxG 2.103e-04kgxm2
IoyG 2.084e-04kgxm2
IozG 2.06e-05kgxm2
IxyG 4.593e-11kgxm2
IxzG 5.004e-10kgxm2
IyzG -1.737e-05kgxm
Principal Moments / G
M1 1.901e-05kgxm2
M2 2.1e-04kgxm2
M3 2.103e-04kgxm2
Principal Axis
A1X -2.627e-06
A2X 8.299e-08
A3X 1
A1Y 0.091
A2Y -0.996
A3Y 3.226e-07
A1Z 0.996
A2Z 0.091
A3Z 2.609e-06
OK
Cancel

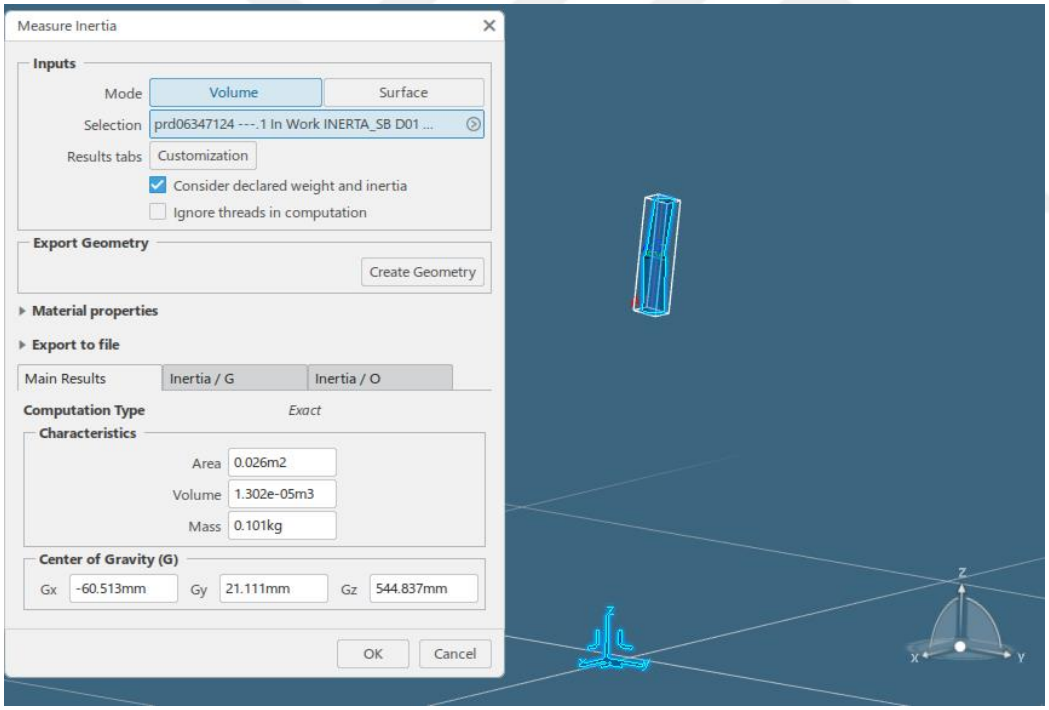
Measure Inertia
Inputs
Mode
Volume
Surface
Selection
prd06347124 ---.1 In Work INERTA_SB D01 ...
Results tabs
Customization
Consider declared weight and inertia
Ignore threads in computation
Export Geometry
Create Geometry
Material properties
Export to file
Main Results
Inertia / G
Inertia / O
Computation Type
Exact
Characteristics
Area 0.026m2
Volume 1.302e-05m3
Mass 0.101kg
Center of Gravity (G)
Gx -60.513mm
Gy 21.111mm
Gz 544.837mm
OK
Cancel

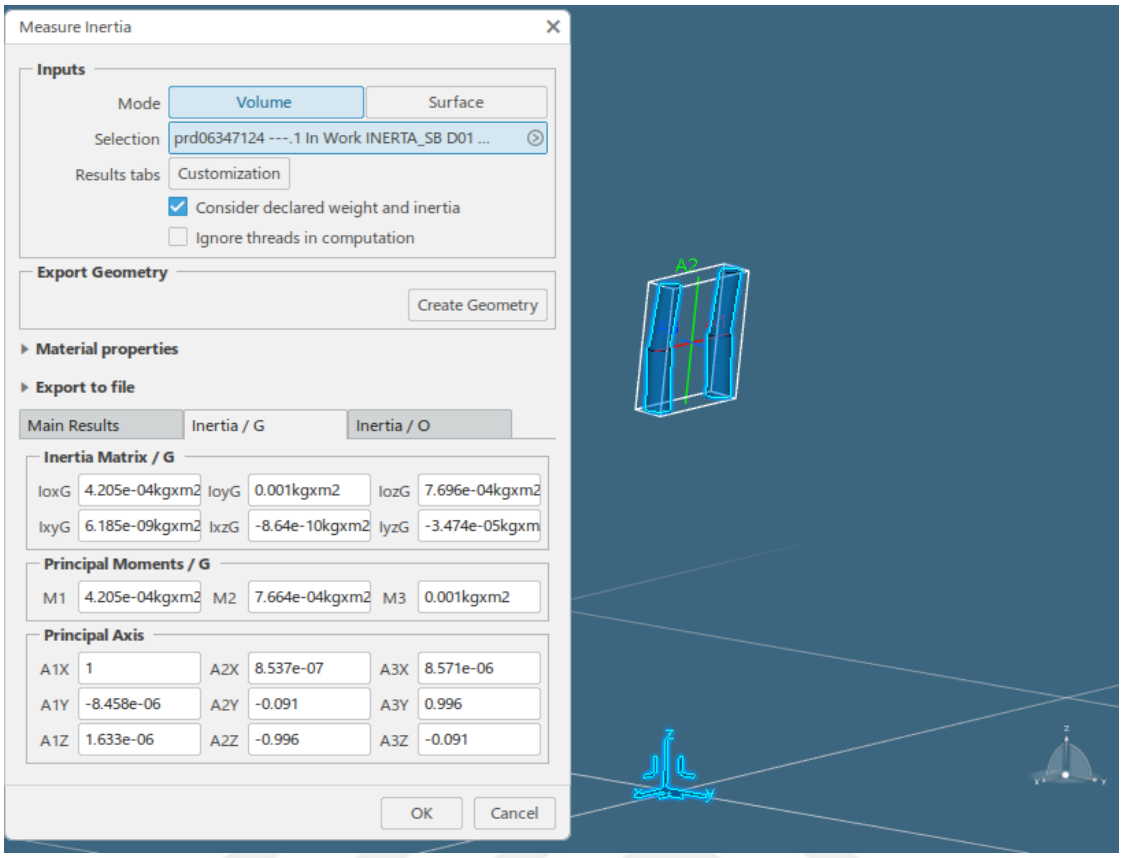
Measure Inertia
Inputs
Mode
Volume
Surface
Selection
prd06347124 ---.1 In Work INERTA_SB D01 ...
Results tabs
Customization
Consider declared weight and inertia
Ignore threads in computation
Export Geometry
Create Geometry
Material properties
Export to file
Main Results
Inertia / G
Inertia / O
Inertia Matrix / G
IoxG 4.205e-04kgxm2
IoyG 0.001kgxm2
IozG 7.696e-04kgxm2
IxyG 6.185e-09kgxm2
IxzG -8.64e-10kgxm2
IyzG -3.474e-05kgxm
Principal Moments / G
M1 4.205e-04kgxm2
M2 7.664e-04kgxm2
M3 0.001kgxm2
Principal Axis
A1X 1
A2X 8.537e-07
A3X 8.571e-06
A1Y -8.458e-06
A2Y -0.091
A3Y 0.996
A1Z 1.633e-06
A2Z -0.996
A3Z -0.091
OK
Cancel

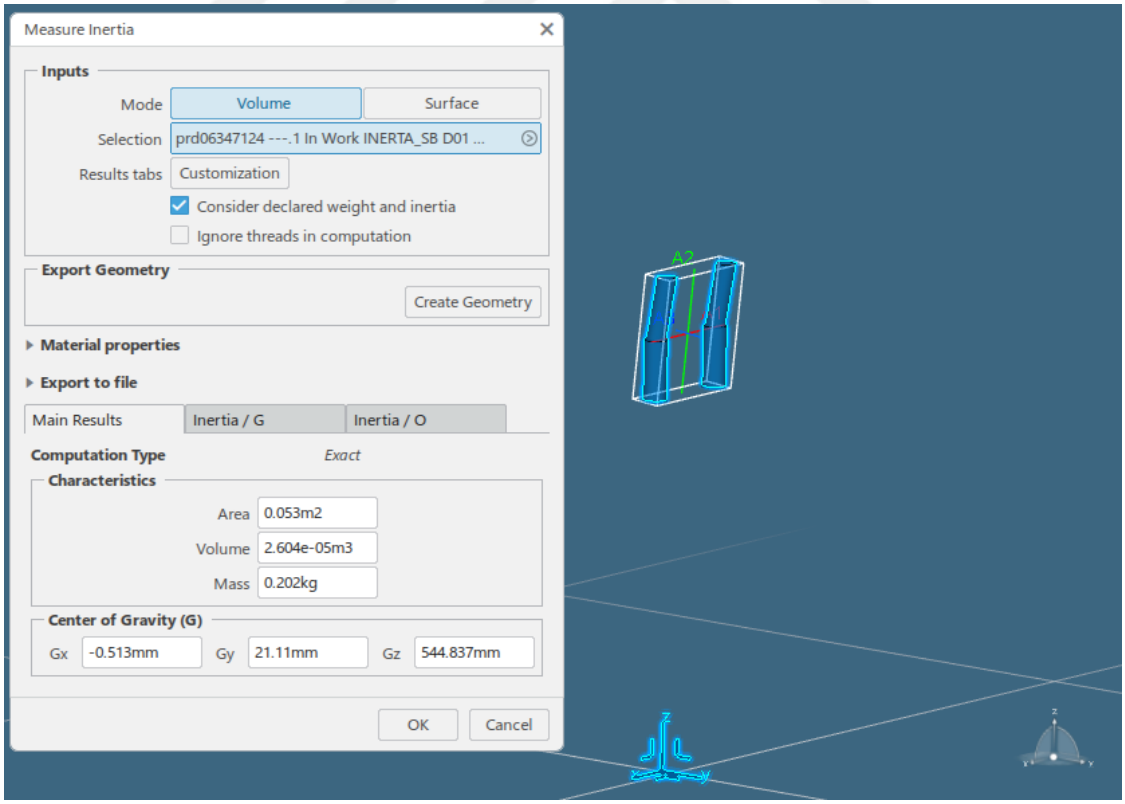
Measure Inertia
Inputs
Mode
Volume
Surface
Selection
prd06347124 ---.1 In Work INERTA_SB D01 ...
Results tabs
Customization
Consider declared weight and inertia
Ignore threads in computation
Export Geometry
Create Geometry
Material properties
Export to file
Main Results
Inertia / G
Inertia / O
Computation Type
Exact
Characteristics
Area 0.053m2
Volume 2.604e-05m3
Mass 0.202kg
Center of Gravity (G)
Gx -0.513mm
Gy 21.11mm
Gz 544.837mm
OK
Cancel

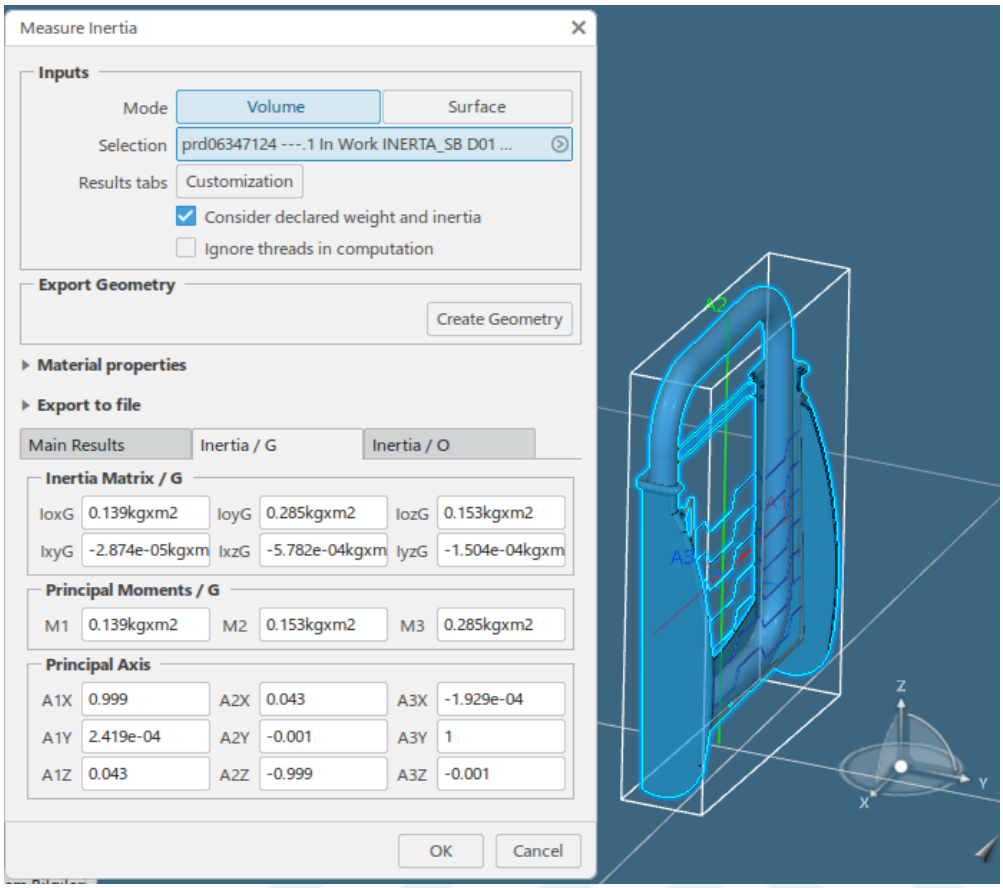
Measure Inertia
Inputs
Mode
Volume
Surface
Selection
prd06347124 ---.1 In Work INERTA_SB D01 ...
Results tabs
Customization
Consider declared weight and inertia
Ignore threads in computation
Export Geometry
Create Geometry
Material properties
Export to file
Main Results
Inertia / G
Inertia / O
Inertia Matrix / G
IoxG 0.139kgxm2
IoyG 0.285kgxm2
IozG 0.153kgxm2
IxyG -2.874e-05kgxm
IxzG -5.782e-04kgxm
IyzG -1.504e-04kgxm
Principal Moments / G
M1 0.139kgxm2
M2 0.153kgxm2
M3 0.285kgxm2
Principal Axis
A1X 0.999
A2X 0.043
A3X -1.929e-04
A1Y 2.419e-04
A2Y -0.001
A3Y 1
A1Z 0.043
A2Z -0.999
A3Z -0.001
OK
Cancel

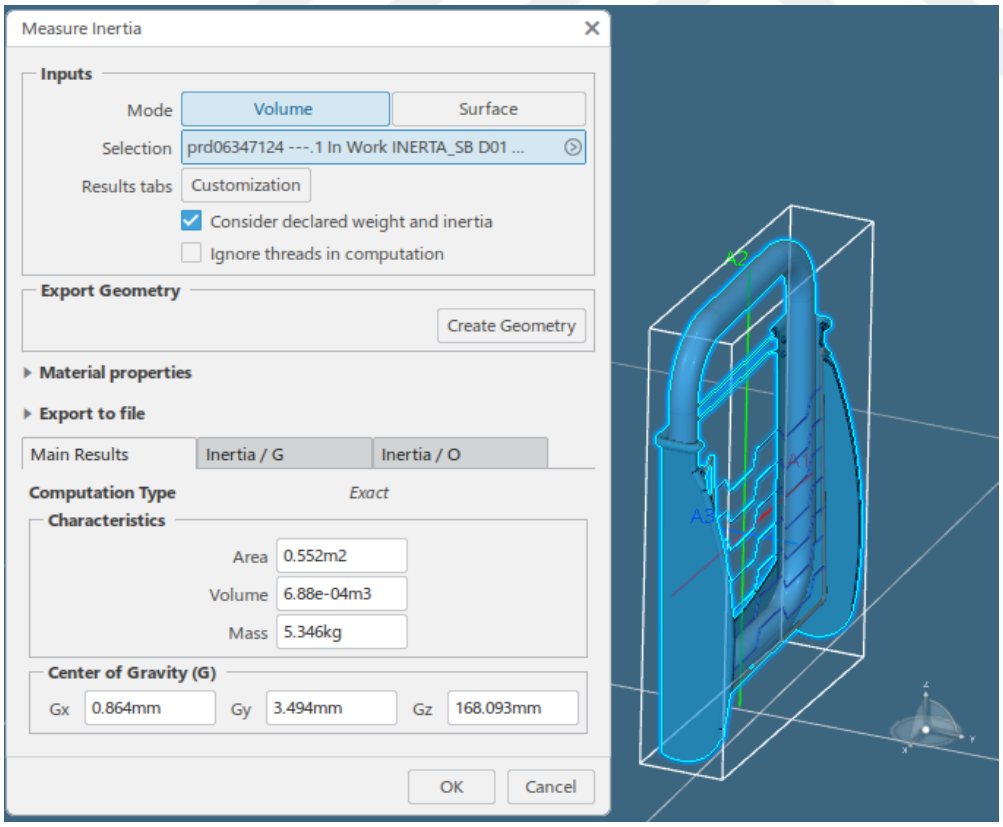
Measure Inertia
Inputs
Mode
Volume
Surface
Selection
prd06347124 ---.1 In Work INERTA_SB D01 ...
Results tabs
Customization
Consider declared weight and inertia
Ignore threads in computation
Export Geometry
Create Geometry
Material properties
Export to file
Main Results
Inertia / G
Inertia / O
Computation Type
Exact
Characteristics
Area 0.552m2
Volume 6.88e-04m3
Mass 5.346kg
Center of Gravity (G)
Gx 0.864mm
Gy 3.494mm
Gz 168.093mm
OK
Cancel

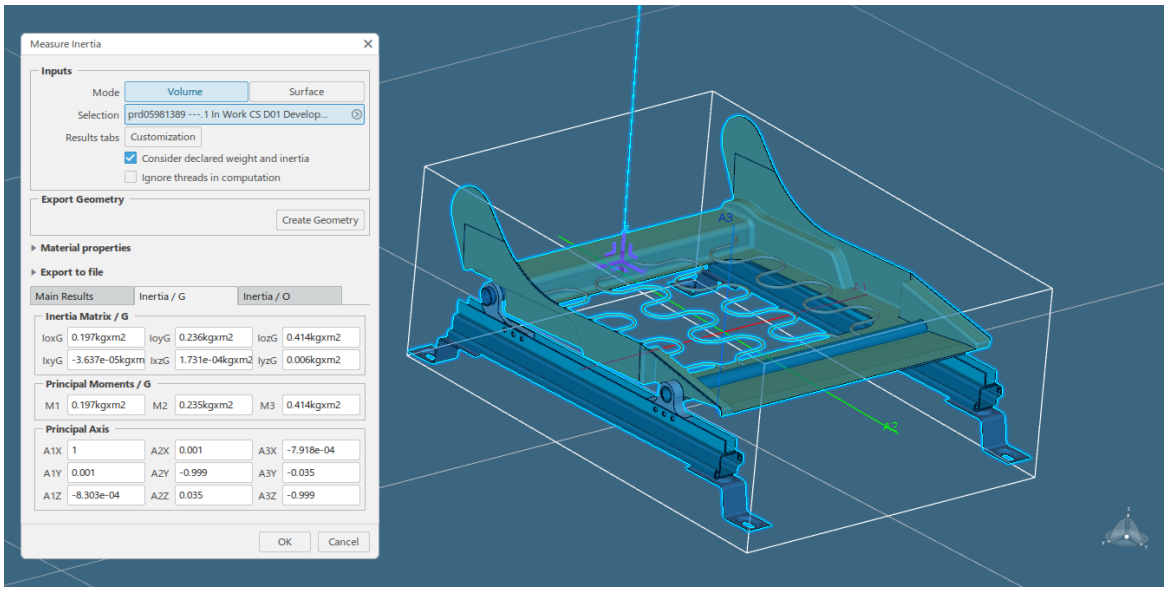
Measure Inertia
Inputs
Mode
Volume
Surface
Selection
prd05981389 ---.1 In Work CS D01 Develop...
Results tabs
Customization
Consider declared weight and inertia
Ignore threads in computation
Export Geometry
Create Geometry
Material properties
Export to file
Main Results
Inertia / G
Inertia / O
Inertia Matrix / G
IoxG 0.197kgxm2
IoyG 0.236kgxm2
IozG 0.414kgxm2
IxyG -3.637e-05kgxm
IxzG 1.731e-04kgxm2
IyzG 0.006kgxm2
Principal Moments / G
M1 0.197kgxm2
M2 0.235kgxm2
M3 0.414kgxm2
Principal Axis
A1X 1
A2X 0.001
A3X -7.918e-04
A1Y 0.001
A2Y -0.999
A3Y -0.035
A1Z -8.303e-04
A2Z 0.035
A3Z -0.999
OK
Cancel

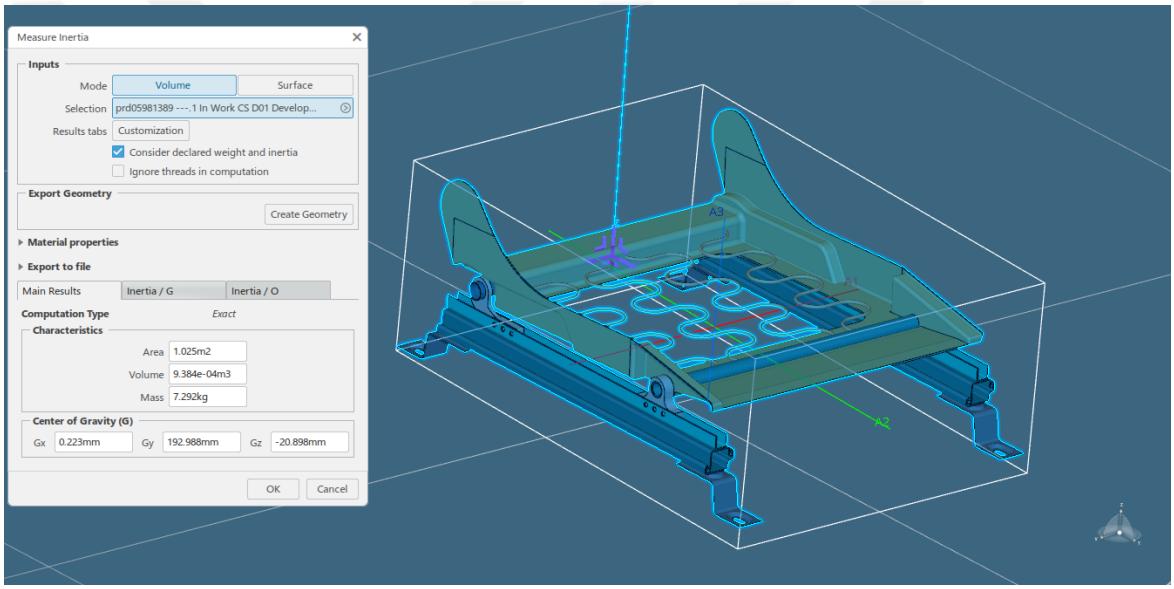
Measure Inertia
Inputs
Mode
Volume
Surface
Selection
prd05981389 ---.1 In Work CS D01 Develop...
Results tabs
Customization
Consider declared weight and inertia
Ignore threads in computation
Export Geometry
Create Geometry
Material properties
Export to file
Main Results
Inertia / G
Inertia / O
Computation Type
Exact
Characteristics
Area 1.025m2
Volume 9.384e-04m3
Mass 7.292kg
Center of Gravity (G)
Gx 0.223mm
Gy 192.988mm
Gz -20.898mm
OK
Cancel

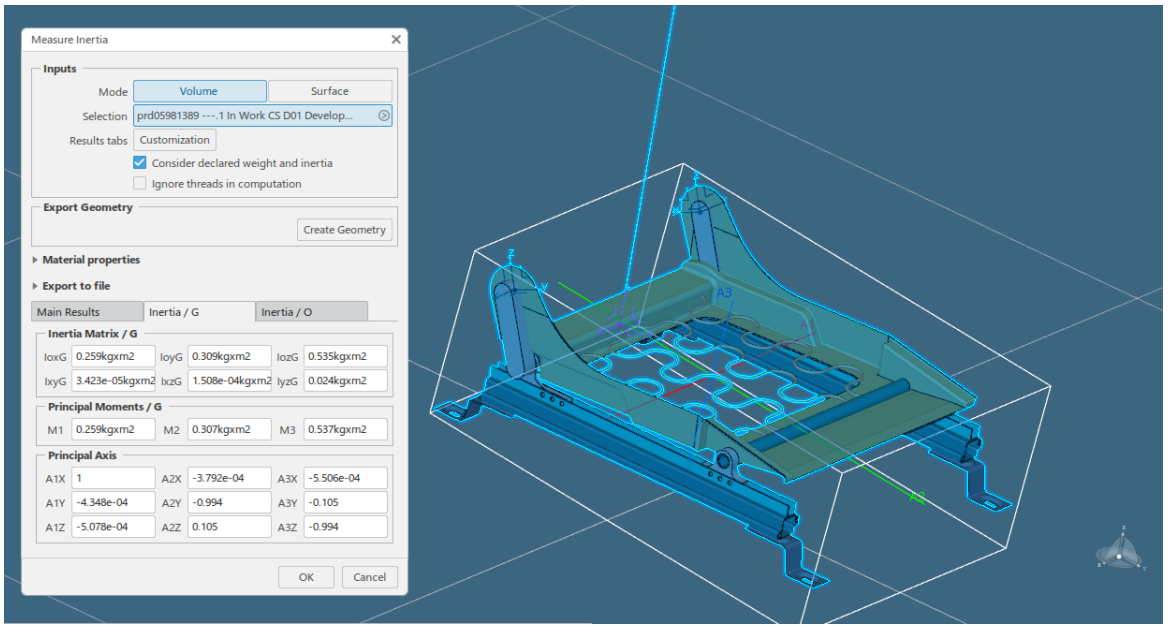
Measure Inertia
Inputs
Mode
Volume
Surface
Selection
prd05981389 ---.1 In Work CS D01 Develop...
Results tabs
Customization
Consider declared weight and inertia
Ignore threads in computation
Export Geometry
Create Geometry
Material properties
Export to file
Main Results
Inertia / G
Inertia / O
Inertia Matrix / G
IoxG 0.259kgxm2
IoyG 0.309kgxm2
IozG 0.535kgxm2
IxyG 3.423e-05kgxm2
IxzG 1.508e-04kgxm2
IyzG 0.024kgxm2
Principal Moments / G
M1 0.259kgxm2
M2 0.307kgxm2
M3 0.537kgxm2
Principal Axis
A1X 1
A2X -3.792e-04
A3X -5.506e-04
A1Y -4.348e-04
A2Y -0.994
A3Y -0.105
A1Z -5.078e-04
A2Z 0.105
A3Z -0.994
OK
Cancel

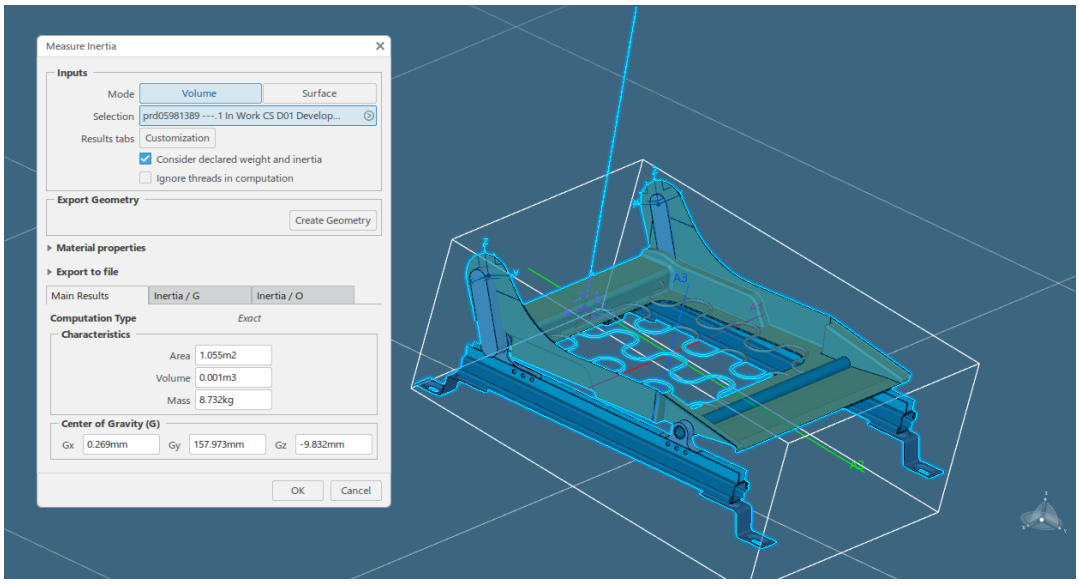
Measure Inertia
Inputs
Mode
Volume
Surface
Selection
prd05981389 ---1 In Work CS D01 Develop...
Results tabs
Customization
Consider declared weight and inertia
Ignore threads in computation
Export Geometry
Create Geometry
Material properties
Export to file
Main Results
Inertia / G
Inertia / O
Computation Type
Exact
Characteristics
Area 1.055m2
Volume 0.001m3
Mass 8.732kg
Center of Gravity (G)
Gx 0.269mm
Gy 157.973mm
Gz -9.832mm
OK
Cancel